POLITECNICO DI TORINO

Master's Degree in Automotive Engineering

Application of a P2 mild hybrid functional model with dual clutch transmission on a complete vehicle model

University Supervisors:

Prof. Enrico GALVAGNO

Prof. Alessandro VIGLIANI

FCA Supervisor:

Ing. Silvio FILECCIA

Candidate:

Andrea GUABELLO

Academic Year 2020/2021

Contents

Abstract

Automotive manufacturers are currently facing several challenges, brought by contrasting factors, like the pursuit of mechanical performances, environmental and safety regulations and also market demands, that very frequently ask for conflicting approaches. From this point of view, constructors are required to develop more and more complex systems, to control a wide range of features belonging to different fields. This is leading to an increasingly extensive use of systems modelling and simulations, an approach that is rising to be quite dominant in the automotive field, that prioritizes the functionality of a component and assesses its integration into a larger system at each stage of the development, before the physical prototype is created. Further widening the perspective, the co-simulation, a technique consisting in simulating more conjoined sub-models developed in different dedicated software, can bring additional benefits in the vehicle development process.

In the hereby paper it is presented the co-simulation of a driveline model with a complete vehicle mode, developed in two different software. In particular, it is evaluated the dynamics of a 48V mild hybrid vehicle, equipped with a P2 parallel architecture of the hybrid system, and a dual clutch transmission. This type of driveline, besides offering advantages in terms of energy efficiency and vehicle dynamics, is particularly interesting for the variety of driving modes in which it can operate.

The driveline is represented in a Simulink model, previously built and here developed in order to further enlarge its working modes possibilities. The aim of this first model is to compute the torque that arrives at the differential in the different manoeuvres. For better representing the vehicle response and simulate its real dynamics, a complete vehicle model is built on VI-CarRealTime, a dedicated software able to replicate a wide range of the vehicle data and features. A simple vehicle

model was also present in the Simulink model, but giving the complexity of the system, a more dedicated environment was preferred.
The ultimate goal of this work will be to effectively co-simulate the Simulink driveline model, in which we can reproduce all the possible longitudinal manoeuvres of a P2 mild hybrid 48V DCT vehicle and obtain the torque generated and arriving at the differential, with the VI vehicle model. This latter, inserted in a co-simulation model in Simulink, will receive in input the differential torque computed by the joined submodel, and provide us with an overview of the whole vehicle longitudinal dynamics.
In particular, in this paper are also evaluated the effects of the engine mounts, how they are going to work in a longitudinal dynamics manoeuvre and their influence on the ride comfort.
The final results are later going to be correlated with the ones obtained by the simple vehicle model developed in the Simulink environment.
The thesis is subdivided in five chapters: the first chapter presents a state of the art concerning model design and simulation and the advantages it can bring to the automotive field.
The second chapter describes the P2 DCT driveline of a mild hybrid vehicle, the main components it includes, and all the possible driving modes it can ensure, which will later be simulated.
In the third chapter the Simulink driveline model will be analysed: in particular, it is shown in which way the real system functioning is replicated and how the previously built model was further developed in order to guarantee an even wider range of solutions for its application. The effectiveness of the model will be shown in the simulations post-processing.
The following chapter focuses on the development of the vehicle model on the VI-CarRealTime environment, and the differentiation between the rigid powertrain model and the one in which engine bushings were inserted.
In the fifth and last chapter the co-simulation of the two sub-models is presented, and a correlation between the simple vehicle model and the new model can be shown with simulation results. An overview of the possibilities offered by the described co-simulation is provided here, including the powertrain suspensions analysis.

Chapter 1

Model-based design and simulation

In the last years, the automotive field has seen a dramatic increase in the complex systems within it. Manufactures are continuously working not only on mechanical improvements, but even more in the electronics area and in control strategies. This is leading automotive houses to face challenges like shortened development times, high safety requirements, and growing complexity of systems' codes and functionalities.

Because of the graphical tools' limitations, engineers of the past era heavily relied on text-based programming and mathematical models, that was time consuming and often prone to errors. To face the previously mentioned challenges, car producers are moving to a new paradigm in the software development, from hand-coded to model-based design [1]. A model-based approach enables a shift of focus; computer-modelling techniques are used throughout the design process, while the code is generated automatically when the model is already simulated and approved. This way, the model-based design prioritizes the functionality of a component and assesses its integration into a larger system at each stage of the development, before the physical prototype is created.

One of the most used tools for model-based design, that is largely going to be used in the development of this paper, is Simulink, a software integrated in MATLAB used for the modelling and the simulation of dynamic systems.

The described paradigm change can result in an improvement of product quality and reduction of development time by 50% or more.

1.1 Modelling and simulating

Modelling consists in creating a virtual representation of a real-world system by means of a dedicated software. The model must be a faithful representation of its real counterpart, incorporating its most important features, but at the same time it should not be too complex, in order to have a good understanding of its functioning and reasonable simulating times. When building a model, a good trade-off between realism and simplicity is fundamental.
Once the model has been created, a good technique for its validation is to compare the model outputs with the real system ones. Iterating between modelling and simulating can improve the quality of the system design, especially in the early phases. This will lead to a reduction of errors found later in the design process.
In model-based design, the system model is at the foundation of the workflow and, starting from it, it is possible a fast and cost-effective development of the dynamic systems, including control systems, signal processing systems, and communications systems. It is possible to:

- Use a common design environment across project teams.
- Link design directly to requirements.
- Identify and correct errors continuously by integrating testing with design.
- Refine algorithms through multi-domain simulation.
- Automatically generate embedded software code and documentation. [2]

The model-based design has earned much popularity in the automotive industry quickly making traditional software development methodology outdated. This is due to the great benefits it grants to automotive companies:

- Decreased development time and cost: model-based design is associated with rapid prototyping and validation of models and with the automation of coding, which considerably speeds up the overall development process. Since testing is performed at each stage, the development team can avoid costly and risky product changes in the later stages.

- Ability to introduce major changes late in the development process: block-oriented workflow and automatic code generation allow automotive engineers to correct erroneous specifications and replace large functional blocks, even if the product is late into the development cycle.

- Consistent documentation and implementation: the model description becomes the basis for system documentation, substantially reducing its cost and the associated errors.

- More reliable systems: the functionality of the system as a whole is a key focus from the very beginning of individual component development. In addition, extensive simulations, early testing, and automatic code generation eliminate the possibility of code errors and reduce the need for in-system debugging.

- Simple reuse of the solutions: the generated models can be reused under various operating conditions, or even in the development of other models. [3]

Once the model is created, by simulating its operation the system can be studied, and its behaviour represented and deduced. Simulation is a tool to evaluate the performance of a system under different configurations of interest and over long periods of time. It is used before an existing system is altered or a new one built, to reduce the chances of failure, to meet specifications, to eliminate unforeseen bottlenecks, to prevent under or over-utilization of resources, and to optimize system performance. [4]
Unlike physical modelling, simulation modelling is computer based and uses algorithms and equations, being the simulation software that provides the dynamic environment for the analysis. It presents different advantages, like consisting in a risk-free environment, providing a safe way to explore different "what-if" scenarios and the reduction of development costs and times. Moreover, a simulation model can capture much more details than an analytical model, providing for increased accuracy and more precise forecast. [5]
There are different uses for simulation technologies, like for process analysis, or decision support. What we are most interested in, are simulation technologies to support

product design and engineering: this category includes all those simulation tools used to predict the behaviour of a product or a portion of it. The main technologies used nowadays includes Multi-body simulation, Boundary Element Modelling simulation, Finite Element Method, CFD simulation.
The simulation environment must allow the modelling to consider different physical phenomena and their iterations with the appropriate degree of detail. Others key features are the accuracy of the results and the ability to model the equations and constraints of the system in a coherent manner, and the ability to be integrated with other systems. Simulation, therefore, not only allows data or information to be obtained from models, but also enables new forms of collaboration whereby designers can pass their simulation models, in order to run more advanced simulations, validate their results, or interact with production or customers.

1.2 Co-simulation

Co-simulation is a technique used to enable the simulation of a system through the composition of more simulators; it is the set of simulations computed by the coupled simulation units.
The simulation units can be independent black boxes, representing the constituent systems, developed and provided by the responsible teams, with an orchestrator coupling them and controlling how the simulation time progresses in each unit, and moving data from outputs to inputs according to a co-simulation scenario. Alternatively, models can be described in a unified language and then simulated; there are advantages to this approach, but each domain has its own particularities, making it impractical to find a unified language and a simulation algorithm that can be good for all. In contrast, co-simulation technique allows each team to configure their system with their own software and tools, without having to worry about the coupled systems. [6]
When performing a co-simulation, an algorithm is taking care of the synchronization and the interactions between the sub-simulators. These interactions are only synchronized and performed at specified discrete communication points, while sin-

gle systems are assumed to be independent out of the linking points; thus, each sub-simulator will behave like a black box, it will accept inputs from the other subsystems, perform its own simulation independently, and compute its outputs, which can later be used as other subsystems' inputs.

Co-simulation can provide a unique, more comprehensive, and more complete understanding of performance through the coupling of multiple simulation disciplines, since different types of analysis, from acoustics to multi-body dynamics, from CFD to structural analysis and crash dynamics, can now be linked through joint analyses. Multi-physics co-simulation guarantees greater accuracy, and improved performance by helping to avoid over-simplifying assumptions and thus leading to better correlation between virtual simulation and physical testing, so that engineers gain a deeper understanding of the real product performance without over-engineering. Besides offering higher levels of precision, co-simulation allows to comply with design timelines; simulating an event in a non-dedicated environment with a non-specific analysis can result in high time losses.

There are generally three approaches for combining models for full-system simulation:

1. The entire full-system model is built in one tool (Co-modelling).

2. The exchange of models between tools (Model exchange).

3. Coupling two or more simulators (Co-simulation).

Co-simulation advantages over the other two options are:

- Its modular nature and high flexibility, whereby a full-system simulation is built from several sub-simulators.

- Models can be developed efficiently in parallel and they can easily be re-used.

- The ability to leverage specialized tool chains and domain-specific knowledge already in use by participants and partners.

- The open nature of co-simulation together with a black box approach that protects Intellectual Property Rights.

- Sub-simulators can run in parallel with the potential to speed up the full-system simulations. [7]

Due to its characteristics and advantages, co-simulation is mostly used for complex and heterogeneous systems. This technique is worth considering if the model presents a high degree of flexibility, and the involvement of several sub-models from various fields and disciplines. The systems can have wide range of physical and engineering domains, and even adopt different time scales. Additional benefits can be obtained when sub-models are developed by different partners, especially if there are already substantial investments made in knowledge, tools, people, and if IPR protection is a concern.
In the automotive scenario, due to the complexity of the vehicle systems, it is always necessary to use a combination of simulation tools; control systems, mechanical, electrical, and hydraulic systems design require different development environments. The method of co-simulation is then applied to allow the communication between the various processes during the simulations.

Chapter 2

P2 48V hybrid vehicle with dual clutch transmission

2.1 Driveline architecture

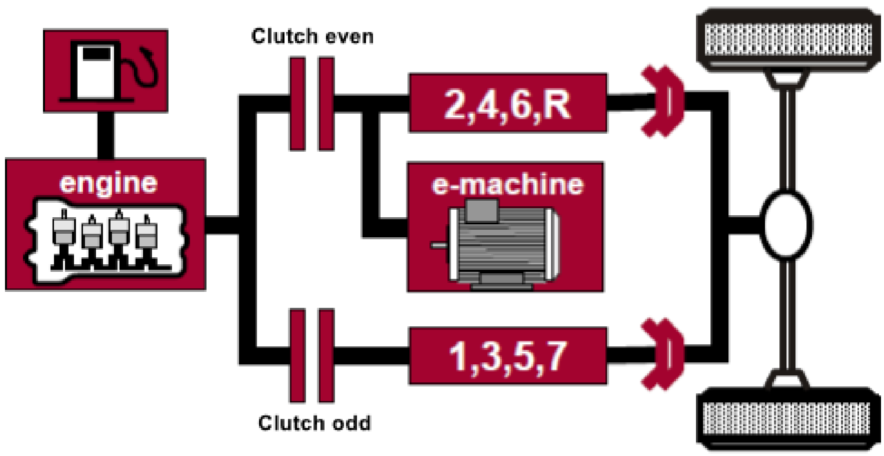

Figure 2.1: *Driveline of a P2 hybrid architecture with DCT*

The model that is going to be analysed in this paper has the purpose of predicting and evaluating the dynamics and the comfort of a given vehicle in its longitudinal manoeuvres. In particular, we want to assess the performances of a mild hybrid vehicle, with a P2 configuration of the hybrid architecture and a dual clutch transmission.

This particular type of architecture is quite peculiar: it mounts a DCT, so with the possibility of using two clutches and divide the produced torque alternatively and

smoothly between even and odd gear side of the gearbox. Moreover, being the vehicle a mild hybrid, it features a 48V battery and the electric motor in a P2 position, so between the engine and the transmission. In particular, the machine is mounted in the even side of the transmission, after the clutch pack and before the even gears.
The combination of the hybridization, the e-Motor positioning, and the presence of the DCT, opens up a wide range of possible driving modes of usage, conferring high flexibility to this type of vehicle.

2.2 Possible driving modes

2.2.1 Pure electric drive mode

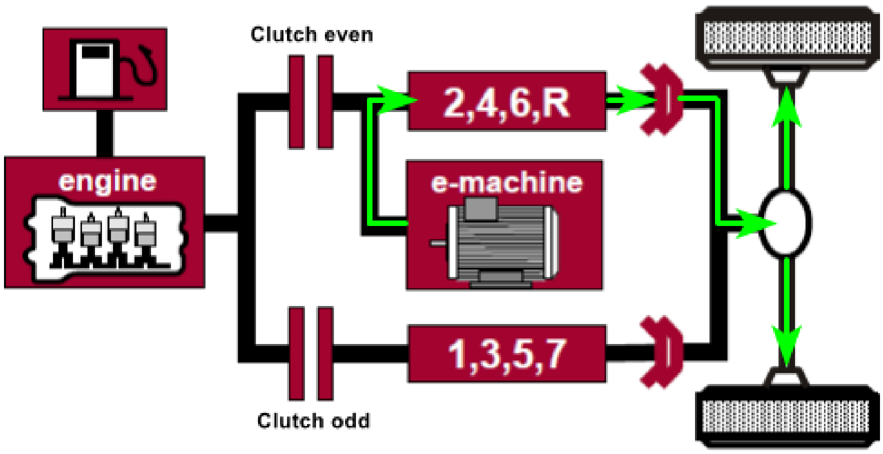

Figure 2.2: *Pure electric drive mode*

In an electric drive situation, the power flows from the electric motor to the differential, while the two clutches are open, and the ICE is off. It is possible to change the gear, using even gears, but it will not be possible to use the functionalities of the dual clutch transmission, so a torque cut will occur in the gearshifts. It could theoretically be possible to engage also the odd gears, but with both clutches closed the energy flowing will also drag the ICE, resulting in a loss of power at the wheels. It will be seen later how this effect could result useful if the aim is to switch the engine on.

2.2.2 Pure thermal drive mode

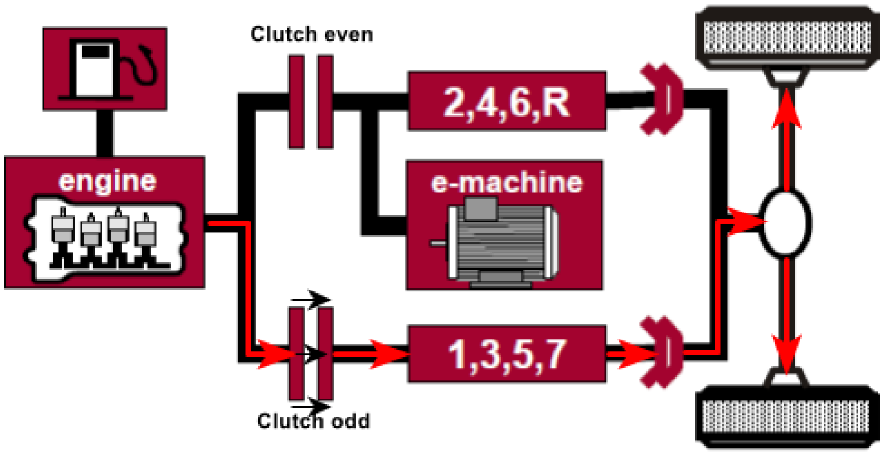

Figure 2.3: *Pure thermal drive mode*

In this case we have that the ICE is the only power source, while the electric motor is passive. We can exploit the functionalities of the DCT, with the torque transfer alternatively going through the two sides of the gearbox, accordingly to the gear changing in the developing of the manoeuvre.

2.2.3 Hybrid drive modes

There are different solutions of usage when both power sources are exploited for the drive, depending on how the torque flow is proceeding through the driveline.

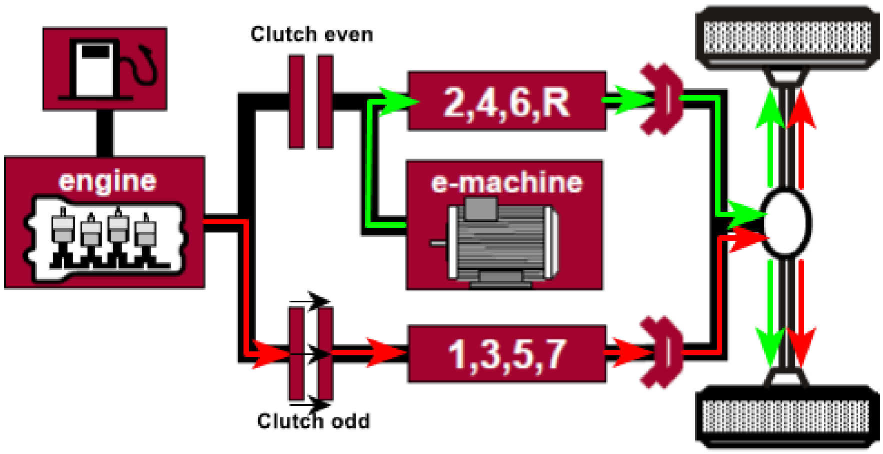

Figure 2.4: *Hybrid drive mode with ICE on odd gear and EM on even gear*

In the solution described in Figure 2.4, we have that both ICE and EM are transferring power to the wheels, but using two different gears: the electric motor is giving power through the even gear side, with the corresponding clutch that will be open. At the same time the thermal engine is transferring the power through an odd gear, passing through the closed clutch. This is the more natural and simpler mode of usage of this hybrid architecture.
There is no limitation on the gear selection, but of course a smart choice is to have the ICE that works with an even gear that differs by one unit with respect to the one used by the EM in the even side: this way, when a gearshift happens, the next gear for the ICE is already engaged, and there will be only the need of the clutches' movement.
Starting from this scenario, we can see in Figure 2.5 the second of our possible energy flows, that is when both ICE and EM are delivering the power through the same even gear.

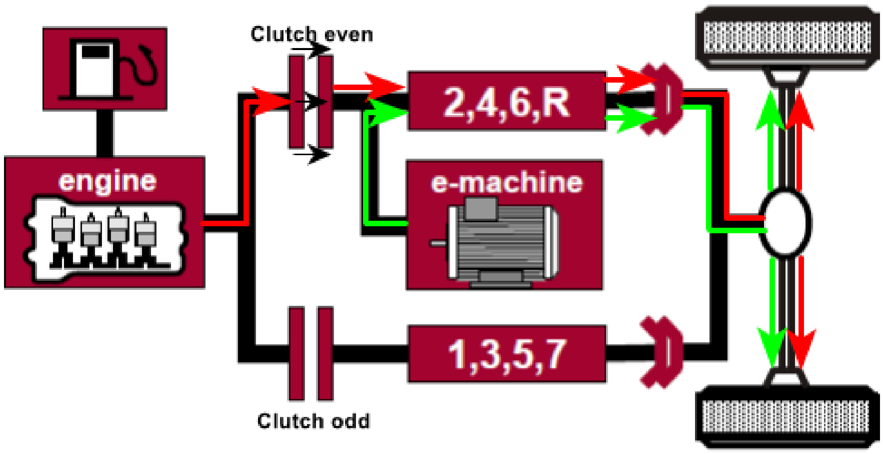

Figure 2.5: *Hybrid drive mode with ICE and EM on the same even gear*

The internal combustion engine energy will pass through the closed even clutch, while the odd clutch will be completely open. This condition can be particularly critical for the amount of torque acting on a single gear, that has to be analysed to prevent structural damages. Moreover, using the same gear for the thermal and the electric machine might be a drawback from the optimal use of the electric motor, since it is preferable to use it at low speed for the high torque capability and high efficiency, both in drive mode and in generation mode.

Another particular case of usage is when both motor and engine engage the same odd gear.

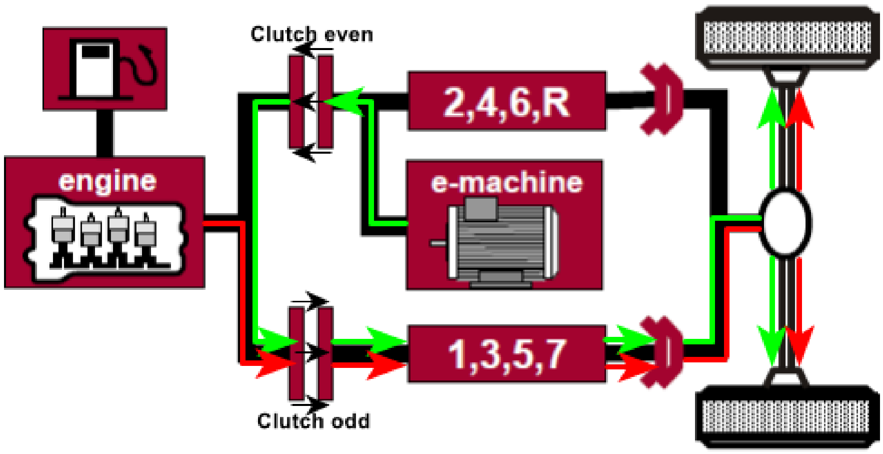

Figure 2.6: *Hybrid drive mode with ICE and EM on the same odd gear*

To do so, as shown in Figure 2.6, both the clutches will have to be closed, so that the ICE transfers the torque through the odd clutch, and the e-Motor power has to pass through both clutches. Again, we will have the same limitations seen for the second case about using the same gear. It can also result in a complex and unsmooth gear change, determining poor effects on the vehicle dynamics.

2.2.4 Thermal engine start

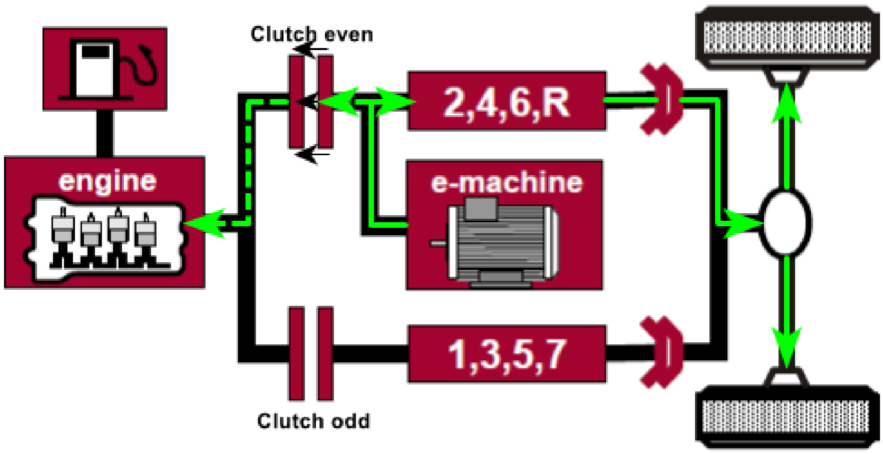

Figure 2.7: *Engine clutch start with the electric motor*

The P2 DCT architecture permits different solutions for the engine cranking.
In a simple standstill situation, the electric motor can start the engine, without engaging any gear, passing through the even clutch, and acting like a starter motor. The only resistance will be the one coming from the engine.
A solution that is made possible by this type of driveline is the clutch start. This particular cranking can happen in a moving-vehicle situation, starting from a pure-electric drive mode. The electric motor is transferring the driving power to the wheels, through the even gears, and at the same time can transfer some of the energy produced to the engine, to start it. This last energy transfer can both happen closing either the even or the odd clutch. The higher the gear engaged, the lower the corresponding gear ratio, and therefore the lower will be the impact of the missing torque at the wheels.

2.2.5 Regenerative braking

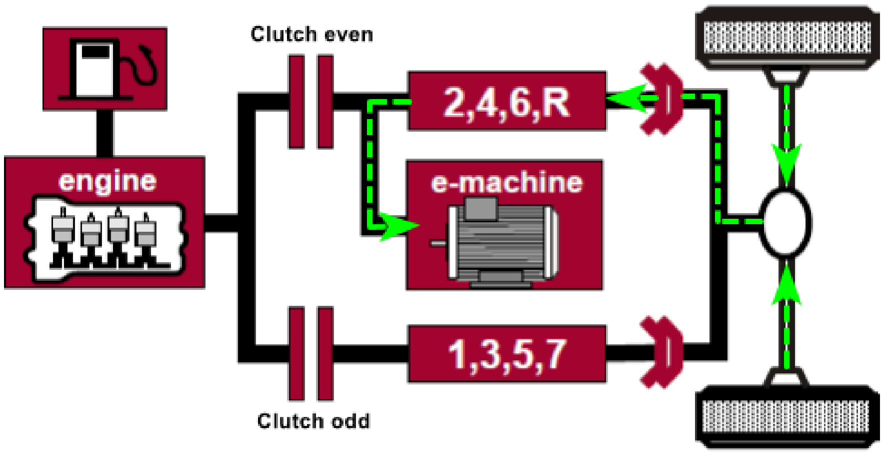

Figure 2.8: *Regenerative braking*

The presence of an electric machine consents to have a reverse conversion of the energy, so the possibility to transfer power from the wheels to the battery, to recharge it. This transfer, again, can happen passing from both sides of the transmission. Normally we have that the electric motor engages an even gear, so that the torque transfer does not have to pass through clutches in order to reach it. Therefore, the alternative solution consists in a less efficient case. For the recovered energy to reach the EM through an odd gear both the clutches must be closed, that means a longer path and lower mechanical efficiency involved, and it has to be considered that in this path we will also have the drag of the ICE.
A different analysis has to be done if the regenerative braking is happening with the gear changing. In this case, shifting gears using also the odd side could represent a good trade-off: in fact, we must consider that shifting the gear using only the even side will mean not to use the DCT and to interrupt the torque flow, losing power. Shifting using also the odd side will have a lower efficient path, but it will permit to have a better torque continuity.

Chapter 3

Simulink driveline model

The final objective of this work is to develop a model able to co-simulate a functional driveline model, previously built in Simulink, with a complete vehicle model created in VI-Grade.

The starting model, representing the driveline type presented in Chapter 2, was previously developed in Simulink by Riccardo Benevento as described in his thesis [8], and contains all the blocks to simulate the main features of a P2 mild hybrid vehicle equipped with a dual clutch transmission. In particular, we will have both the ICE and the EM blocks, the DCT block, the gearbox block and finally the vehicle model block. This last one is bound to be a simple model, since the Simulink environment is not so dedicated to have a full vehicle representation. For this reason, we are later going to develop a complete vehicle model on VI-Grade that will be linked to and driven by the Simulink driveline model and by the simulations we run on it, which results will be the inputs for the co-simulated model.

3.1 Model overview and functioning

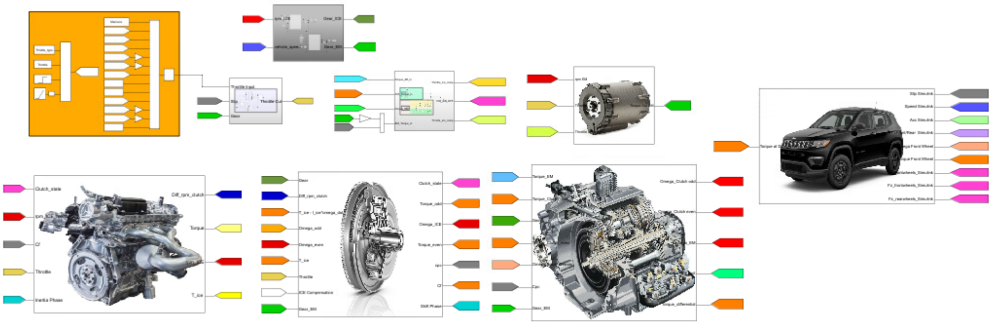

Figure 3.1: *Driveline model in Simulink*

It is now presented a general overview of the Simulink model of the driveline, its functioning, and how it was further expanded in order to have the possibility to perform all the driving modes described in the previous chapter.

3.1.1 Thermal engine block

The internal combustion engine block will be in charge of creating the engine torque.

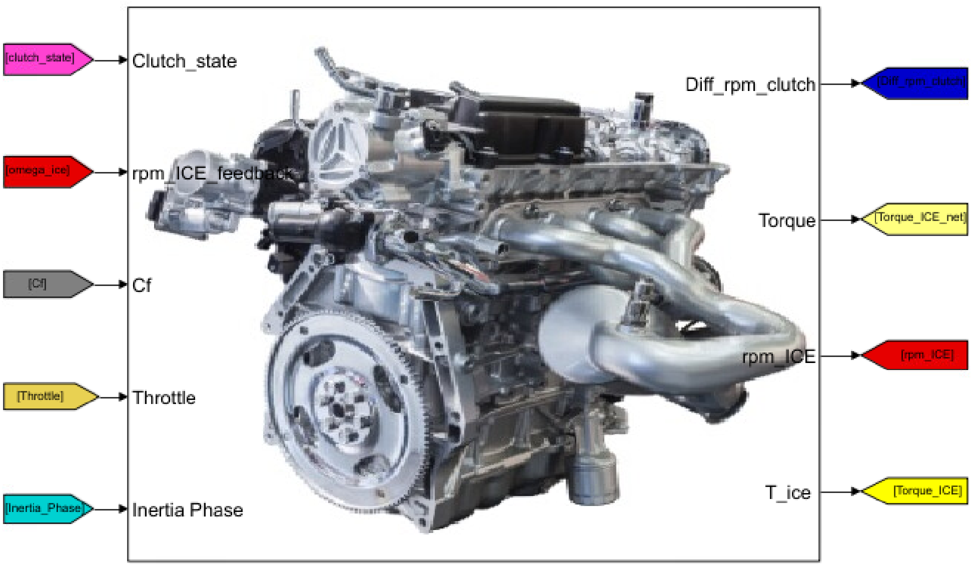

Figure 3.2: *ICE block*

A lock-up table is provided, which links the engine rpm feedback signal computed to the engine torque output, that will be cut accordingly to the chosen throttle profile, established by the user on the MATLAB script.
From the engine torque, the input torque at the dual clutch is obtained. Since in this model the synchronizers and the flywheel are not represented, meaning that a gear is practically always selected, there is a direct link between engine and clutch. This is a simplification, for making the overall system more robust and cutting the simulation time. The simplest case that can be considered is that of an engaged clutch situation, where there is only one D.O.F and the equation of motion can be written as:

$$T_{ICE} - \frac{d\omega}{dt} I_{ICE} = T_{clutch} \tag{3.1}$$

For the gear shifting alternative, the equation is used inversely, so the inputs will be the engine torque and the torque at the clutches, which will be used to compute the angular deceleration of the engine. If this is the case, the torque will be lowered in the inertia phase of the upshifts, when the engine rpm need to synchronize with the new transmission side rpm; a controller is inserted to cut the value of throttle.

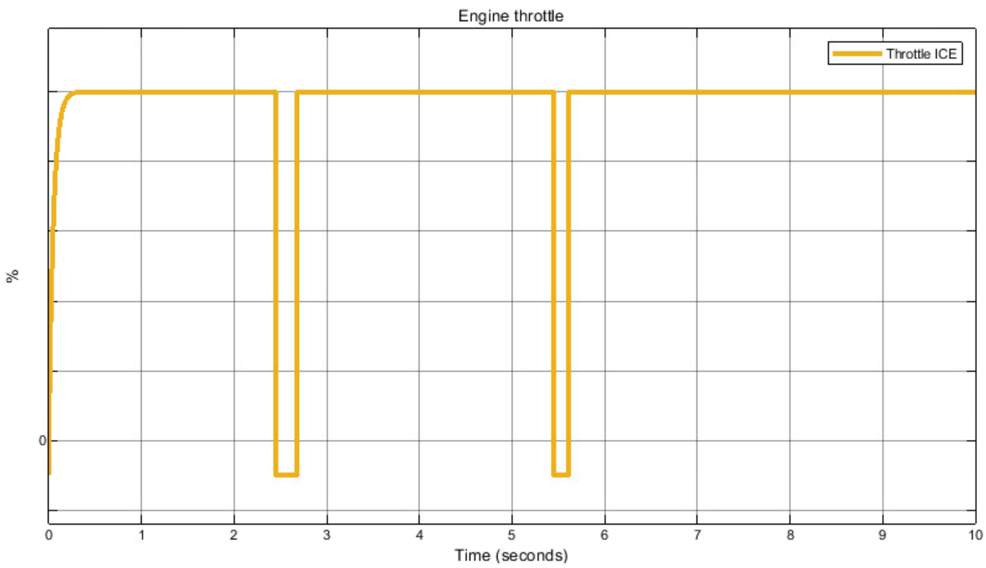

Figure 3.3: *Throttle cut in the inertia phase of the DCT*

3.1.2 Dual clutch block

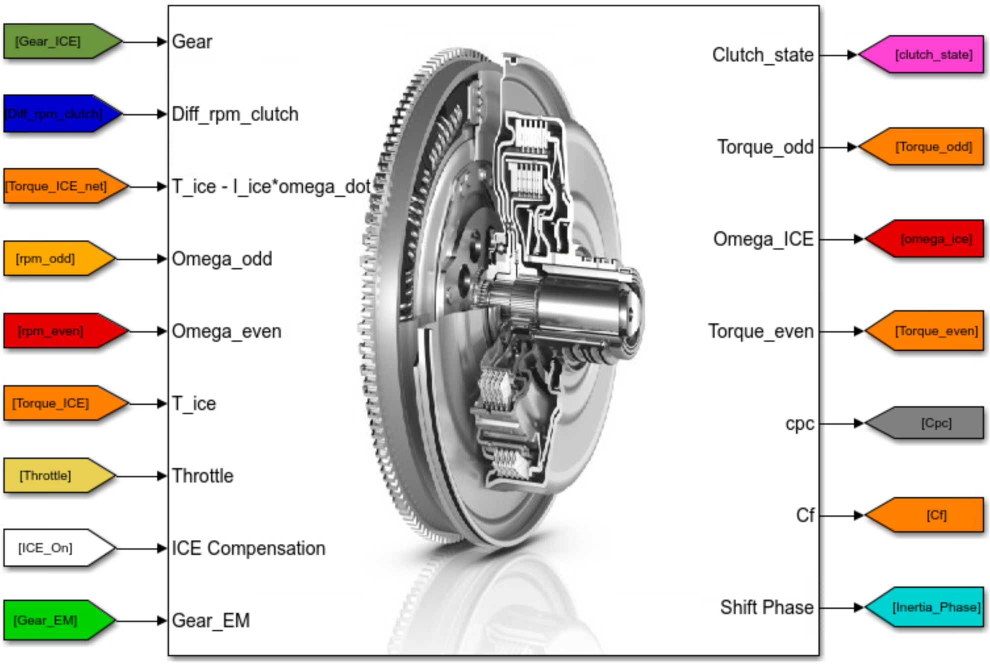

Figure 3.4: *DCT block*

The block representing the two clutches is fundamental for the functioning of this specific driveline. The DCT modelled has to simulate the real behaviour of a dual clutch transmission, so taking into account all the possible driving conditions, and all the phases of its usage, fixed gear or gear shifting phase.

Here some modifications were necessary in order to obtain all the possible drive modes previously explained. Specifically, the initial model did not include the possibility of using odd gears for the electric motor as well, so some major changes had to be made.

The DCT block functioning is guaranteed by a controller that acts on the pressures on the two clutches; in the model this controller is represented by a pressure generator block. Here, an algorithm performs the task to simulate the pressure path acting on the two clutches surfaces. In the fixed gear phase, it takes care of giving the maximum pressure at the clutch in use, in order to guarantee the torque transfer, setting at zero the pressure at the twin clutch.

$$T_{clutch_{capability}} = n \, \mu_f \, r_m \, (p(t) \, A) \tag{3.2}$$

$$T_{ICE} - \frac{d\omega}{dt}\, I_{ICE} \leq T_{clutch_{capability}} \tag{3.3}$$

In the gearshift, the controller will recreate the cross path of the two pressures, in order to smoothly pass the torque from one side of the gearbox to the other. A constant value, lower than the maximum, is set for the closing clutch when we are in the inertia phase of the shifting, in order to synchronize the engine speed with the speed of new gearbox side in use.
For the electric motor to engage an odd gear, since the machine is linked to the even side of the gearbox, the system will have not only to close the odd clutch but also the even clutch. To implement this feature on our driveline model, a function is created that will modify the original pressure path of the even side clutch. While when using an even gear the electric motor torque will pass through no clutch and arrive untouched at the gearbox, in this case it will go through the clutches pack, meaning that the torque produced will be inevitably influenced by the pressure path, as it happens for the ICE torque. For the sake of simplicity, and not to distort the initial model for an isolated case, the electric motor torque will not be included in the general equation of motion for the computation of the torque at the clutch, but it will be considered externally, and the described influence of the clutches on the torque is taken into account separately.
In the more conventional usage, in a hybrid driving mode with the electric motor exploiting only the even side of the gearbox, the DCT is working independently of the even gear selected by the EM; the normal cross path of the pressures at the clutches' surfaces can be observed.

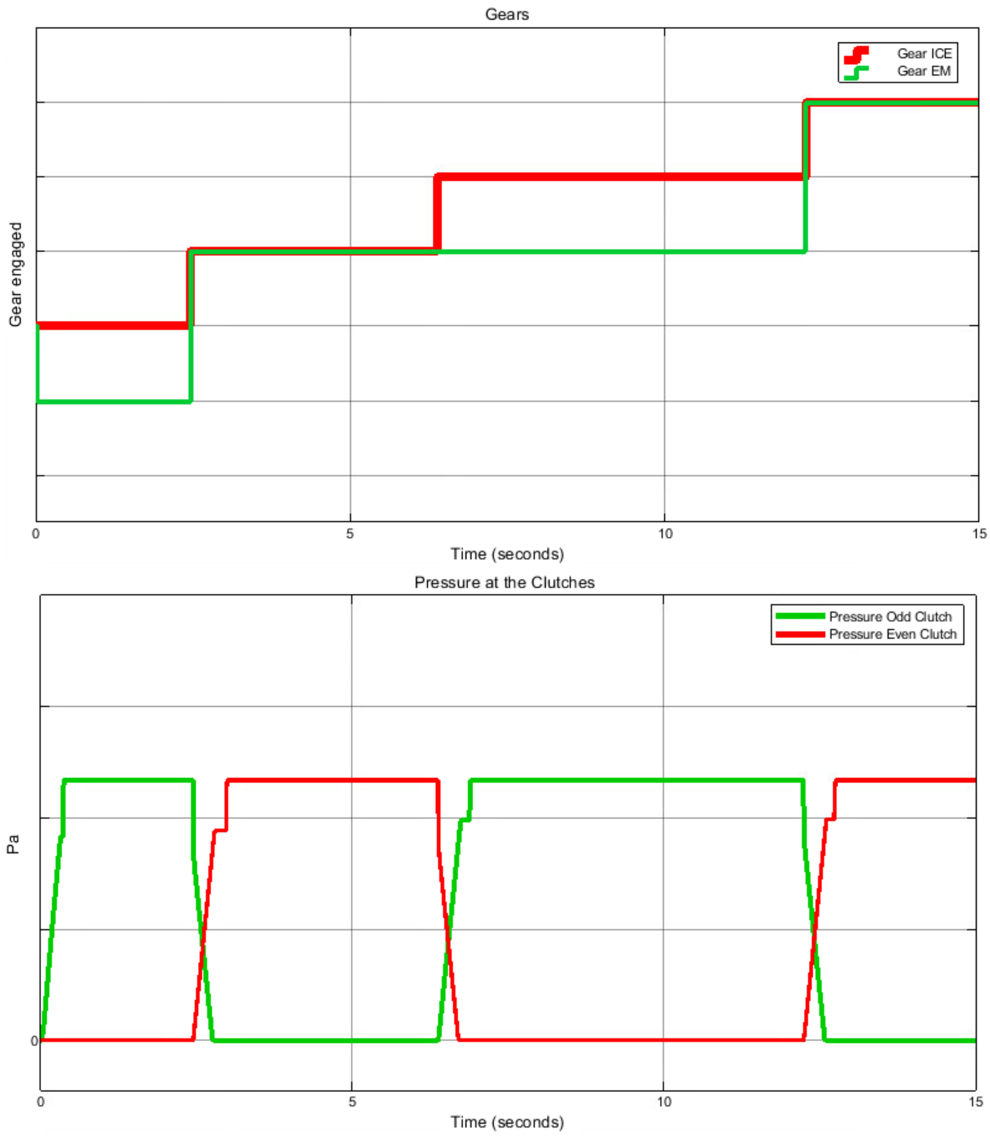

Figure 3.5: *Pressure path acting on the two clutches' surfaces in a normal operation*

Now the goal is to have the possibility to close the even side clutch when an odd gear is selected both for the ICE and the EM. To reach it, a newly implemented algorithm is rebuilding the even clutch pressure trend; when an even gear is selected, the pressure follows the pre-established path. When an odd gear is selected, in the gear changing phase, the pressure on the even clutch is initially starting a cross path, falling as it was in the previous case, while the odd side pressure is rising; once the two pressures intersects, the crossing is ended and the even pressure is now following the odd one and rises again, so that both clutches are simultaneously closing, and both ICE and EM torques are transferred through the odd clutch side.

In results, in an upshift procedure from an even gear to an odd one, the odd-numbered clutch will close in accordance with the normal DCT logic to transfer the torque from both motors, while the even-numbered clutch is now following the previous opening curve only for an initial stretch, and then it closes simultaneously with the odd-numbered clutch.

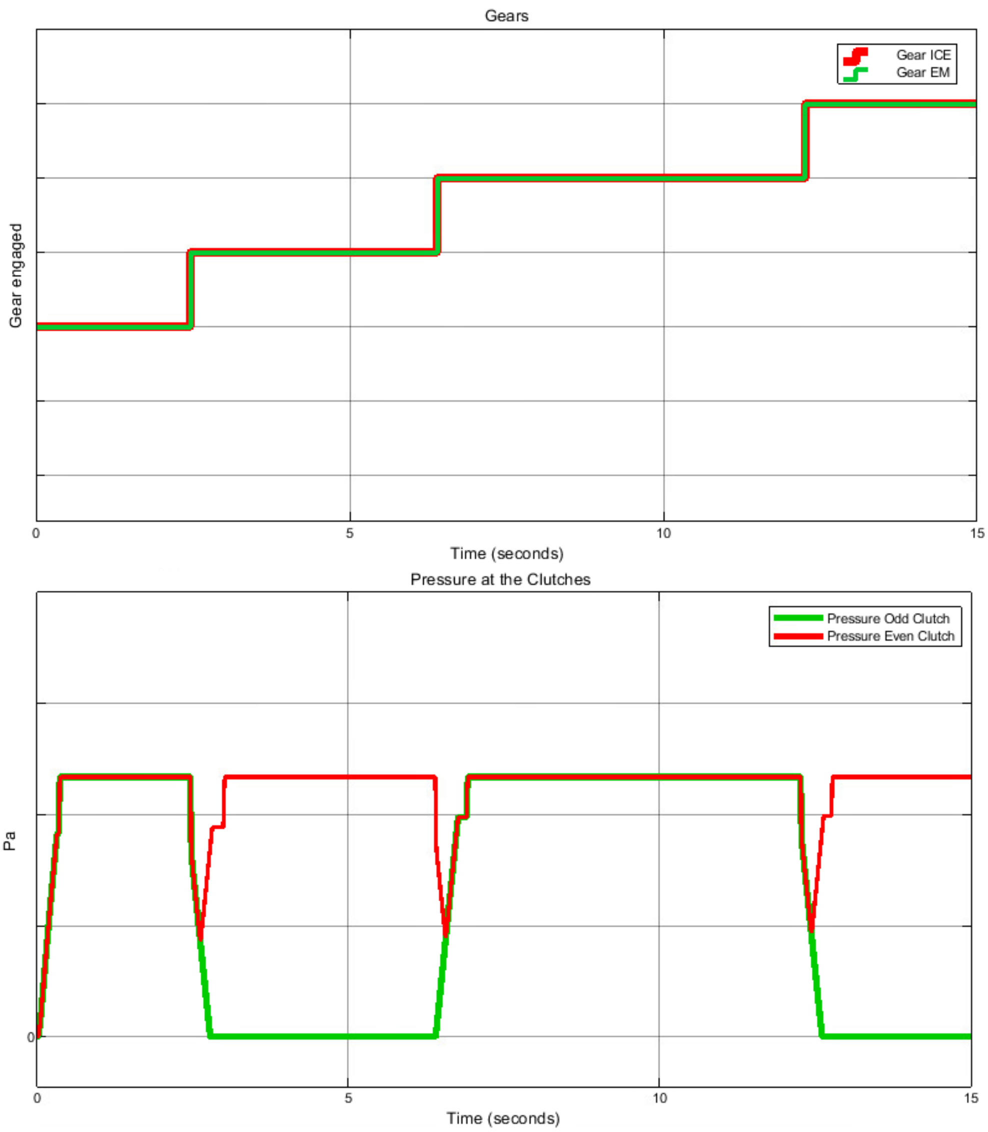

Figure 3.6: *Pressure path acting on the two clutches' surfaces when EM engages odd gears*

A possible alternative was to have the even clutch always closed for these manoeuvres. The described path was preferred, firstly to maintain a solution more consistent with the other modes of operation, and also in order to have a smoother and more controlled transition of the electric power from the even side to the odd side.

In this type of operation, as previously mentioned, when the electric motor is using an odd gear we cannot think anymore that the power produced will arrive untouched to the differential; it must be considered the influence of passing through the clutches.
It is assumed that the engine transfers its torque, according to the gear selected, independently from the new even clutch pressure trend, so as if the cross path was maintained unmodified. As we have seen in the equation, the engine torque that is transferred through the clutch, will be lower than the clutch capability, that is proportional to the clutch pressure. A proportionality has now to be considered also for the electric motor torque, when it passes through the clutches.
Following a simplistic logic, avoiding to create a new equation of motion, a loss coefficient is created, which considers that the clutch is not always fully closed during the manoeuvre. This coefficient will therefore be given by the ratio between the pressure at the even clutch and the maximum pressure value, corresponding to the transfer of the entire torque, and will be multiplied by the torque produced by the electric motor. Of course, when the gear is even, this coefficient is always considered to be equal to unity, since in that condition the electric motor can transfer its power directly to the gearbox, bypassing the clutches pack.

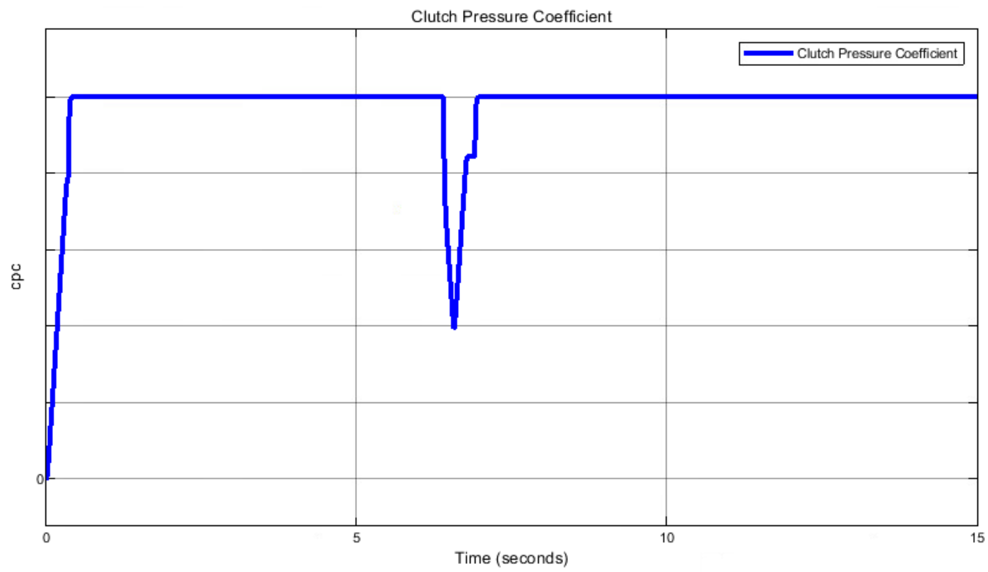

Figure 3.7: *Clutch pressure coefficient*

3.1.3 Electric motor block

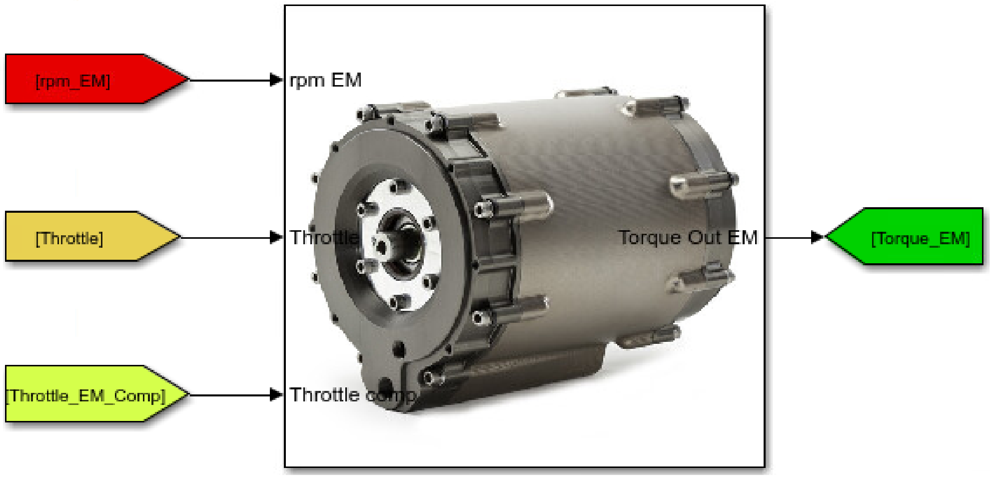

Figure 3.8: *EM block*

The electric motor block is simply built to give the torque produced through the use of lock-up tables. According to the motor rpm, a corresponding torque is attributed as output. Different tables are present, in order to guarantee that the shorter is the period of usage, the higher is the torque that the machine can produce, mainly for overheating prevention; the actual output torque will be regulated during the manoeuvre by a clock.

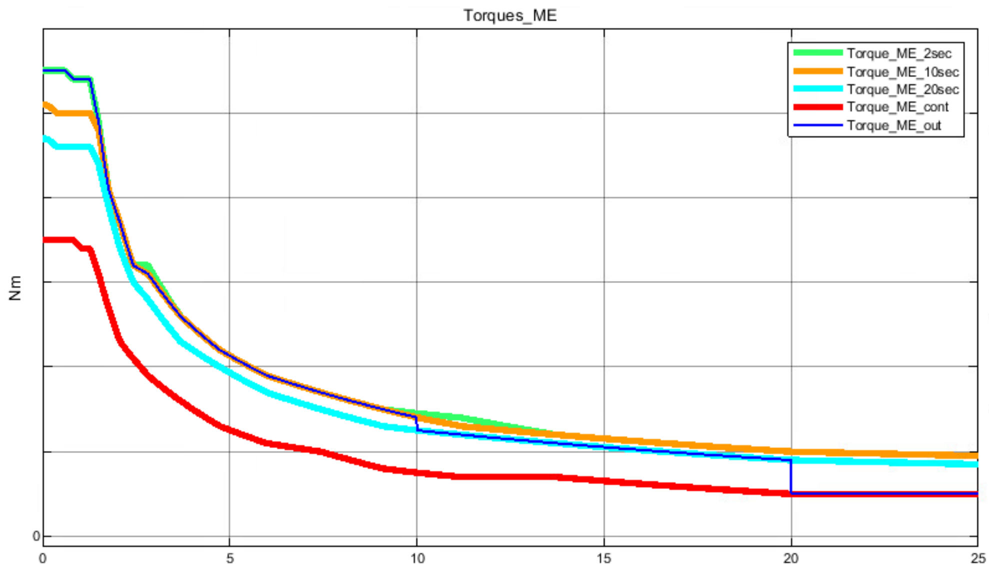

Figure 3.9: *Electric motor torque produced according to its time usage*

The electric motor has also to guarantee a reverse operation, in order to perform the regenerative braking and to recharge the battery. In the dedicated manoeuvre, the functioning is the same, of course with an inverse trend of the table values.

3.1.4 Gearbox block

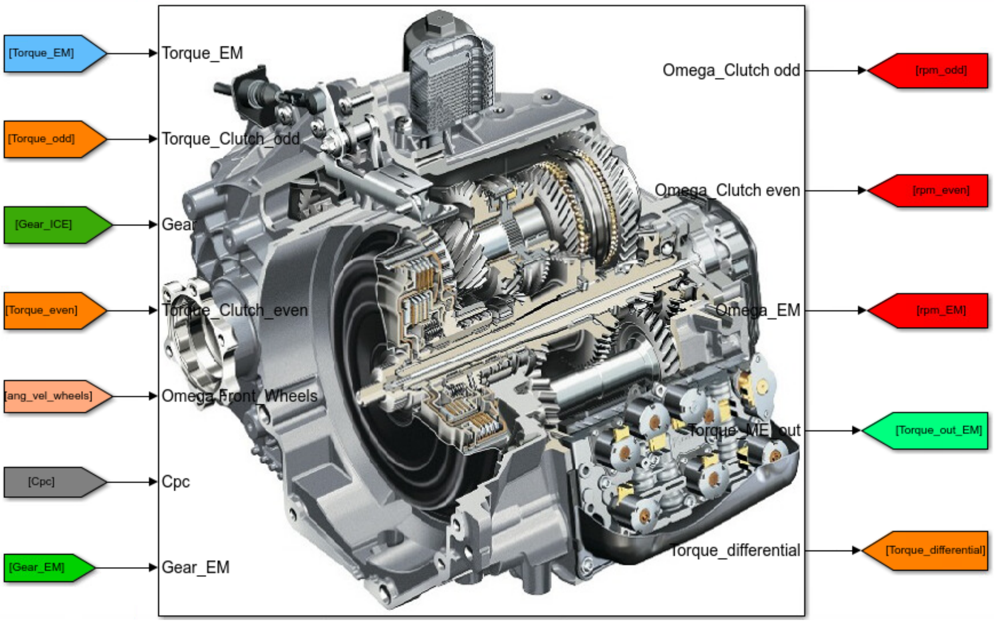

Figure 3.10: *Gearbox block*

The gearbox block takes in input the torque coming from the clutches and has the job to compute the torque arriving at the differential from both the even and the odd gears sides of the transmission.

Again, some modifications were necessary in this block in order to consider the new possibility for the electric motor to engage an odd gear. The basic equations used for the gearbox are now:

$$T_{GB_{even}} = \eta\, \tau_{even}\, (T_{evenClutch} + T_{EM_{even}}\, \tau_{finEM}) \tag{3.4}$$

$$T_{GB_{odd}} = \eta\, \tau_{odd}\, (T_{oddClutch} + T_{EM_{odd}}\, \tau_{finEM}) \tag{3.5}$$

The torque output of the clutches is gained by the gear ratio τ, and now on both side is considered the contribution of the electric motor torque T_{EM} with its own final ratio τ_{finEM}. As previously explained, in the odd side the torque produced by the electric machine is considered as external to the one arriving at the clutch. In the two equations is considered a mechanical efficiency η .

Three internal blocks are present, one for the electric motor torque, and two for the ICE torques. The block dedicated to the electric motor will compute the related gearbox output torque according to the gear ratio and the final ratio, and divide it in the two sides depending on the gear selected. The two blocks for the ICE will perform the same task, with the only difference that the two sides differentiation is already taken into consideration at the clutches level, for that reason the torque arrives already divided and two separated blocks are used.

Now the two output torques can be computed and the torque in input at the differential can be obtained summing the two machines contributions.

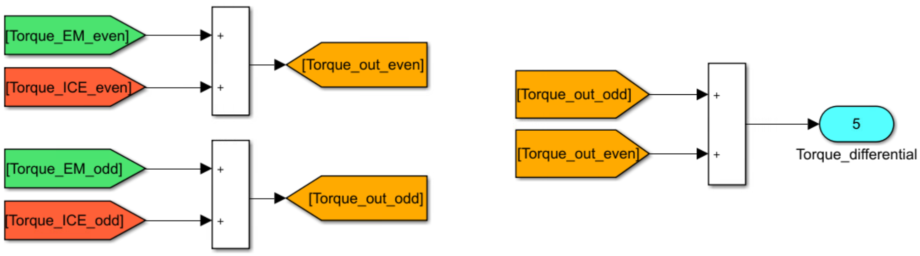

Figure 3.11: *Torque at the differential computation*

3.1.5 Controllers blocks

In the model are included three controllers blocks.

The first controller present is for traction control: it is a PID controller that, only at first gear, cuts the torque according to the slip value of the wheel in order to avoid slippage.

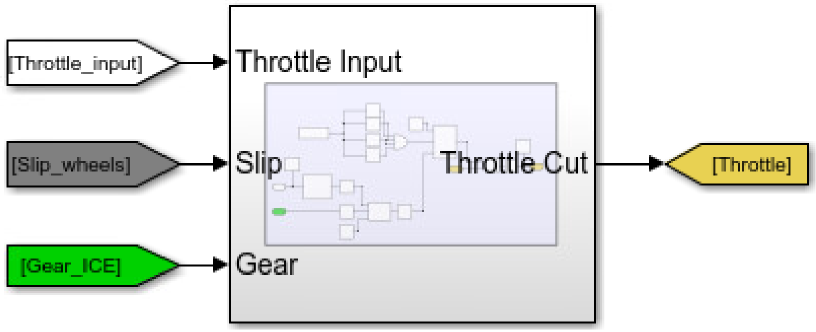

Figure 3.12: *Traction controller*

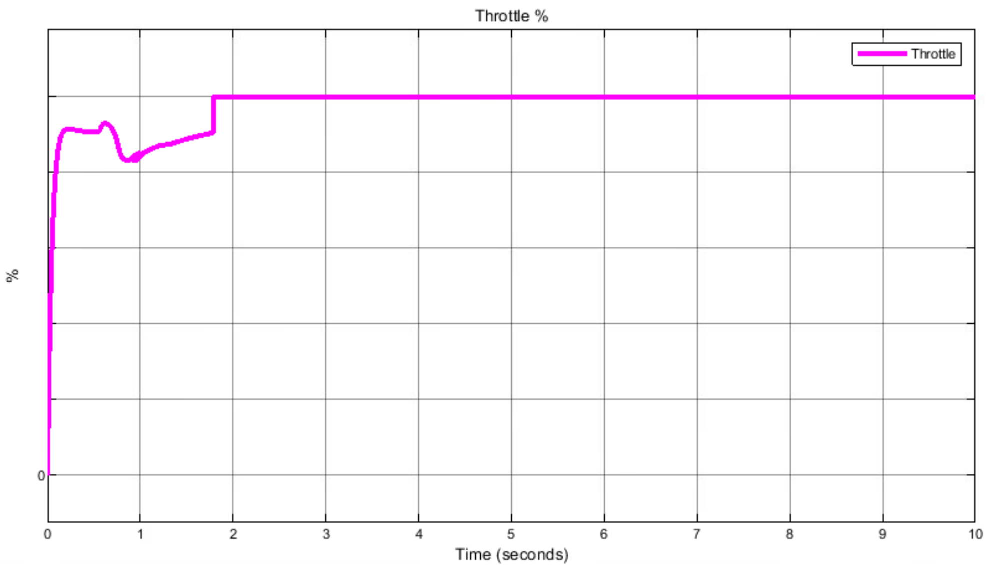

Figure 3.13: *Throttle control action*

The second controller showing in Figure 3.14 is the automatic gear shifter. This is the block controlling the gears engaged during the simulations. Some changes were introduced for our model, since we needed to embody a new logic for the electric motor gear, that before was only bound to the ICE gear. Now, this controller will be responsible also for the controlling of the gearshift during the regenerative braking.

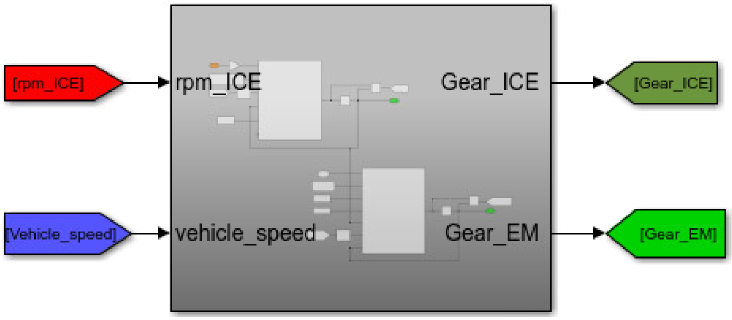

Figure 3.14: *Automatic gear shifter*

The gear shift control for the ICE was already present; a function is controlling the gear according to the engine speed. Following the same scheme, a new function was created in order to control the electric motor gear. This block action will be determined by the chosen manoeuvre; the new logic comprehends the gear control during regenerative braking and during hybrid drive mode with the EM on odd gear.

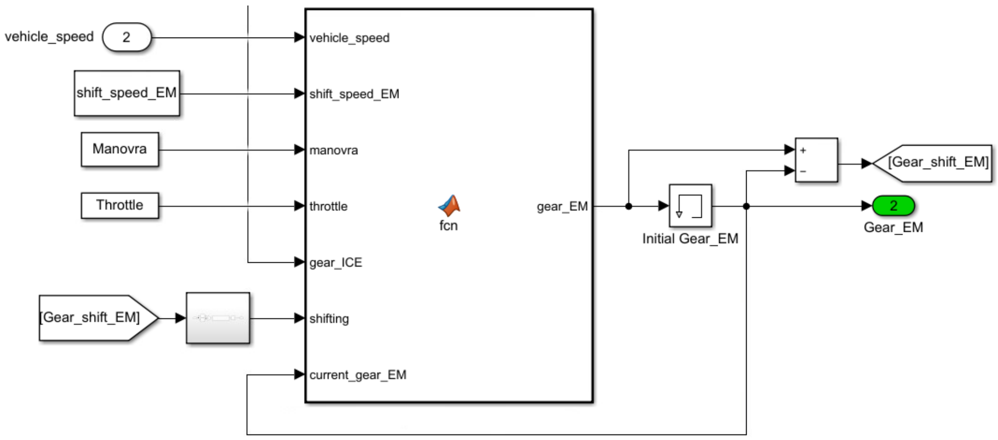

Figure 3.15: *EM gear shifter*

For the acceleration case, the ICE gear information is used, so that the electric motor will transfer the power using the same gear.
For the braking case we have to differentiate two manoeuvres, according if we want to downshift using or not the odd gears. In both scenarios the logic implemented in the function is the same: differently from the ICE controller case, where the gear was selected according to the engine rpm, here the dependence is based on the vehicle speed. This choice was made for the sake of simplicity, being that in the downshift the electric motor rotational speed would highly increase, while in the rest of the

braking manoeuvre is decreasing with the vehicle speed, so a complex control logic would be needed to determine how actuating the gear change according to the rpm. In the created function the various speed ranges to which a given gear corresponds are specified; the ranges are determined after evaluating the gears used in a WOT manoeuvre, so that, imagining switching to an acceleration manoeuvre, the proper gear would already be engaged. The solution of using pre-established longitudinal speeds instead of rpm can even be preferable, if we consider that in a braking manoeuvre with regenerative purpose is reasonable to act following a convenience criterion.

The last controller implemented is the torque components controller. This controller acts in two distinguished operations, both in the case of a hybrid drive mode.

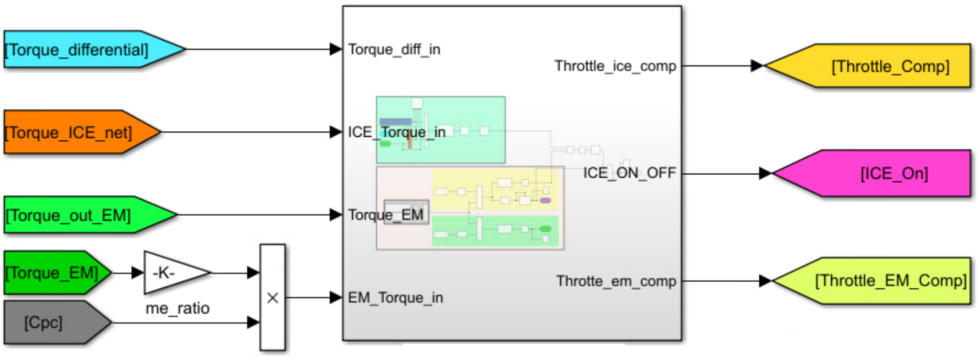

Figure 3.16: *Torque components controller*

Firstly, it operates in a throttle management consideration for a compensation manoeuvre: this means that the controller acts on the contributions of torque coming from the ICE and from the EM. In particular, a target torque is implemented in the model, taken from a simulation of the same manoeuvre in a full throttle operation with only the thermal engine, and considered when the compensation manoeuvre is selected. The logic behind the controller action can be divided in two cases:

- When the electric motor is able to fulfill the whole torque request, the thermal engine is off and its torque output is zero.
- When the electric motor is not able to fulfill the whole torque request, it will work at its maximum capability while the engine compensates the remaining torque with a controlled output.

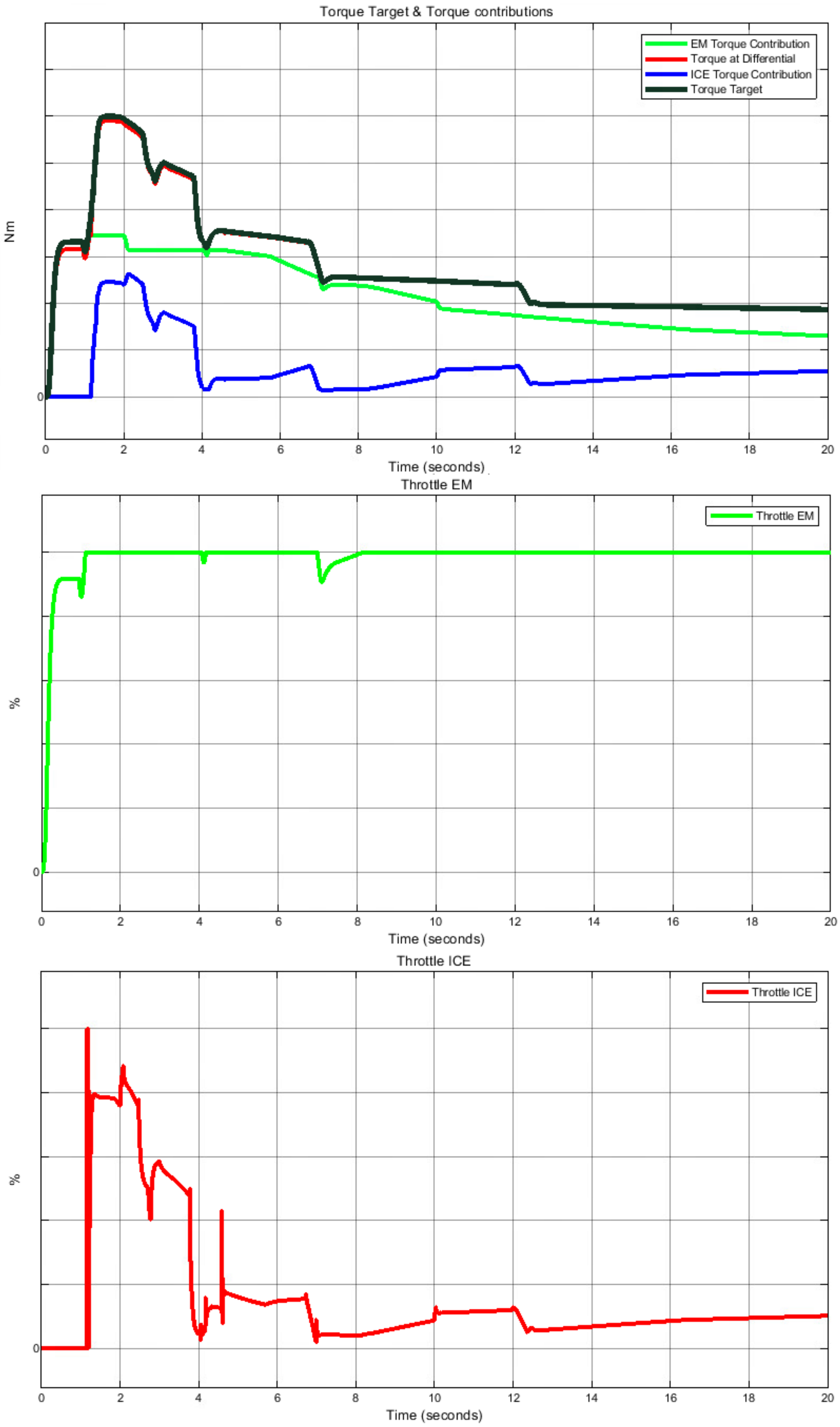

Figure 3.17: *Compensation control action*

The other controlling operation performed by this block is the control of the maximum torque output. Again we have a compensating manoeuvre, so the previously explained controller is still working in the same way, but with the addition of a limitation of the maximum torque entering at the gearbox, for a possible protection of the gear mechanism from structural damage. The maximum torque is a constant value, fixed at a fraction of the maximum torque that the engine can deliver. The torque cut of the control acts only on the ICE throttle.

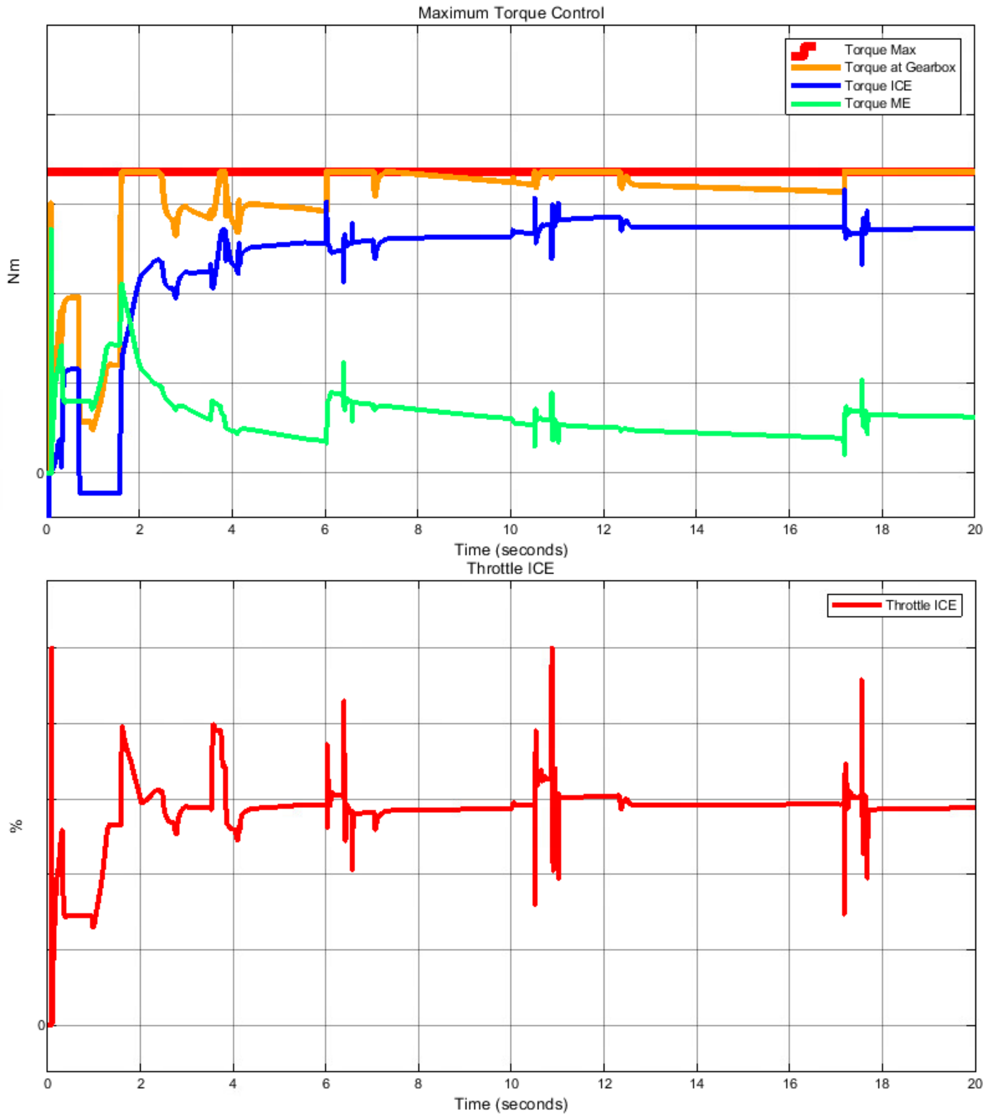

Figure 3.18: *Maximum torque control action*

Simply the controller will take the sum of the two torques contributions, from the engine and from the electric motor, and compares it with the limit value. If the torque exceeds the maximum, the controller cuts the throttle value of the engine.

3.1.6 Vehicle model block

The general goal of the model, that was to compute the torque at the differential, is now accomplished, but in order to obtain the parameters showed in the equations and to run the simulations, a simple vehicle model block is included in the Simulink model. This will result useful to obtain the vehicle acceleration and speed, the tire slip, and the loads at the wheels.
At the end of this paper, the simple vehicle model will be used in order to calibrate the complete model we will later create, and verify its correct functioning.

Figure 3.19: *Simulink vehicle model*

In the vehicle model block, the main equations of the vehicle longitudinal dynamics are represented. Two sub-models can be distinguished, one regarding the tire behaviour, and the other representing the vehicle behaviour, working together and passing inputs to each other.
The torque at the differential is taken as input and used in the dynamic equation of the tire.

$$\frac{d\omega}{dt} J_{wheel} = \frac{1}{2} T_{diff} - (F_x - F_{rot}) R \tag{3.6}$$

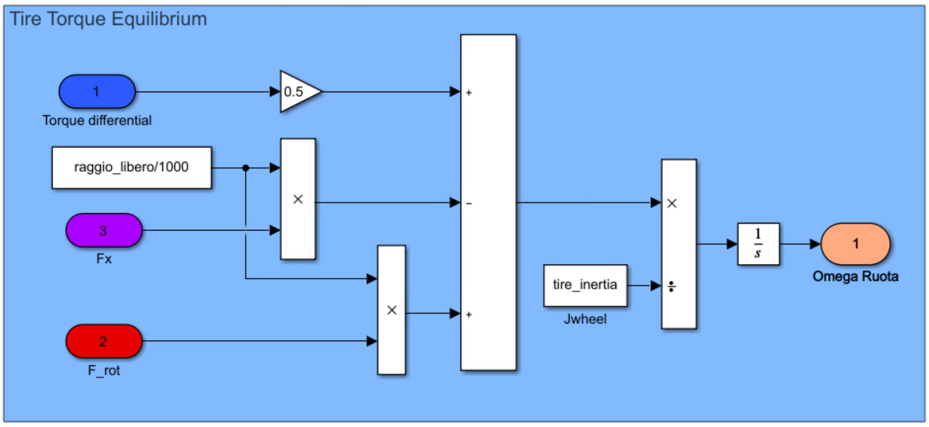

Figure 3.20: *Wheel torque equilibrium*

Integrating the tire angular acceleration, its speed and then the tire slip value can be obtained, being it :

$$\sigma = \frac{\omega\, R\ -\ V}{V} \tag{3.7}$$

Starting from the slip value of the tire, and the normal load given as feedback from the following block, a table of real data is provided to simulate the Pacejka model of the tire, and consequently obtaining the longitudinal loads at the front wheels. The longitudinal force serves as input of the vehicle model and is inserted in the vehicle longitudinal force equilibrium, to compute the vehicle acceleration.

$$F_x\ -\ F_{aer}\ -\ F_{roll}\ = m\, a \tag{3.8}$$

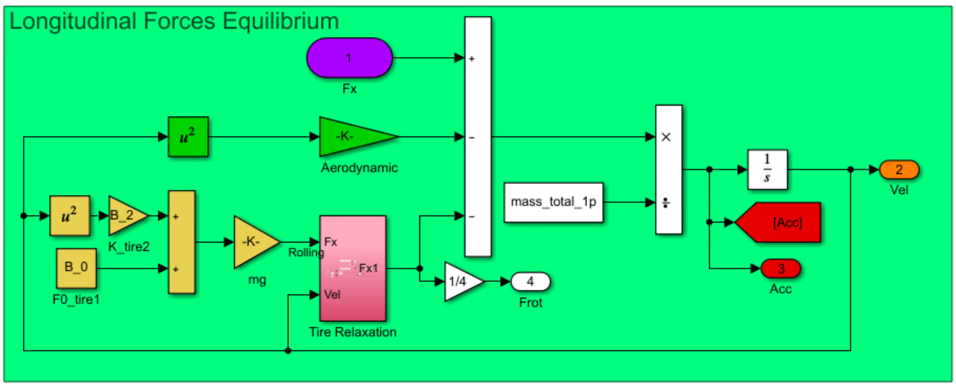

Figure 3.21: *Longitudinal forces equilibrium*

The acceleration value will be used to compute the vehicle vertical load transfer, and to obtain the front and rear wheels normal loads.

$$N_{front} = m\, g\, \frac{b}{l} \; - \; m\, a_x\, \frac{h}{l} \tag{3.9}$$

$$N_{rear} = m\, g\, \frac{a}{l} \; - \; m\, a_x\, \frac{h}{l} \tag{3.10}$$

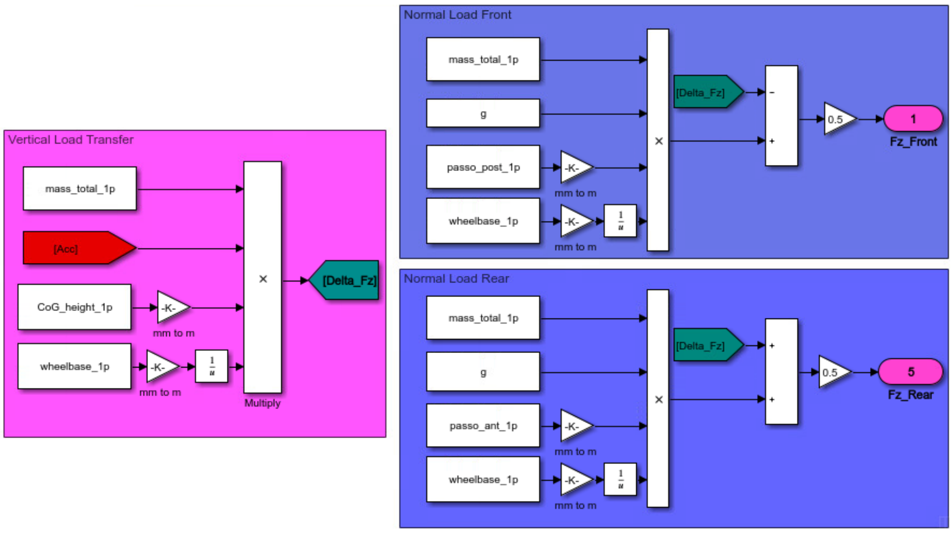

Figure 3.22: *Normal loads computation*

3.2 Driving modes simulations

The updated driveline model, with the aid of a supporting MATLAB code for the creation of the manoeuvres, is effectively able to simulate all the driving modes explained in the previous chapter. All the manoeuvres were simulated, and results confirm the updated driveline to be a satisfactory representation of a real vehicle behaviour.

3.2.1 Pure thermal drive mode

A pure thermal engine drive mode can be simulated, and here is reported the conventional mode of operation of a DCT, with the torque path alternatively going through the even and the odd side of the transmission. It can be verified the torque curve to be smooth and without irregularities

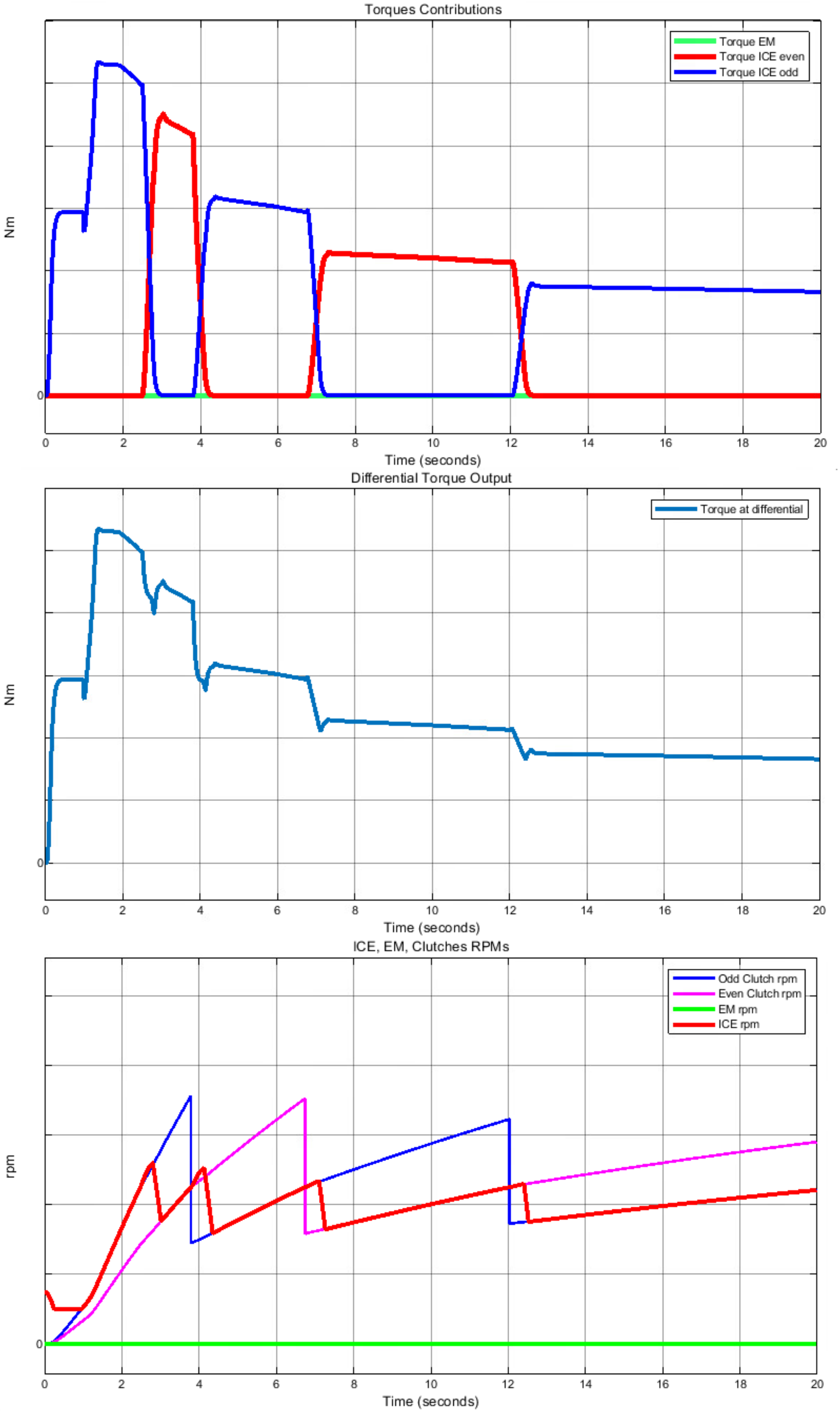

Figure 3.23: *Pure thermal drive manoeuvre*

3.2.2 Pure electric drive mode

In the same way, the engine can be kept shut down, and a pure electric drive mode can be simulated, with all the driving torque coming from the electric motor and without any clutches activity.

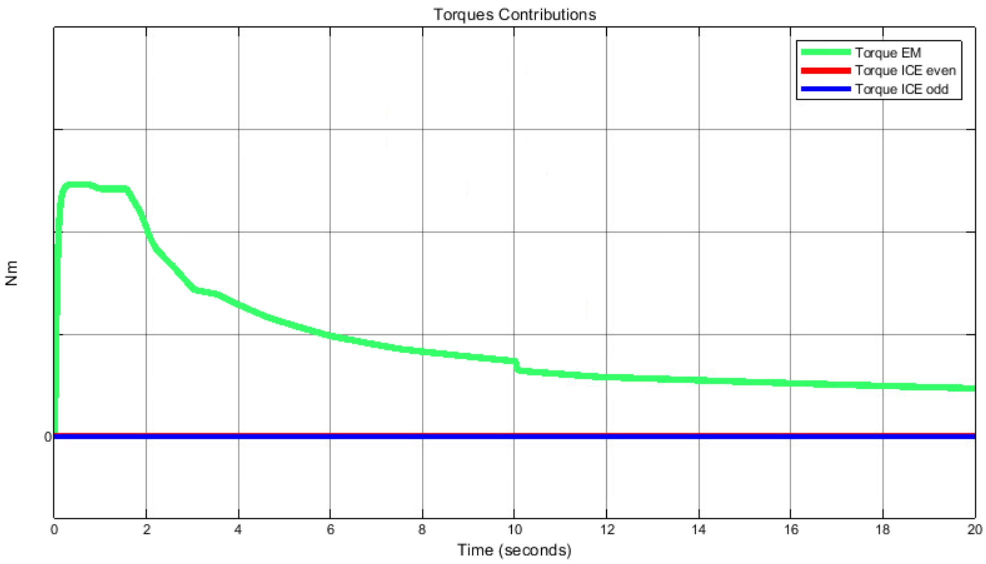

Figure 3.24: *Pure electric drive manoeuvre*

3.2.3 Hybrid drive modes

For what concerns the mixed operation of the driveline power sources, different driving modes are separated in different manoeuvres and can be simulated by the Simulink model.

Overboost manoeuvre

Firstly, an overboost manoeuvre can be performed, to simulate a high load requirement situation, where the main source of power will be the ICE, and the EM is giving a surplus of power to reach higher performances. The two machines work in their maximum capability, providing us with an overview of the potentiality of the propulsion system. This manoeuvre is particularly critical for the tire slip, for this reason the traction controller is calibrated in this condition.

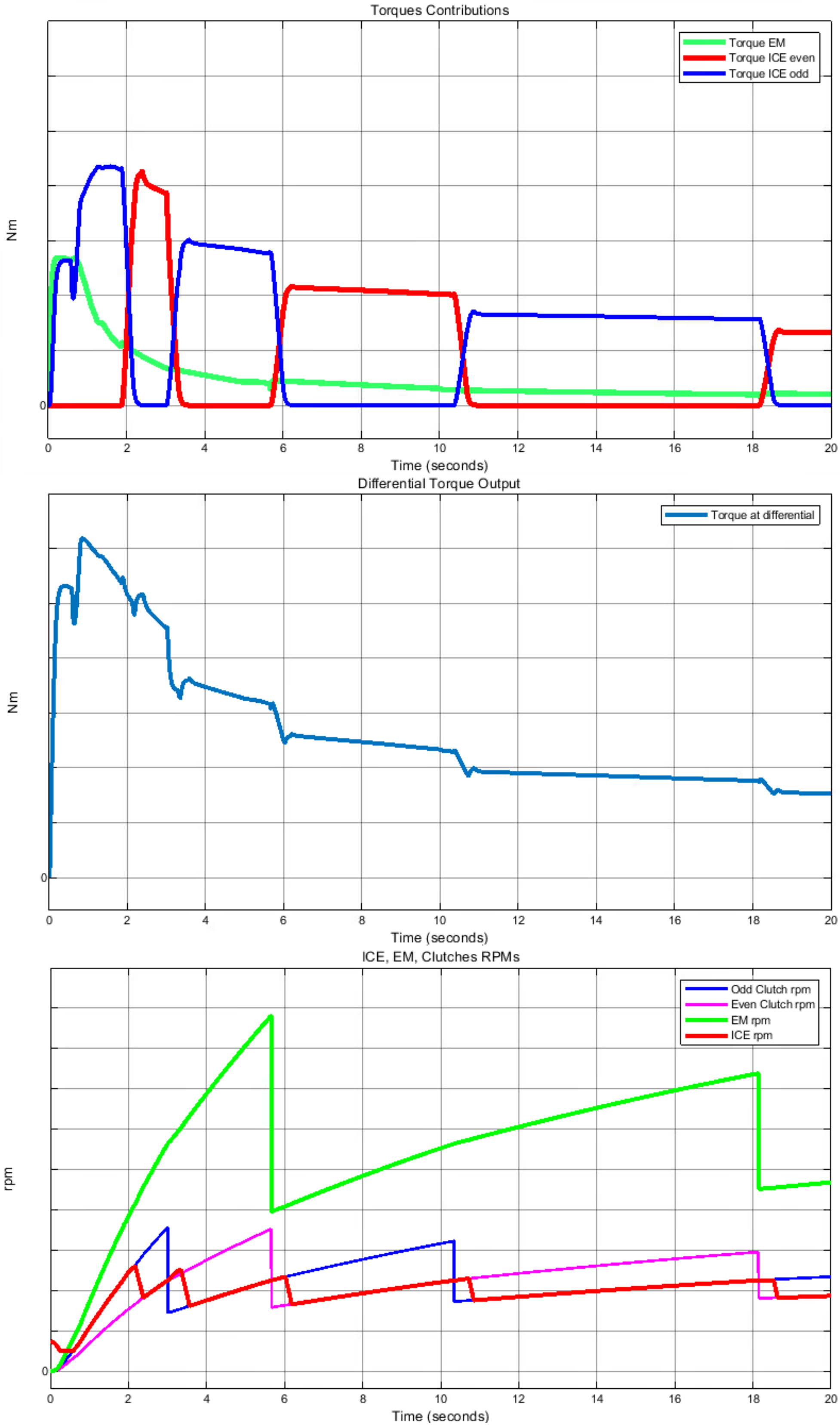

Figure 3.25: *Overboost manoeuvre*

Compensation control manoeuvre

We can simulate and verify the action of the torque controller studying a compensation manoeuvre, where we want the main power source to be the electric motor while the ICE covers the energy missing from the target.

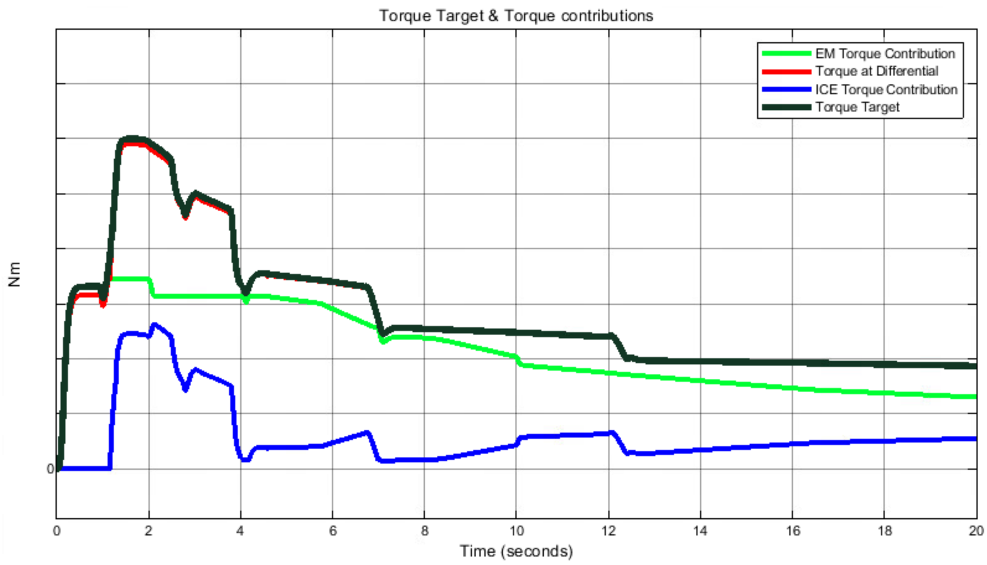

Figure 3.26: *Compensation control manoeuvre*

Maximum torque control manoeuvre

The compensation manoeuvre can also be performed activating the maximum torque controller. We can see how the main target of the control is not to exceed the torque limit at the gearbox input; when that limit is not an issue, then the controlling action has the purpose of following the curve of the target torque at the differential input.

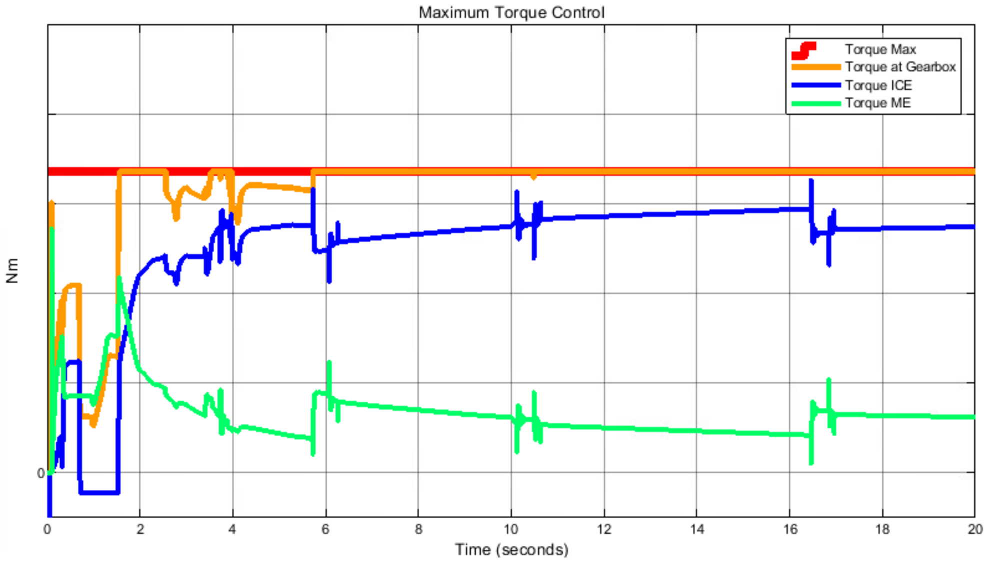

Figure 3.27: *Maximum torque control manoeuvre*

Thermal engine clutch-start manoeuvre

The last mixed power drive mode that can be simulated and analysed is a situation in which we start the manoeuvre in a simple pure electric driving mode, and later the engine is started with a power transfer from the EM, to continue the simulation in a hybrid drive. This condition permits to evaluate the impact of the clutch-ignition of the engine on the vehicle dynamics.

The power transfer to switch on the engine can be done both using the even side or the odd side of the transmission, depending on the gear with which we want to start the engine. A lower gear means lower time needed to synchronize the engine rpm with the clutch, but it also implies a higher transmission ratio, meaning a higher delta of torque, that could be a problem for the comfort perception.

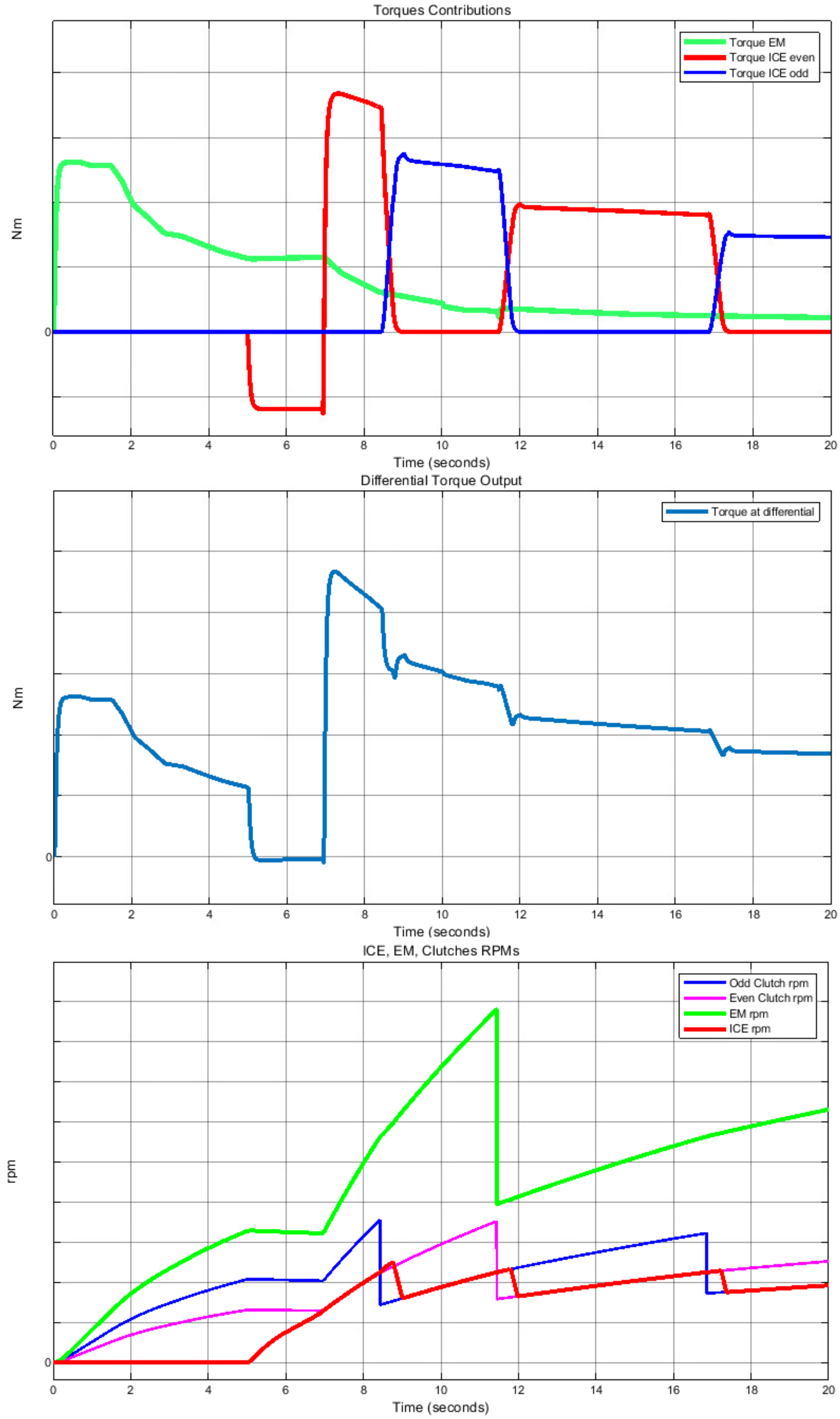

Figure 3.28: *Engine clutch-start manoeuvre*

3.2.4 Regenerative braking

The electric motor can work as a generator too, and a braking manoeuvre with battery recharge can be simulated. In the previously used model it was possible only to select the gear that had to be maintained for the whole duration of the manoeuvre, probably in the perspective of a short-term manoeuvre. From a more general point of view, this was particularly impractical, because a gear too high causes a less efficient braking, and also dangerous, because, with a gear too low, too high motor rpm could be reached. The possible benefits of the newly built controller for this manoeuvre are later going to be analysed.

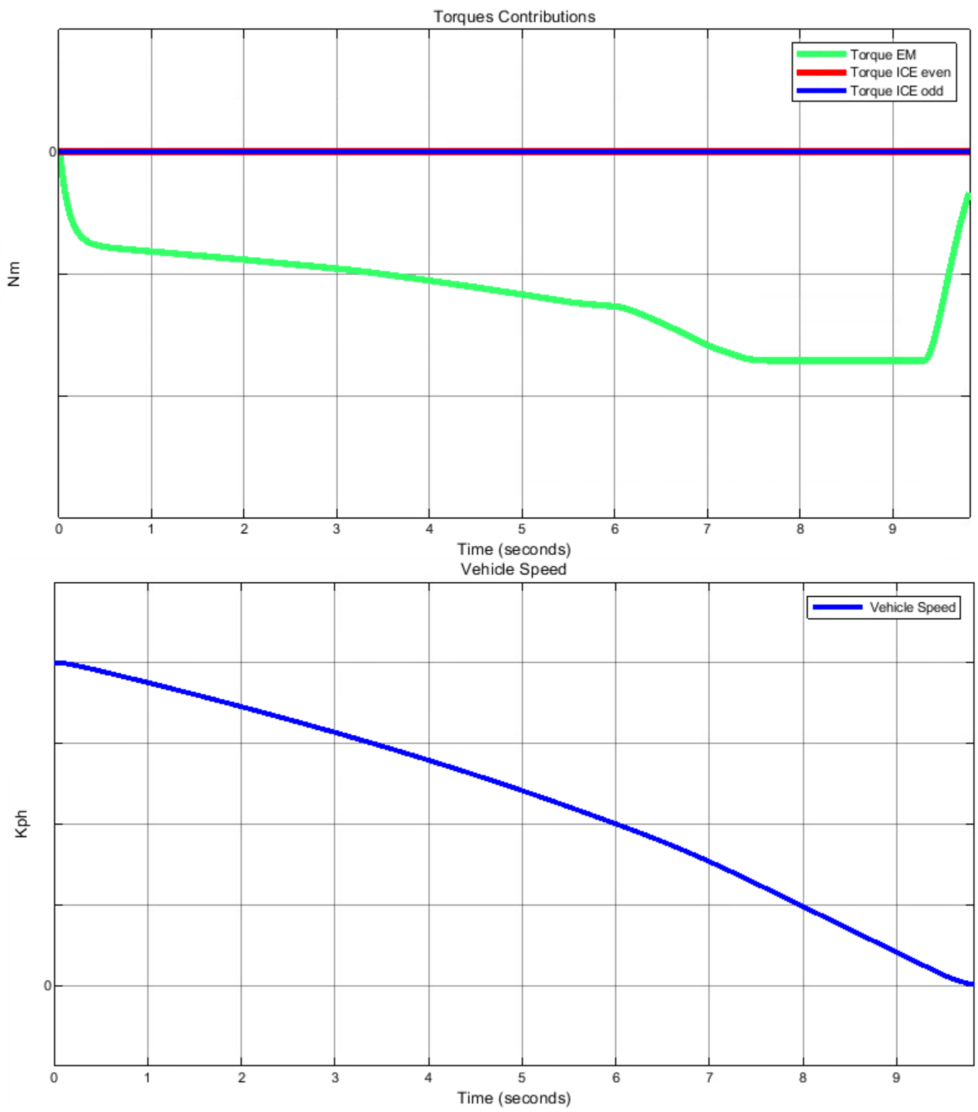

Figure 3.29: *Regenerative braking manoeuvre*

3.3 New model features analysis

The new features supplemented to the initial driveline model give access to additional manoeuvres simulation possibilities, so that their impact can be analysed.

3.3.1 Hybrid drive modes with the electric motor on odd gear

With the described modifications, it is possible to perform the mixed driving modes with the electric motor engaging the odd gears, so practically with the two machines always on the same gear. Let us see the results of this type of manoeuvres, and the impact obtained on torque contributions and on the vehicle dynamics.

Overboost manoeuvre

As seen in section 3.2, this is a manoeuvre at torque values close to those of WOT, where the maximum performance of the driveline is evaluated.
Firstly, we can underline the new functioning of the DCT, with the even clutch closing when the odd gear is selected for the EM.

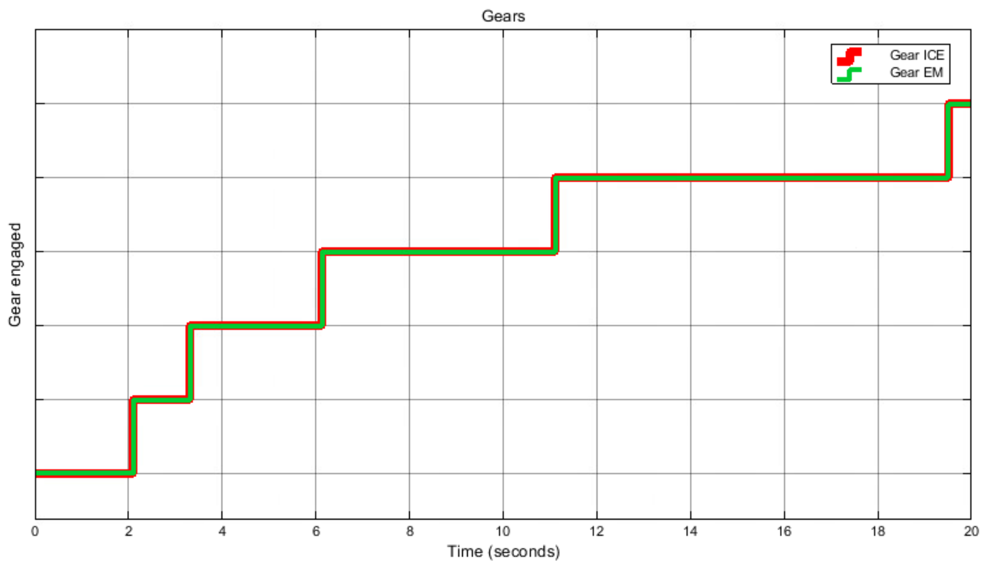

Figure 3.30: *New possible gear selection*

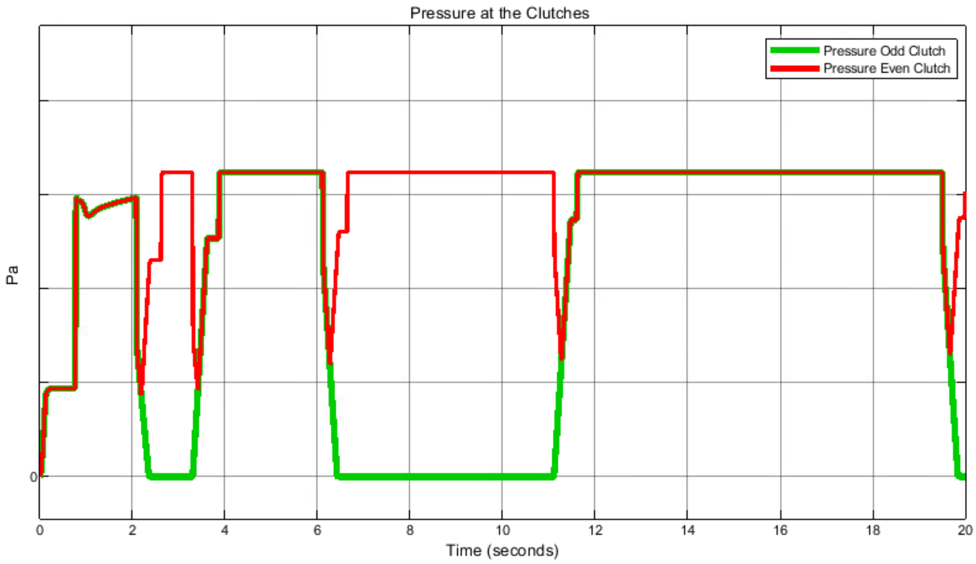

Figure 3.31: *New pressures path related to the new gear selection*

The new torque at the differential, its contributions from the two machines, and their division in the two sides of the transmission, can be assessed in the figures below.

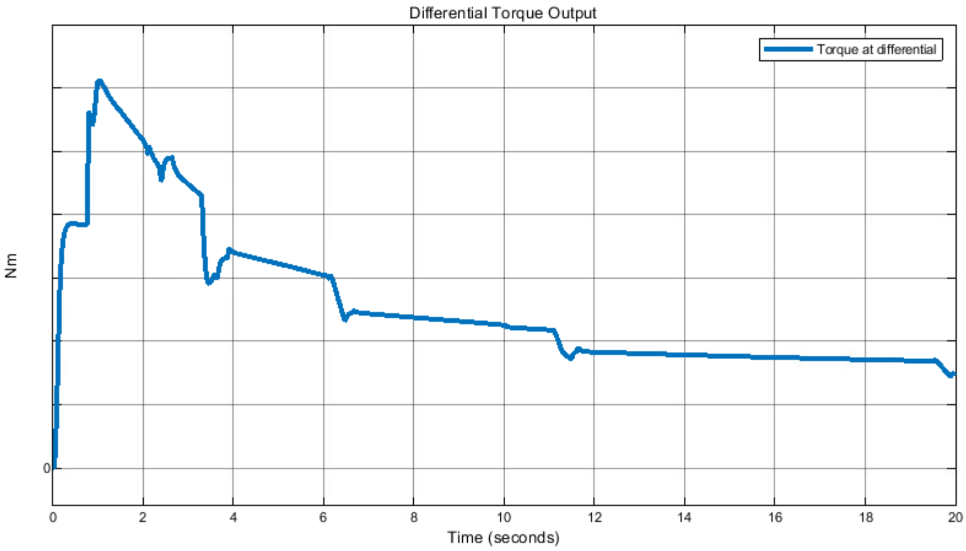

Figure 3.32: *New overboost manoeuvre torque at the differential*

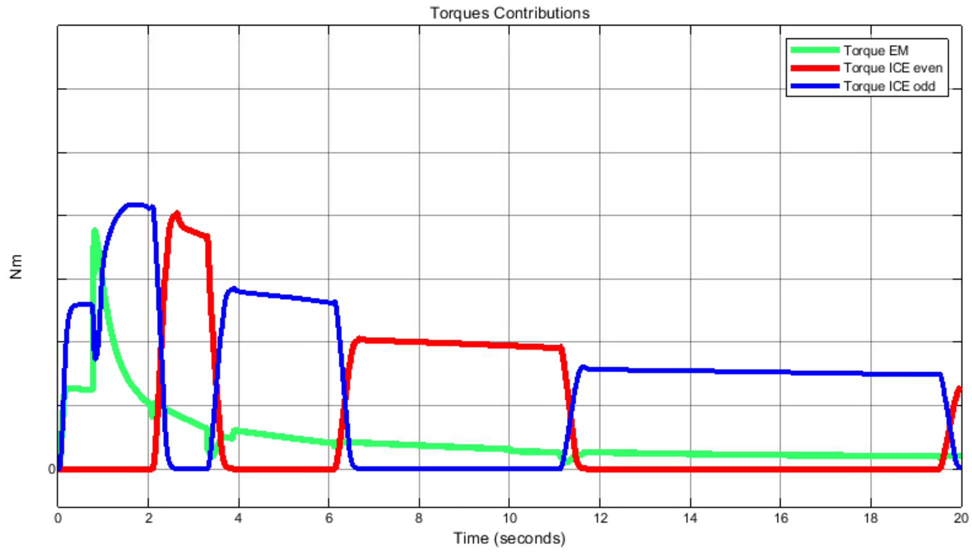

Figure 3.33: *New overboost manoeuvre torque contributions*

After some analysis, it was noted how the losses due to the electric motor power passing through the clutches were particularly relevant in the first phases of the simulation, especially when starting from standstill. This is due to the fact that the clutch pressure at the start, where the electric motor torque is at its highest, is heavily cut at a lower level than the maximum, both by the traction control and by the DCT phase for the synchronization of the engine rpm to the clutch rpm. As explained in section 3.1.2, the electric motor torque lost will be proportional to the clutch pressure cut from its maximum value.

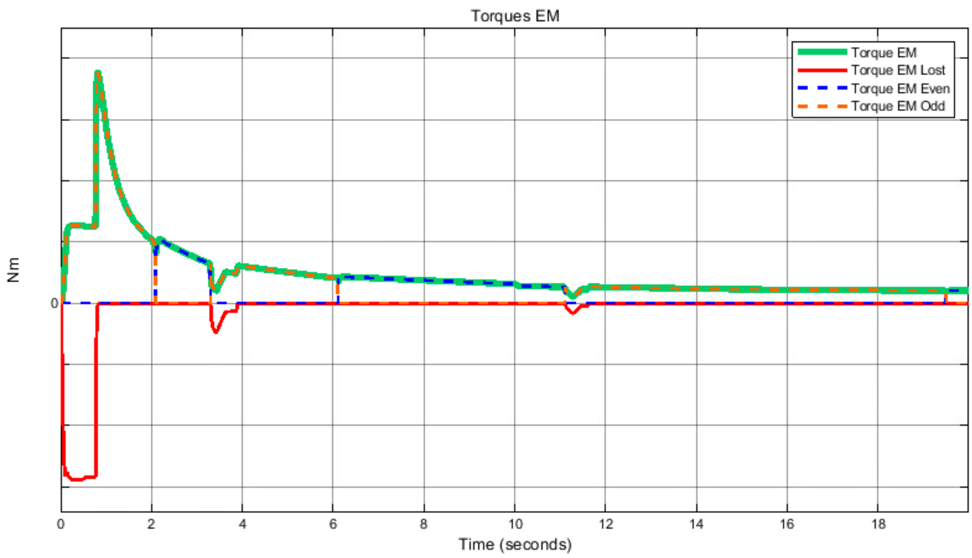

Figure 3.34: *Electric motor torque division and losses*

At the beginning of the manoeuvre, at low speed and high load, it is crucial to have high levels of torque, meaning that a so relevant cut would be inconvenient.
For this reason, for high values of throttle, a controlling action is introduced in the gear shifter block that determines, for this particular manoeuvre, to have the electric motor starting with an even gear. In this way, the first pressure cut, that is the most relevant due to the synchronization time, is avoided, and a more performing start can be obtained.

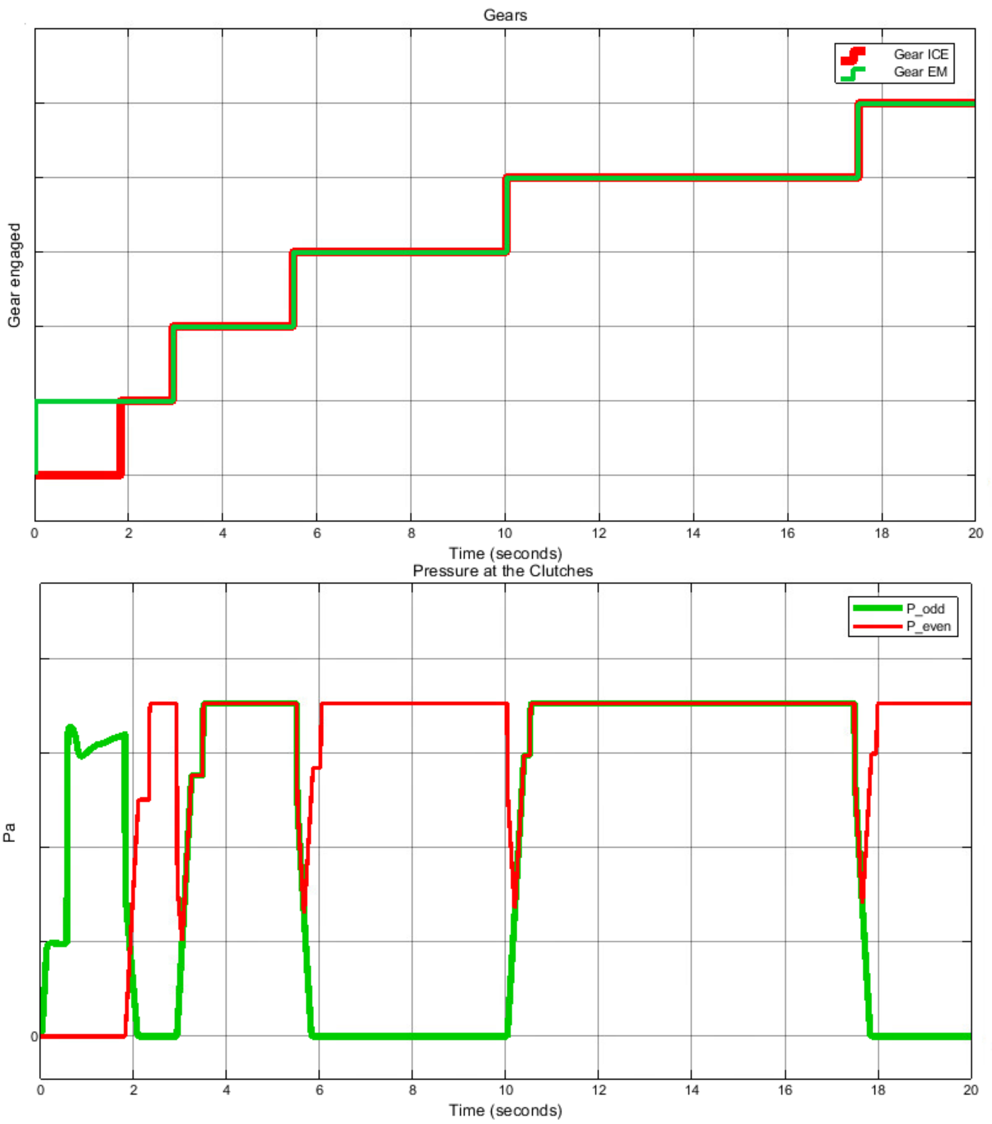

Figure 3.35: *New gear selection and pressure path imposed*

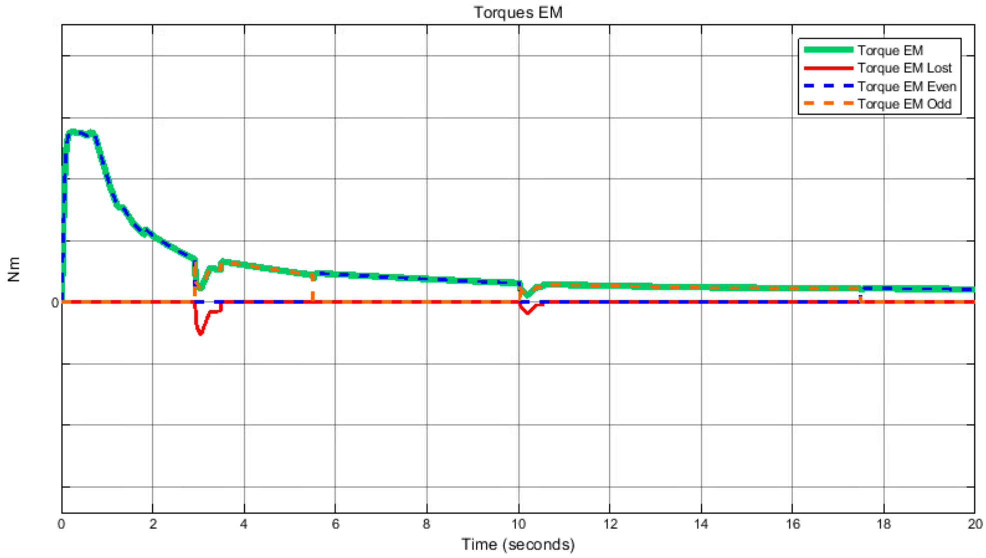

Figure 3.36: *New electric motor torque losses*

Of course, the possibility of using the first gear for the electric motor would be beneficial in terms of peak torque at the start, but this advantage is almost completely compromised by the pressure path of the clutch, so that the new gear selection is preferred for the advantage in terms of energy efficiency.
Confronting the results with the one obtained performing the same manoeuvre with the EM working only in the even side, showed in Figure 3.25, it can be seen how, in general, the torque values arriving at the differential are comparable, even with the torque loss, and how a smooth gear change is still guaranteed, without any additional detrimental impact on the vehicle dynamics.
Using odd gears for the electric motor also has a relevant influence on its rotational speed in this demanding type of manoeuvre, since with more frequent gear changes it can be avoided to reach too high and dangerous rpms values.

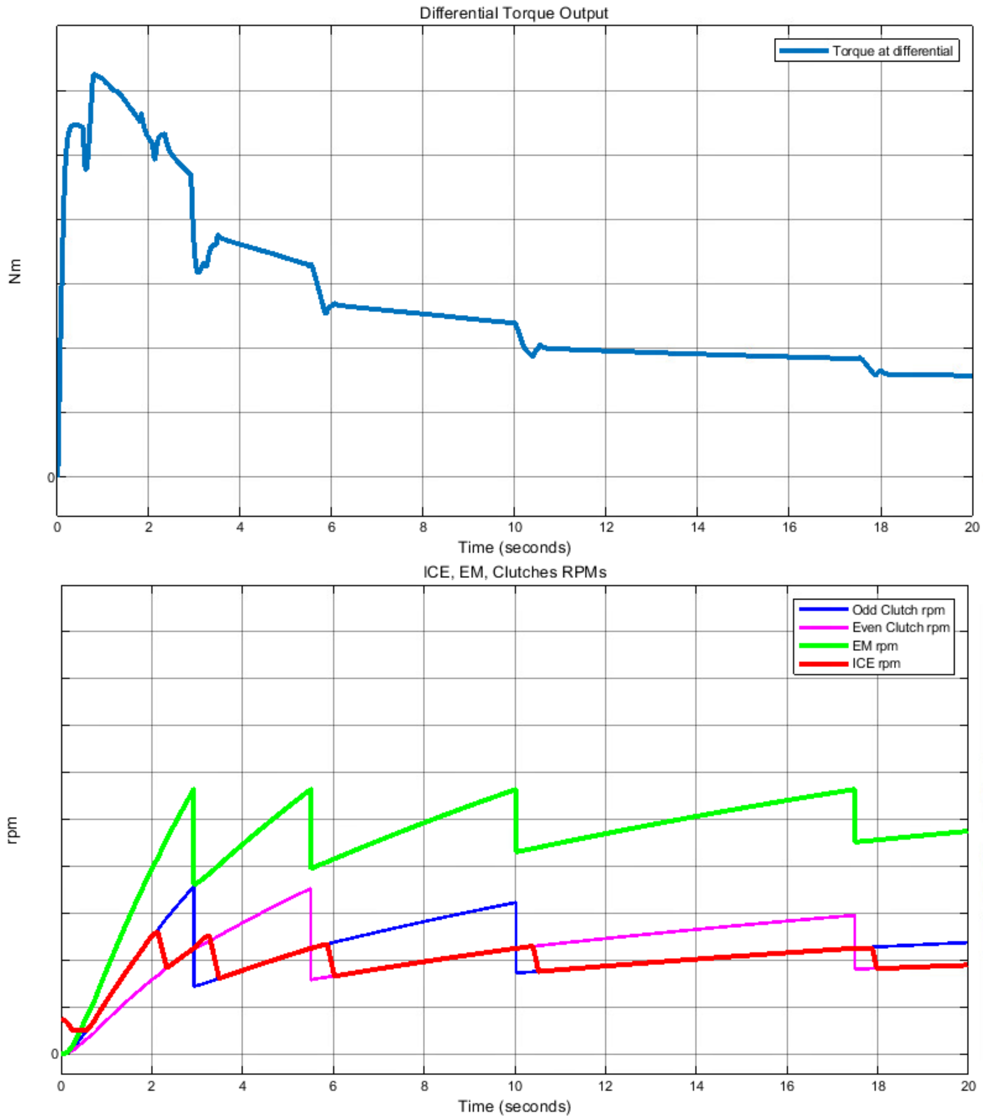

Figure 3.37: *Overboost manoeuvre new results*

Compensation control manoeuvre

Again, a mix mode manoeuvre can be developed, now with the electric motor using also the odd gears. In this type of simulation our goal is to use as less as possible the thermal engine power to reach the target torque, so again we would like to avoid high losses of electric power.

From the simulations performed, the results are found to be consistent with what expected, with the torque target curve that is followed as good as it was in the twin manoeuvre.

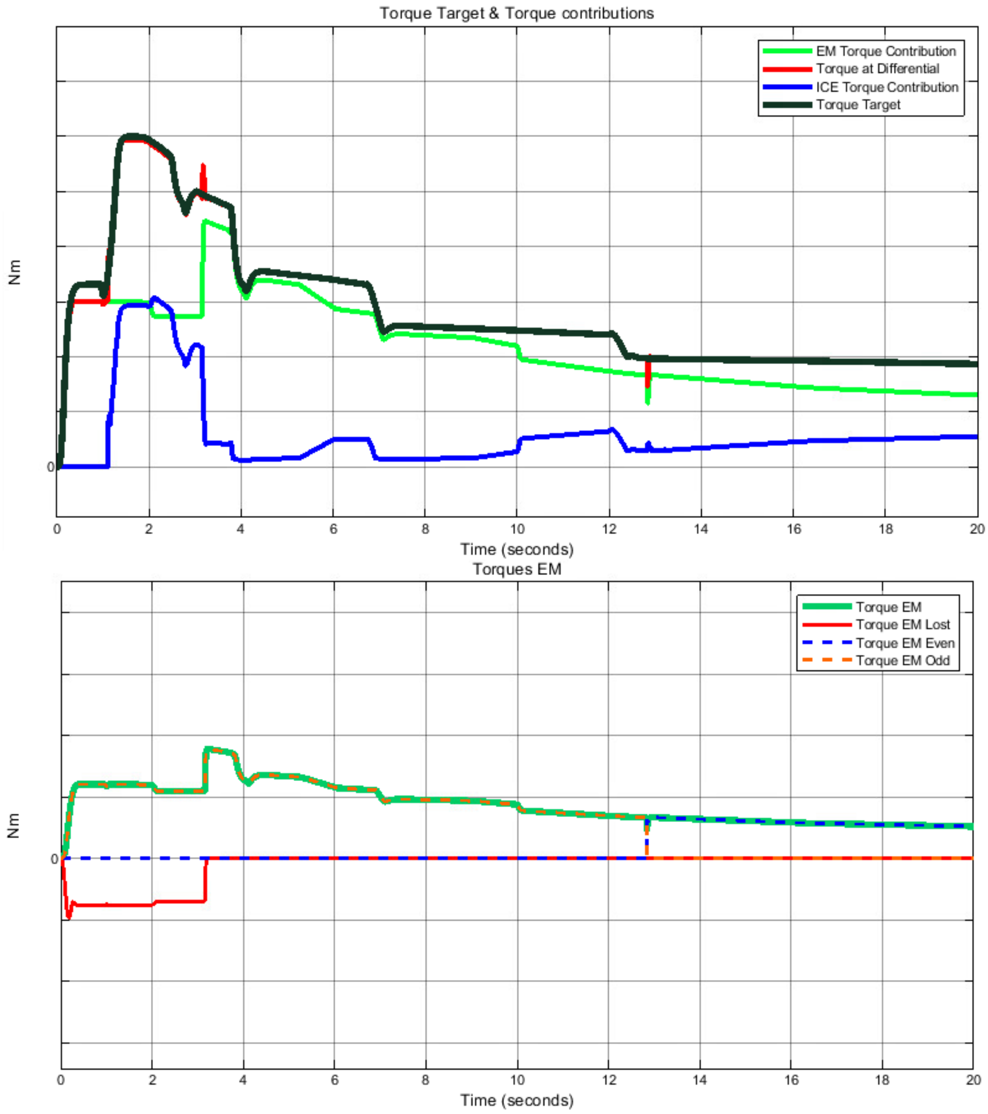

Figure 3.38: *New compensation control manoeuvre*

For the same reasons explained before it is not advisable to start from standstill with an odd gear. However, observing the simulation results, despite the loss in the initial phase, we can see how beneficial can be to have the possibility to engage the odd gears. The previously set manoeuvre was bound to have only even gears for the EM and to start the simulation with the ICE on the same even gear. Using an odd gear lower than the one we used in the only even gears manoeuvre (e.g. 3rd gear instead of 4th), if still consistent with the vehicle speed, can ensure higher torque levels, due to the higher transmission ratio. This results in less ICE usage in the phases successive to the start, and also lower ICE throttle in the initial phase since it uses a lower gear too.

Results comparison can be done with Figure 3.17, where the same manoeuvre is performed with the 4th gear.

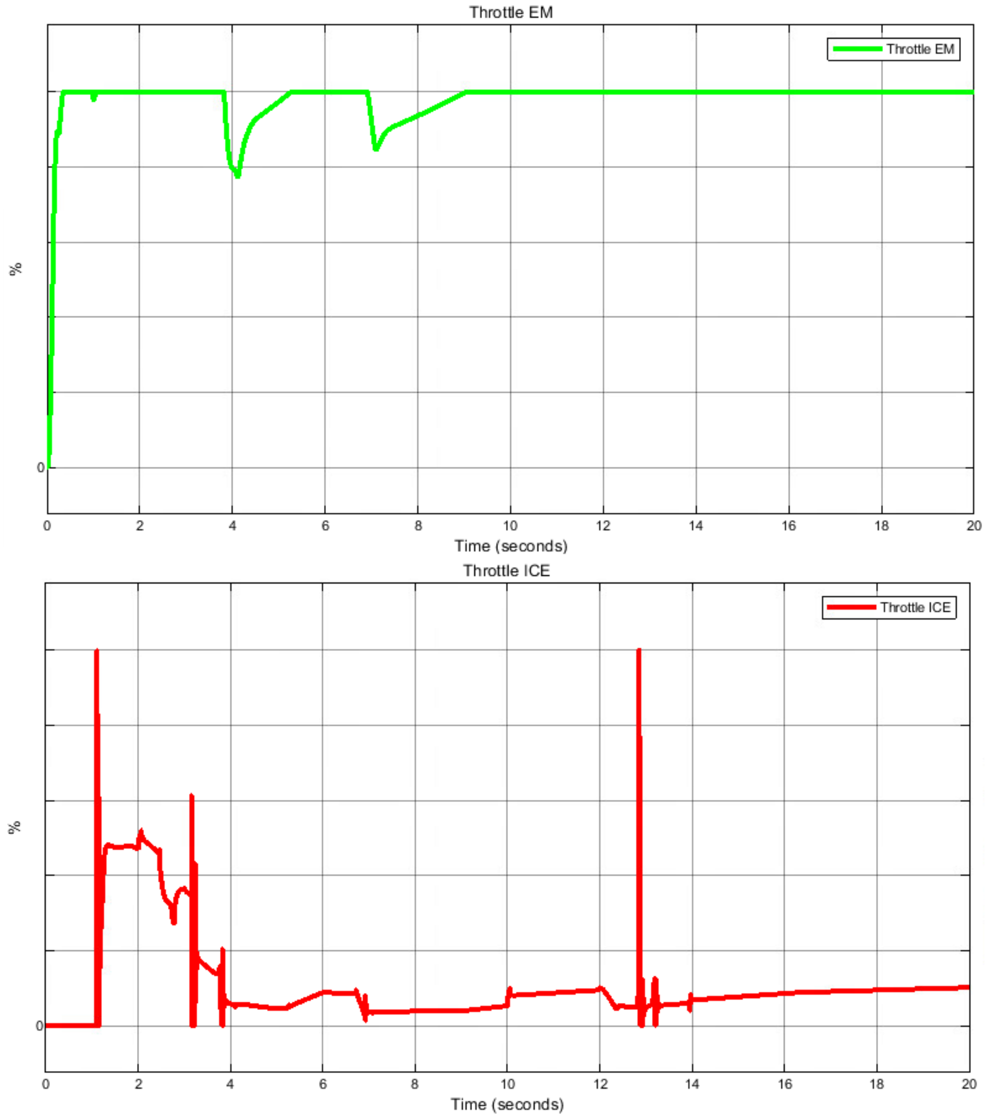

Figure 3.39: *Compensation manoeuvre new throttle control*

Maximum torque control manoeuvre

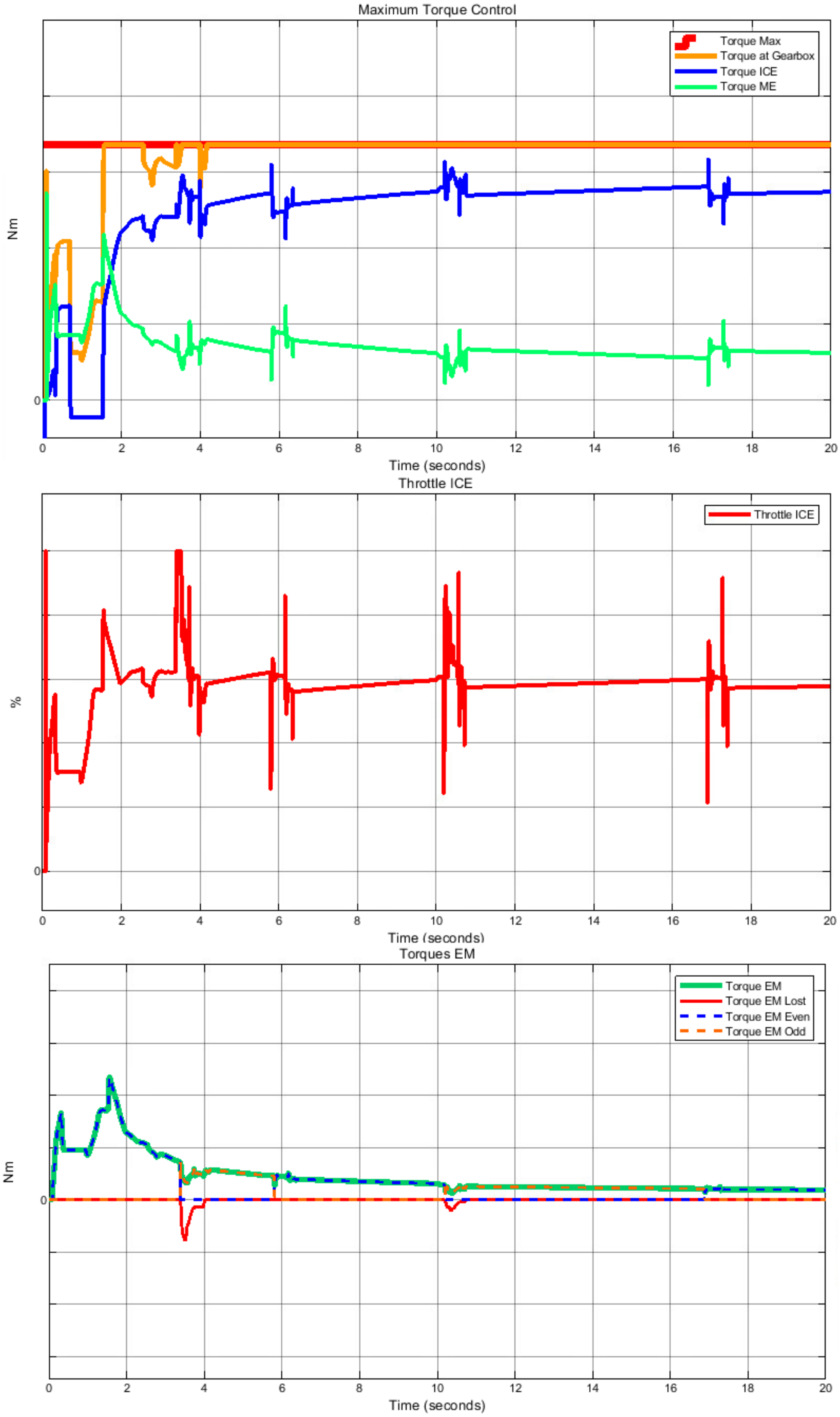

Figure 3.40: *New maximum torque control manoeuvre*

Similar considerations can be made about the maximum torque control manoeuvre. The results show a good capability of the driveline model to maintain the torque at the gearbox input below the maximum permissible value, and again the possibility of using odd gears for the EM introduces some losses during the engagement, but also a higher production of electric motor torque in the odd gear phases of the manoeuvre.

3.3.2 Regenerative braking with gear changes

Two new features were introduced to enhance the regenerative braking manoeuvre: the possibility to shift the gear during braking, and the possibility to use odd gears when performing it. Three braking manoeuvres scenarios are going to be analysed to evaluate the effects of the modifications, considering starting braking at high speed, at medium speed, and at low speed. The same simulation is performed with the fixed gear, with the downshift of the even gears, and with the use also of the odd gears.
All the simulations performed were made until vehicle stop, with 60% of the kinetic energy recovered, and no braking system action. Being the starting and the final velocities the same for the three types of manoeuvres, the kinetic energy recovered is fixed; what differs is the time in which it is recovered, so the braking efficiency, the deceleration dynamics, and the motor rotational speed during simulation.
Before starting, it is important to underline that in this driveline model a gear is always selected, there is almost no time considered for the gear change, so that no torque cut is present in the gear selection. This results in an overestimation of the possibilities of gear downshifting, especially when staying on the even side of the transmission: in this latter scenario, to change the gear a relevant torque interruption would be needed, which is not considered in the model. Instead, when using the odd gears, both sides of the transmission and the gear pre-selection possibility could be exploited, meaning that the torque hole would be highly reduced, as intended by the DCT logic. This differentiated dynamics cannot be taken into account, while it is evaluated the impact of having a wider selection of gear ratios. When using the odd side of the transmission, it is considered a rapid torque cut in the passage from even to odd gear, for the logic explained in section 3.1.2, since, when downshifting, the pressures on the two clutches are set to increase almost instantaneously from zero to

their maximum value, that again is not very representative of the real behaviour of the DCT.

In a high-speed situation, where a high gear would be selected, we can see how downshifting the gear during the manoeuvre can be really beneficial in terms of stopping time. Times of about 30% lower can be obtained, that means a more effective braking, since we can give a higher negative torque and acceleration in the phases with lower gears.

Moreover, choosing a fixed gear in a high-speed situation, could endanger the system: if we would try to diminish the braking time selecting a low gear from the start, critical values of motor rpm could be obtained.

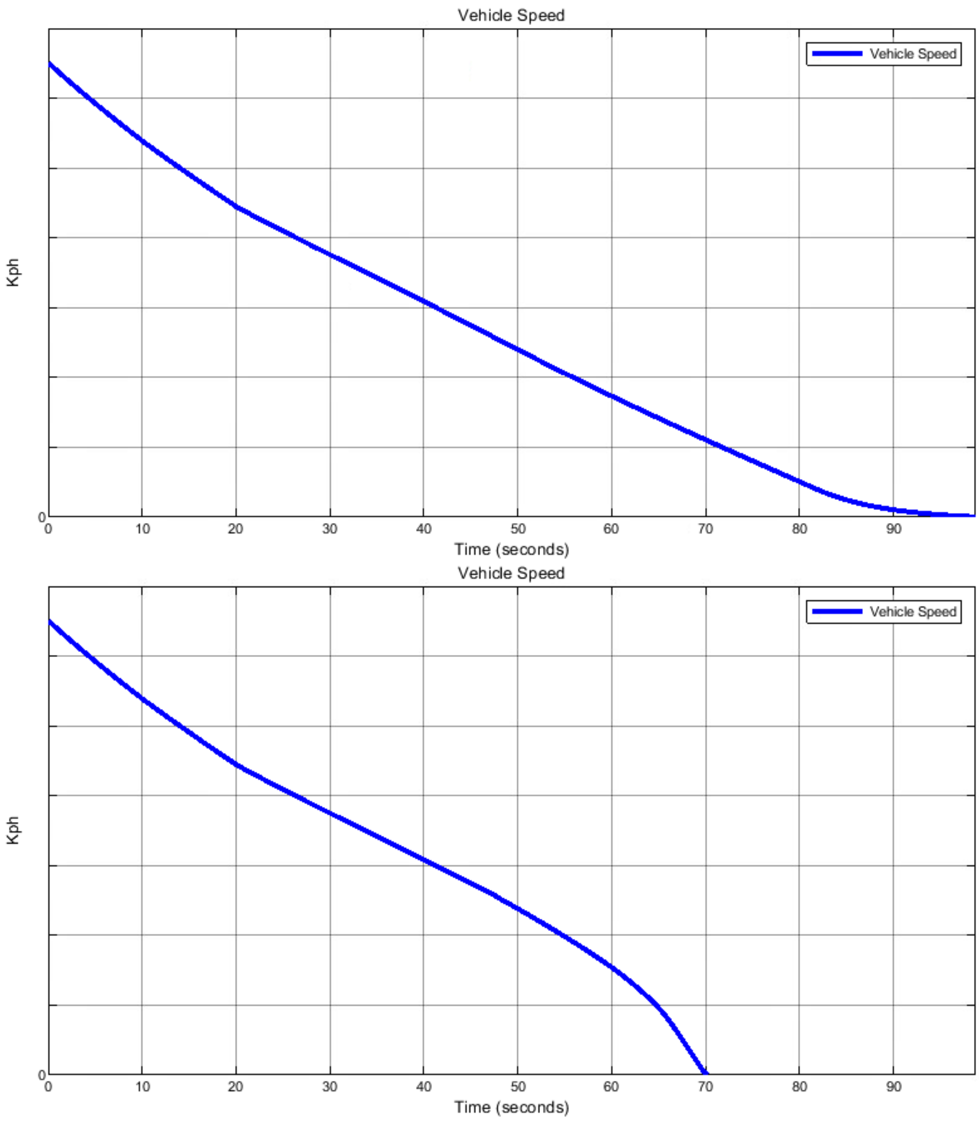

Figure 3.41: *High speed braking manoeuvre; velocity path comparison*

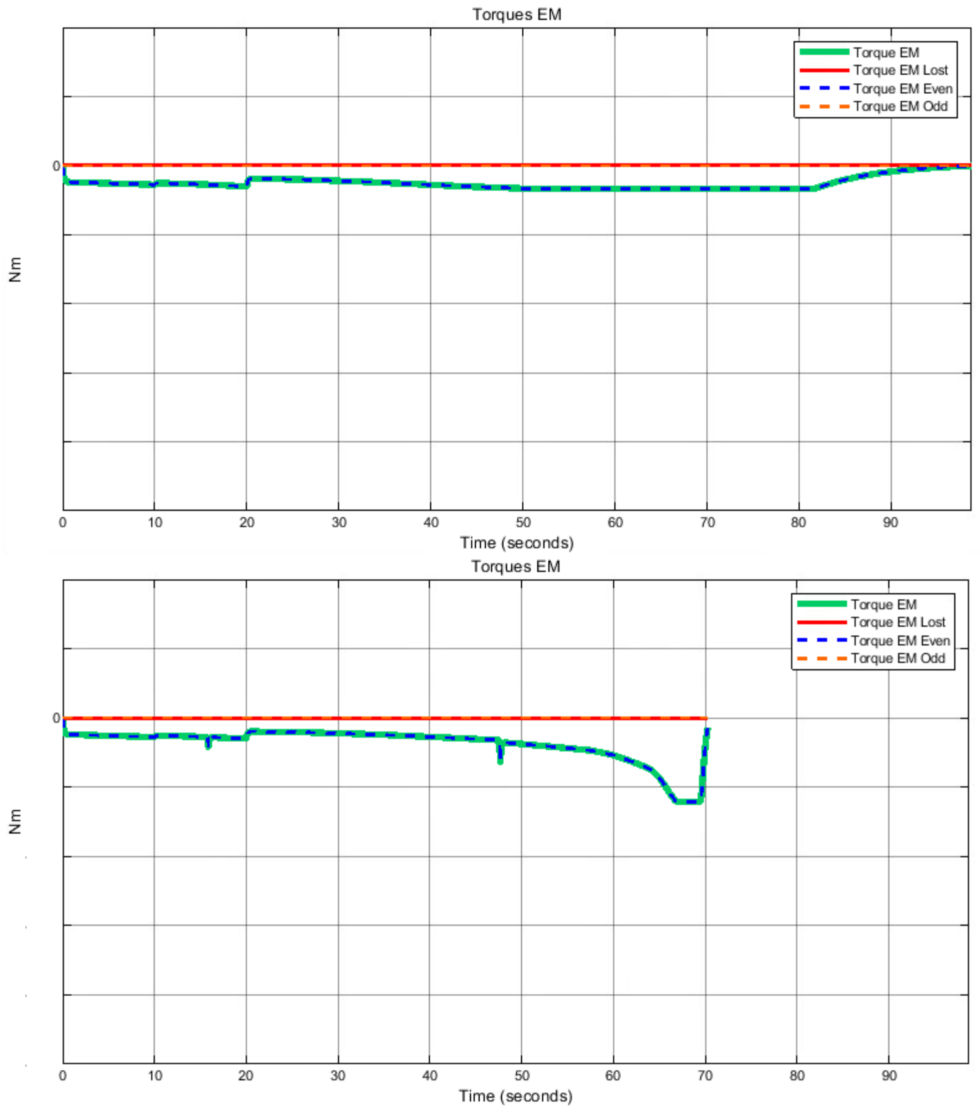

Figure 3.42: *High speed braking manoeuvre; EM torque comparison*

Adding the possibility to use odd gears, would mean to have the more appropriate gear always selected, and for the motor to work in a quite constant range of rpm, with the addition of intermediate gear ratios, and so possible higher level of negative torque. But, with the activation of the clutches, some instantaneous losses in the gear changes are reported, for the previously explained logic. In the end, this results in only slightly lower values of braking times than the previously described manoeuvre, and a less smooth and definite deceleration profile. A more detailed analysis could be done if the real impact of gear selection would be kept into account for both transmission side.

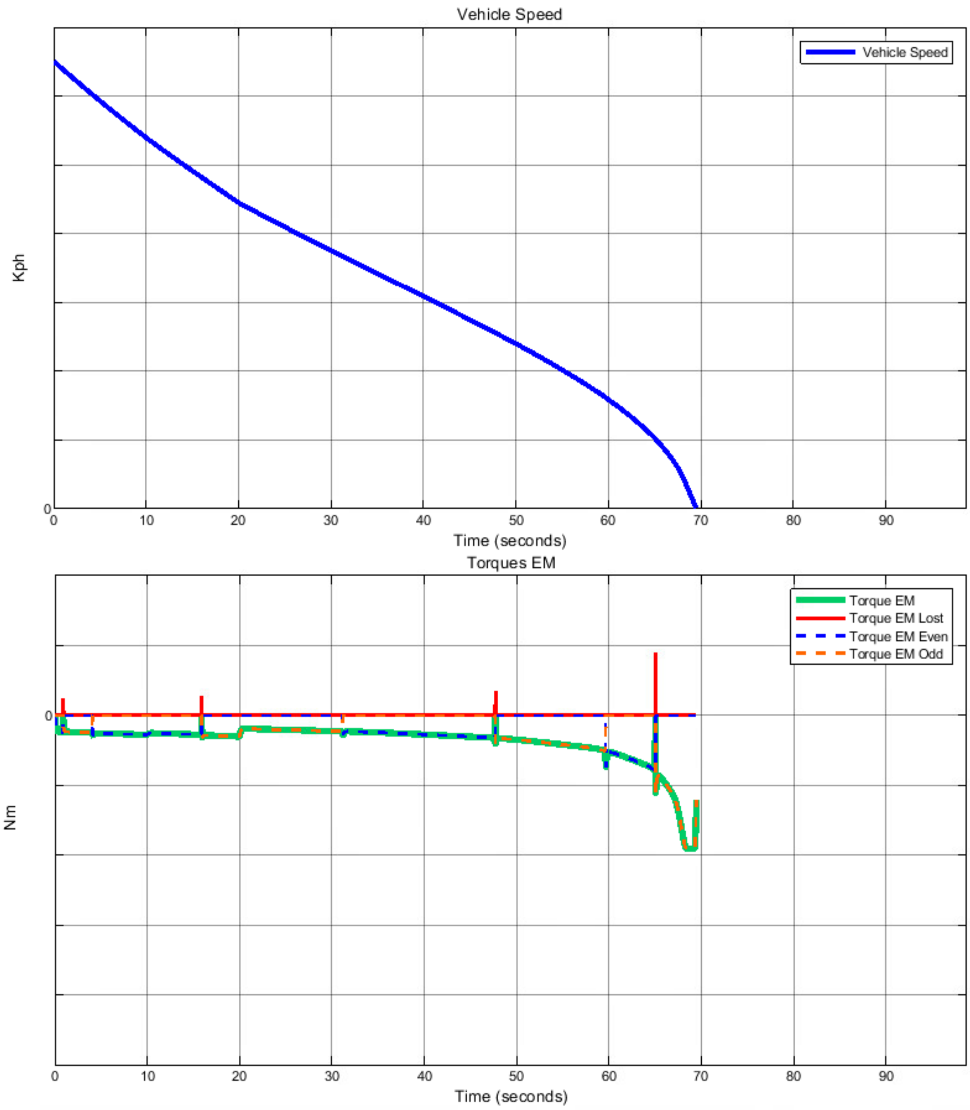

Figure 3.43: *High speed braking manoeuvre using also odd gears*

In a medium-speed situation, starting decelerating with a medium gear, having the possibility to switch it would mean to have a relevant portion of the simulation with the lower gear possible. Obviously, this can give highly lower braking time values and higher decelerations.

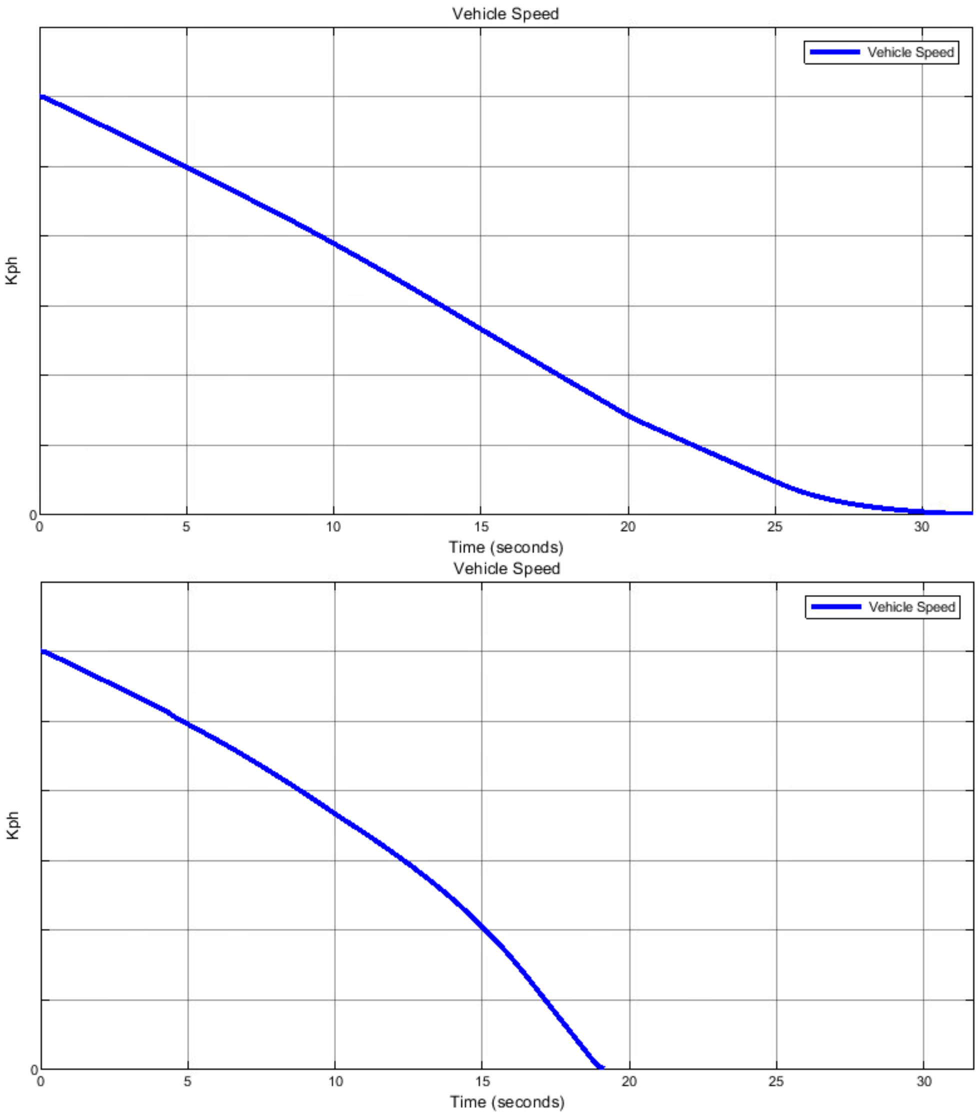

Figure 3.44: *Medium speed braking manoeuvre; velocity path comparison*

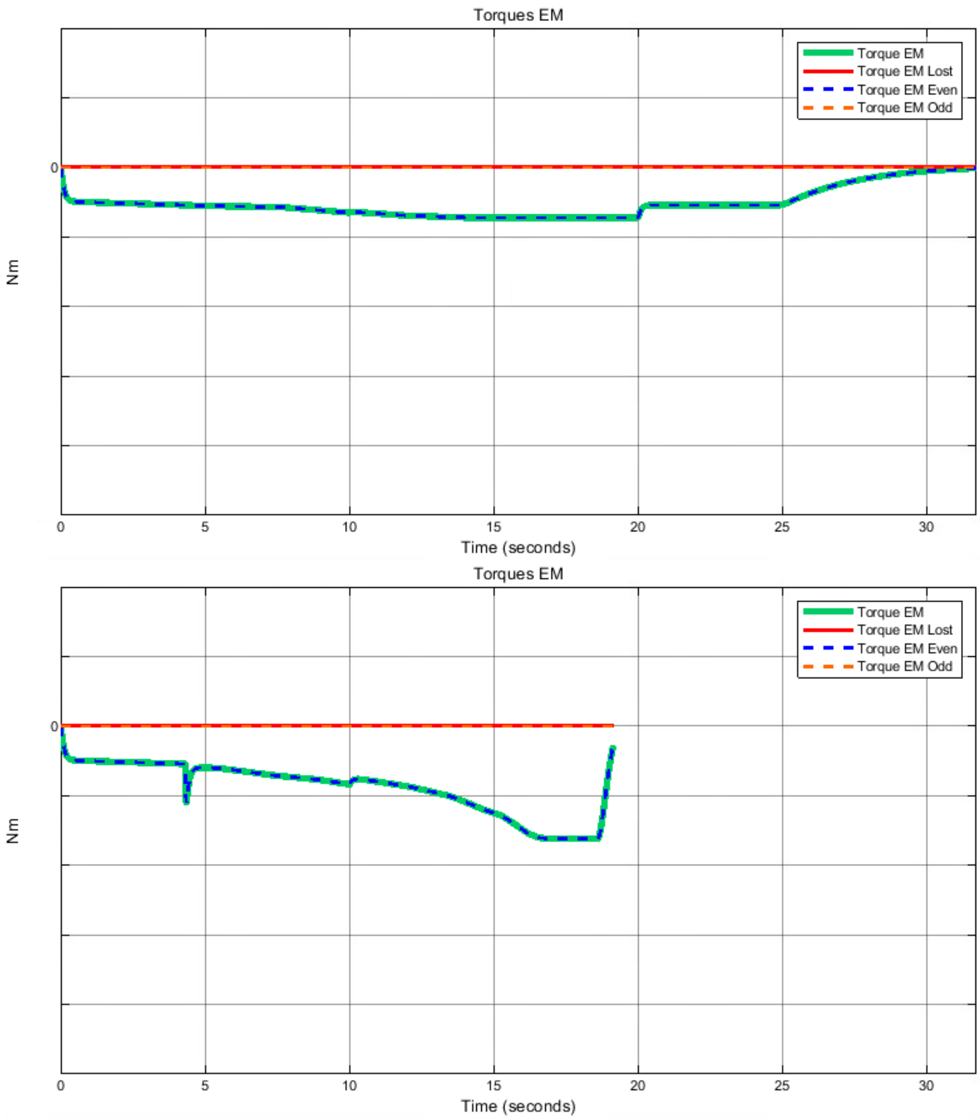

Figure 3.45: *Medium speed braking manoeuvre; EM torque comparison*

The possibility to use odd gears results in similar considerations as before: there is the introduction of losses to be kept into account, that causes a less smooth acceleration profile, but we can have lower and more constant values of rpm and slightly lower values of braking times. Higher peaks of torque and deceleration are reached.

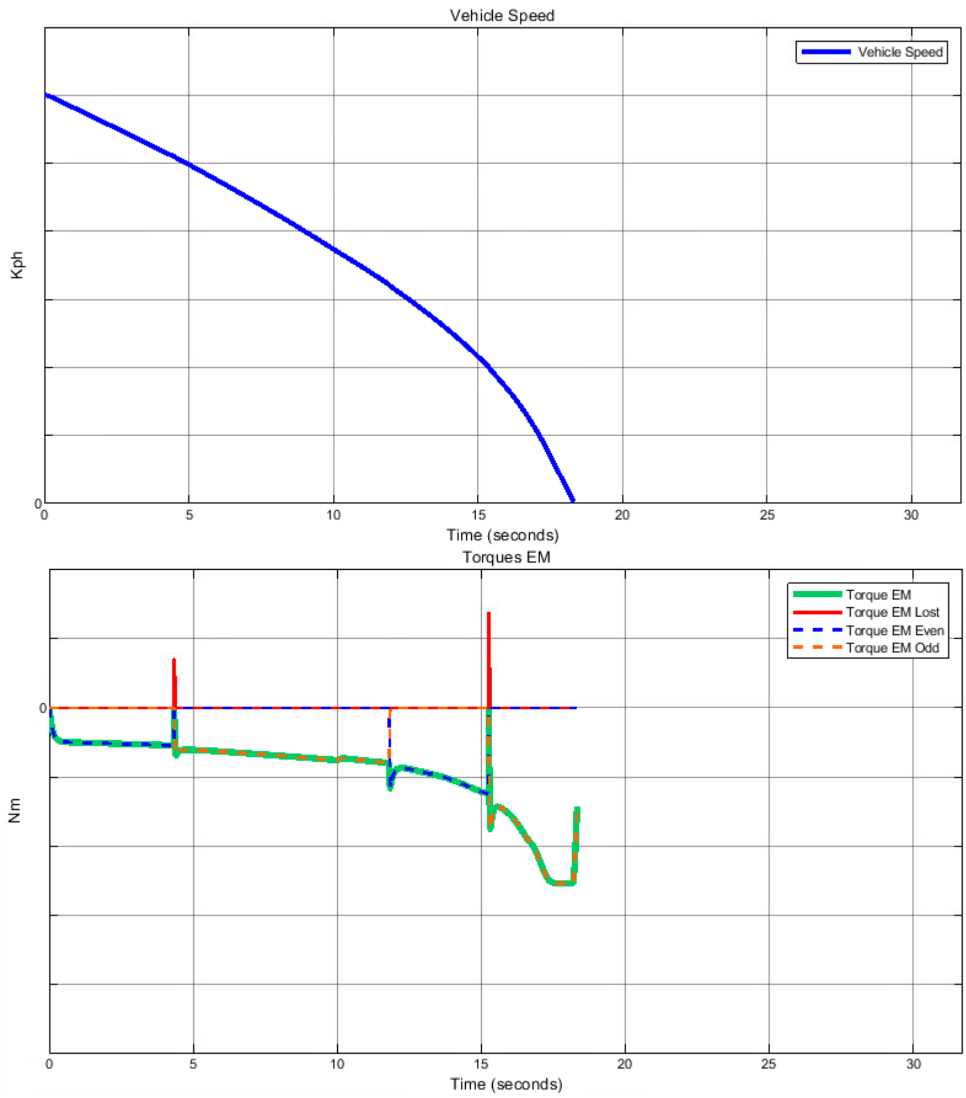

Figure 3.46: *Medium speed braking manoeuvre using also odd gears*

Finally, we can evaluate the impact of the new driveline characteristics in low-speed braking, starting from second gear, so that the downshift can happen only if there is the possibility of closing the clutches and use the odd side.
The possibility to engage the first gear can give a benefit in terms of braking performance, obtaining times of simulation lower of about 15%. The consideration to be made is that a high and rapid drop of acceleration is obtained in the gear change, and with high peak values, that can result in passengers discomfort, even if its magnitude is not so representative of the real dual clutch behaviour.

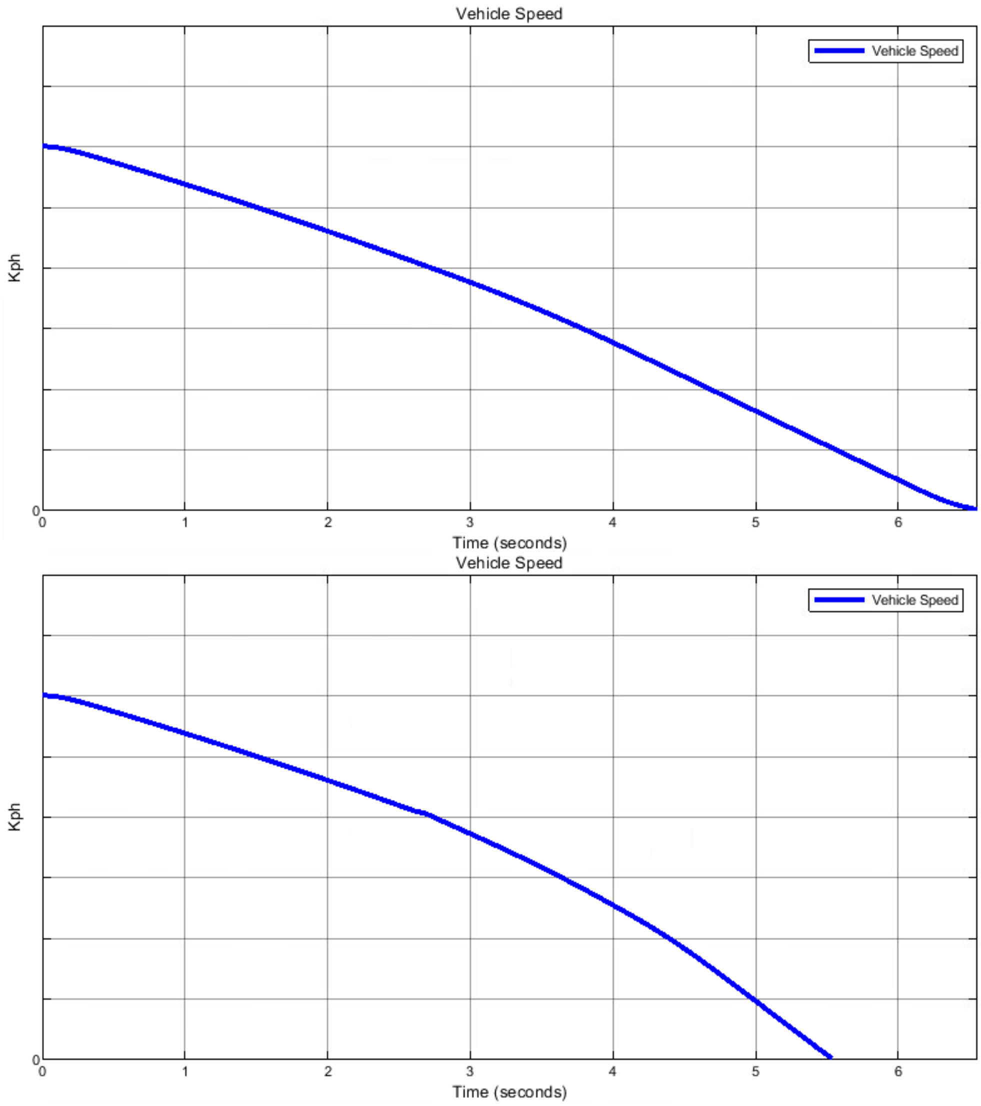

Figure 3.47: *Low speed braking manoeuvre; velocity path comparison*

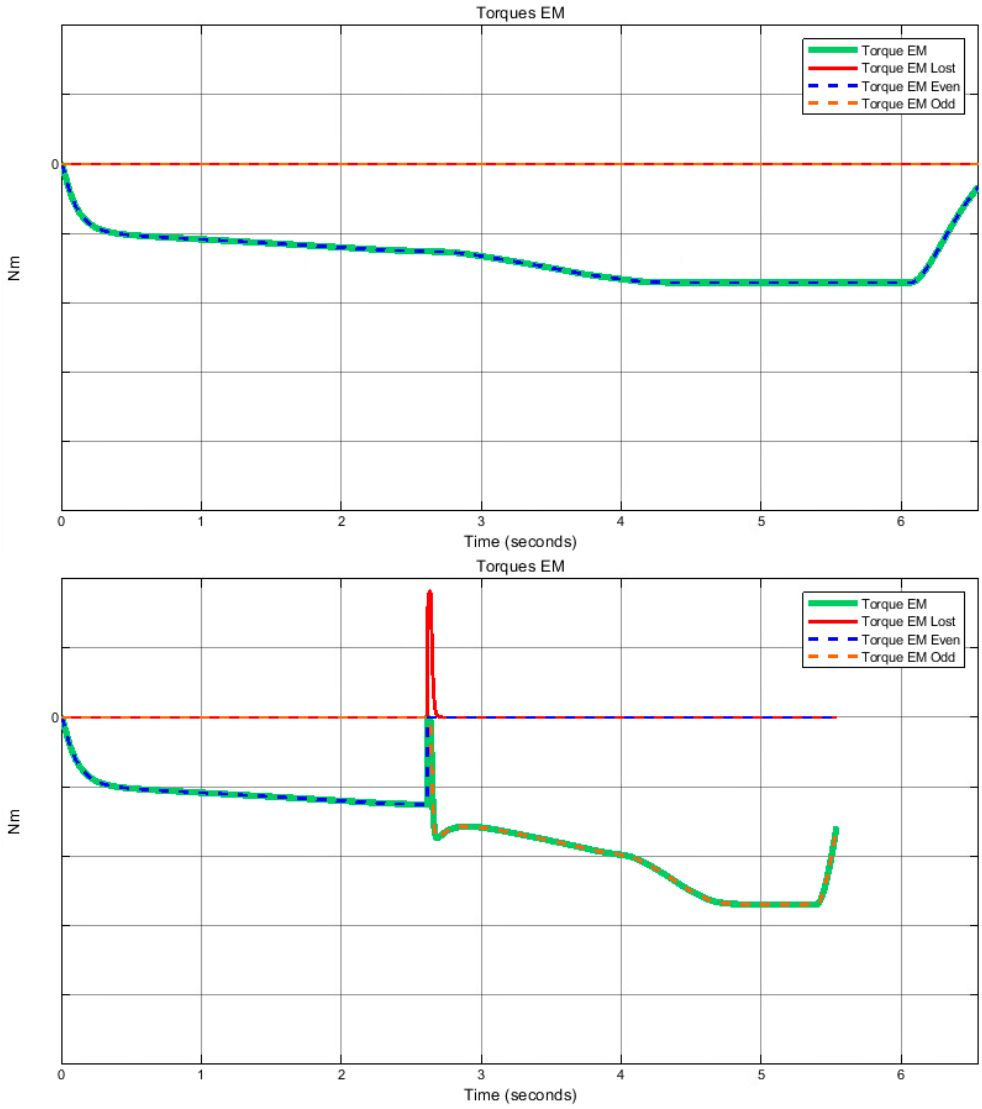

Figure 3.48: *Low speed braking manoeuvre; EM torque comparison*

Chapter 4

VI-CarRealTime vehicle model

4.1 VI-CarRealTime environment

VI-CarRealTime is a real-time vehicle simulation software, dedicated to evaluating the handling and the ride performance of a specified vehicle configuration, and useful to develop and test vehicle controllers or production ECU. It is a comprehensive and user-friendly environment for modelling and simulating vehicles in real-time. It operates with its own graphical interface or can be embedded into another control environment. This software uses a faster-than-real-time equation solver based on Adams/Car, ensuring high quality, and enabling data exchange between different teams in all the phases and disciplines of the whole development process of the vehicle.
Once created, the vehicle model can be tested in a real-time vehicle simulation environment by vehicle dynamics and controls engineers to optimize the vehicle and control system performance. Real world tests can be easily replicated, choosing from a predefined set of events, or directly creating them. VI-CarRealTime can even be associated to a driving simulator, for a test driver feel assessment and for the designers to obtain subjective data of the effects of determined design choices and adjustments. It can easily be paired to a MATLAB-Simulink environment when it can result useful to use another control environment out of its own GUI, or to the Adams/Car software from where obtain components modelling descriptions, reducing the time spent by different teams to get and set the same data. [9]

From our point of view, this type of software corresponds to a good means to reach our purpose, because of its capability to be paired both with Simulink and Adams/Car. This permits to obtain inputs from a comprehensible and well-known environment like the MATLAB-Simulink, and also to implement components, previously developed by other teams, from Adams. Our work in this environment will mostly concentrate in joining together the components of the different subsystems to develop the whole vehicle model, and in adjusting some powertrain features in order to obtain a more detailed assessment of the vehicle dynamics.

4.2 Vehicle model construction

As explained, the main components were taken from an Adams/Car environment and implemented in order to form the main subsystems of our complete vehicle model. In particular, we will have the body subsystem, the brakes, the steering system, the front and rear suspensions, the front and rear wheels models, and the powertrain system. The software permits to easily modify all the parameters whose effects we are interested in studying for each subsystem.
For starter, we must adapt the coordinates of the subsystems implemented in the model, since Adams/Car and VI-Grade use two different reference systems.

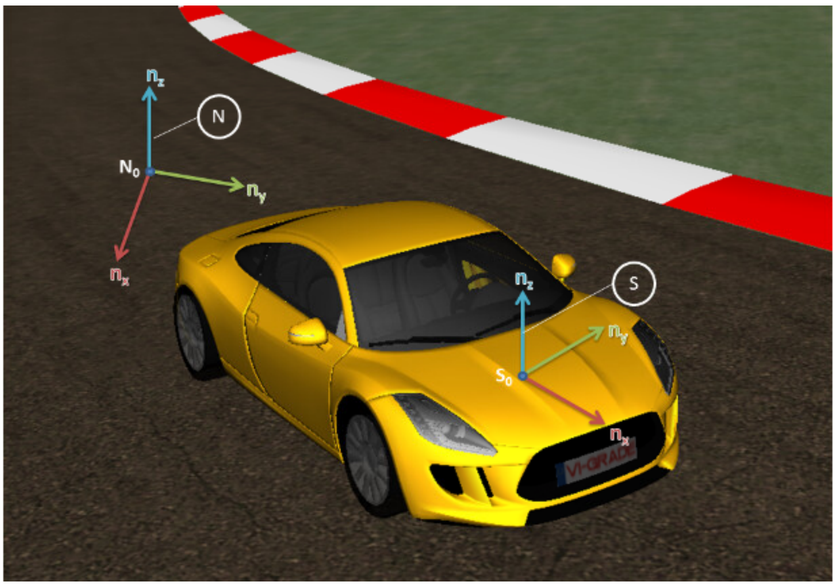

Figure 4.1: *VI reference system*

In particular, we will have to adapt the coordinates of the body centre of gravity, considering the difference in the coordinates of the same point (front left wheel centre) measured in the two references.
The final goal is to obtain a flexible co-simulation model, in which the Simulink driveline model is responsible for reproducing the torque dynamics and provide it as input to the VI vehicle model, which will assess its impact on the car dynamics, independently on how the torque was produced. For this reason, at this stage we are not so interest in replicating precisely all the features of the driveline, that are already faithfully represented in the Simulink environment.
Once the system is set, we can perform some simulations to verify the correct functioning of our vehicle model.

4.3 Powertrain bushings implementation

Since we want to observe the manoeuvres effects on vehicle dynamics and comfort, to expand the analysis, the engine bushings are implemented to include and comprehend their impact.
Up until now the powertrain is considered as a rigid component, so that the only data inserted are about the torque transfer, while its inertial part is considered in the body subsystem. Now, starting from the previous rigid model, we want to detach the powertrain inertial data from the sprung mass subsystem, and create an isolated component in order to consider its dynamics separately.

4.3.1 Sprung mass and powertrain subsystems

From the assigned inertial data of the powertrain and its position, it must be computed the new centre of mass position and the new moments of inertia of the separate sprung mass system.
Initially, in the rigid model, it was assigned to the body subsystem the mass of the sprung mass plus the one of the powertrain, the moments of inertia of the sprung mass including the powertrain, and the centre of mass of the sprung mass and the

powertrain as a single body. Now we have to separate the two entities, so that, having the mass and the inertial data of the powertrain, we have to compute the mass, the centre of gravity and the inertias of the new sprung mass without the powertrain. We can write:

$$M_{sm} = M_{sm+pwt} - M_{pwt} \tag{4.1}$$

And for the new centre of mass of the sprung mass:

$$x_{CG_{sm}} = \frac{M_{sm+pwt}\, x_{CG_{sm+pwt}} - M_{pwt}\, x_{CG_{pwt}}}{M_{sm}} \tag{4.2}$$

$$y_{CG_{sm}} = \frac{M_{sm+pwt}\, y_{CG_{sm+pwt}} - M_{pwt}\, y_{CG_{pwt}}}{M_{sm}} \tag{4.3}$$

$$z_{CG_{sm}} = \frac{M_{sm+pwt}\, z_{CG_{sm+pwt}} - M_{pwt}\, z_{CG_{pwt}}}{M_{sm}} \tag{4.4}$$

For what concerns the moments of inertia, we first have to consider that the given data are referred to the centre of gravity of the given subsystem, and for us to sum them, we must first refer them to the new centre of gravity just computed. In order to do that, we make use of the Huygens-Steiner theorem and write, for the sprung mass:

$$I_{xx_{sm+pwt}} = I'_{xx_{sm+pwt}} + M_{sm+pwt}\, dx^2 \tag{4.5}$$

$$I_{yy_{sm+pwt}} = I'_{yy_{sm+pwt}} + M_{sm+pwt}\, dy^2 \tag{4.6}$$

$$I_{zz_{sm+pwt}} = I'_{zz_{sm+pwt}} + M_{sm+pwt}\, dz^2 \tag{4.7}$$

$$I_{xy_{sm+pwt}} = I'_{xy_{sm+pwt}} + M_{sm+pwt}\, dx\, dy \tag{4.8}$$

$$I_{xz_{sm+pwt}} = I'_{xz_{sm+pwt}} + M_{sm+pwt}\, dx\, dz \tag{4.9}$$

$$I_{yz_{sm+pwt}} = I'_{yz_{sm+pwt}} + M_{sm+pwt}\, dy\, dz \tag{4.10}$$

Where:

$$dx = x_{CG_{sm}} - x_{CG_{sm+pwt}} \tag{4.11}$$

$$dy = y_{CG_{sm}} - y_{CG_{sm+pwt}} \tag{4.12}$$

$$dz = z_{CG_{sm}} - z_{CG_{sm+pwt}} \tag{4.13}$$

And, applying the same method, for the powertrain:

$$I_{xx_{pwt}} = I'_{xx_{pwt}} + M_{pwt}\, dx^2 \tag{4.14}$$

$$I_{yy_{pwt}} = I'_{yy_{pwt}} + M_{pwt}\, dy^2 \tag{4.15}$$

$$I_{zz_{pwt}} = I'_{zz_{pwt}} + M_{pwt}\, dz^2 \tag{4.16}$$

$$I_{xy_{pwt}} = I'_{xy_{pwt}} + M_{pwt}\, dx\, dy \tag{4.17}$$

$$I_{xz_{pwt}} = I'_{xz_{pwt}} + M_{pwt}\, dx\, dz \tag{4.18}$$

$$I_{yz_{pwt}} = I'_{yz_{pwt}} + M_{pwt}\, dy\, dz \tag{4.19}$$

Where now:

$$dx = x_{CG_{sm}} - x_{CG_{pwt}} \tag{4.20}$$

$$dy = y_{CG_{sm}} - y_{CG_{pwt}} \tag{4.21}$$

$$dz = z_{CG_{sm}} - z_{CG_{pwt}} \tag{4.22}$$

The new rigid part of the sprung mass and of the powertrain are now defined.
In order to verify the correctness of our results, a kinematic mount is applied to the new powertrain so that it is rigidly joint to the chassis; in this way its functioning should be the same as the initially created rigid model. Some simulations were performed in order to verify that the responses of the two models coincide.
A steering and a braking manoeuvre can be simulated; the results curves of the two models are not distinguishable, that is what we were looking for. In particular, here reported we can see the centre of mass vertical displacement with respect to the ground and the pitch displacement, so that we can know that the two models are reacting in the same way.

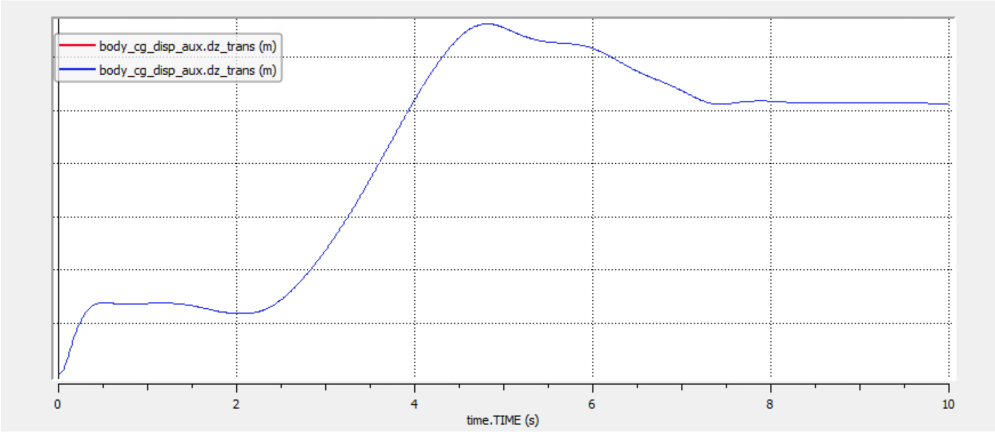

Figure 4.2: *CG vertical displacement in a steering manoeuvre*

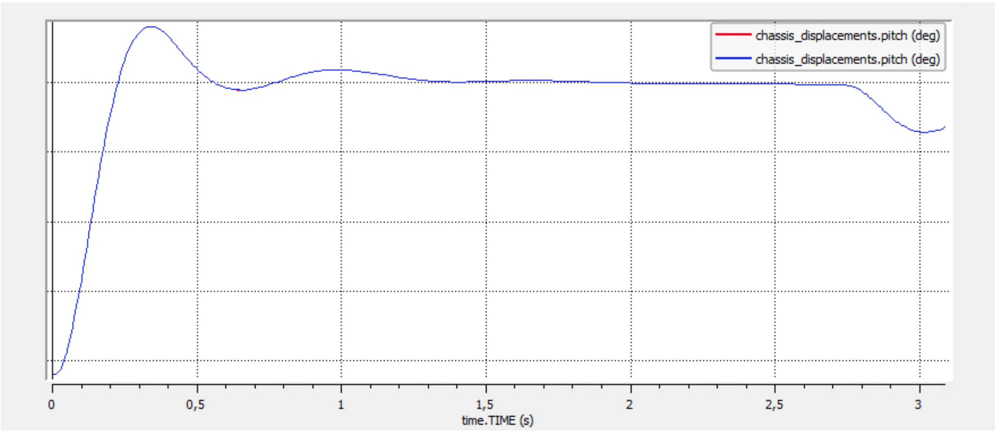

Figure 4.3: *Vehicle pitch displacement in a braking manoeuvre*

4.3.2 Engine mounts activation

Verified that the two models have the same vehicle mass, the same centre of gravity and in general the same inertia, now the mounts can be inserted between the powertrain and the front chassis. In particular, two bushings, one on the engine side and one on the gearbox side, and one torque rod, longitudinally positioned and fixed to the chassis in two points, were used.

Removed the kinematic mount, we can proceed with the bushings' definition; the environment permits to establish the bodies between which the link is provided, the position of the bushing, its stiffness characteristic curves, and its damping properties, all set according to the given data.

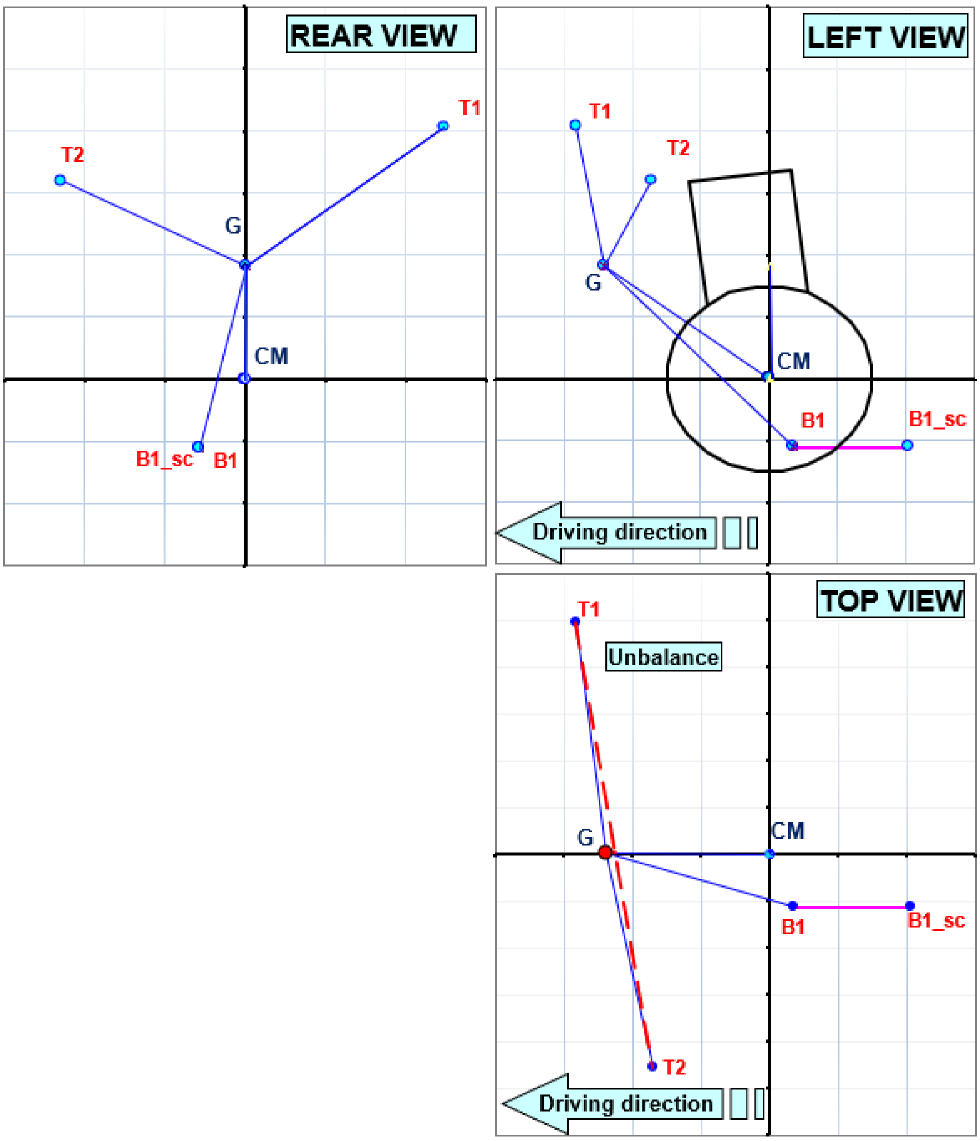

Figure 4.4: *Engine mounts positioning with respect to the engine centre of mass*

Once implemented, it is verified that they work correctly and in accordance with the inserted characteristics.

The more demanding situation to be studied for the ride comfort evaluation in a longitudinal dynamics manoeuvre is the gear shift phase.

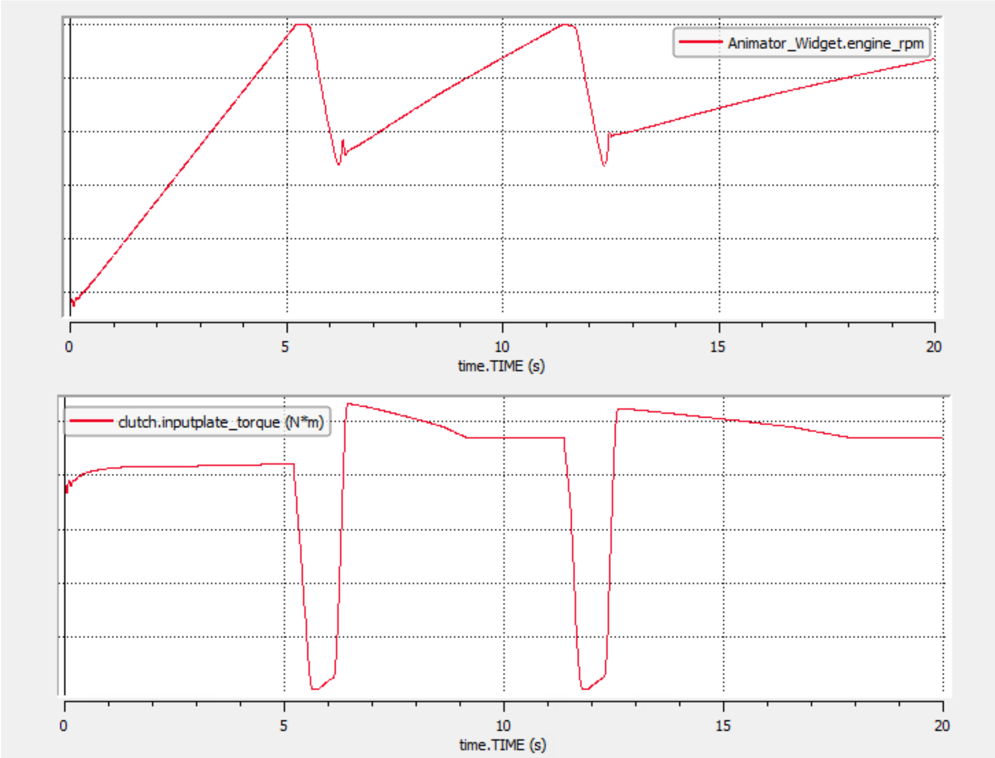

Figure 4.5: *Engine torque and rpm in an acceleration manoeuvre with gear changes*

In that situation, the engine angular speed has high changes in pace, and high torque holes are present, causing the engine to experience heavy vibrations, in all directions.

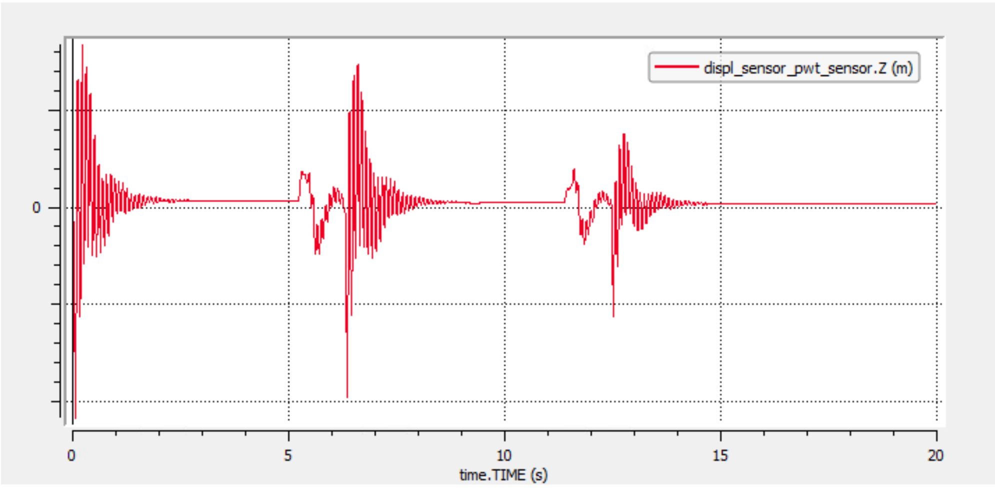

Figure 4.6: *Vertical engine vibrations in the gear changes*

One of the purposes of engine mounts is to damp this type of vibrations, in order for them not to reach completely the chassis and the passengers, and consequently jeopardize the ride comfort.

To understand how the bushings are affecting the engine and, consequently, the vehicle dynamics in such working conditions, initially a rigid versus damped powertrain confrontation has been made.

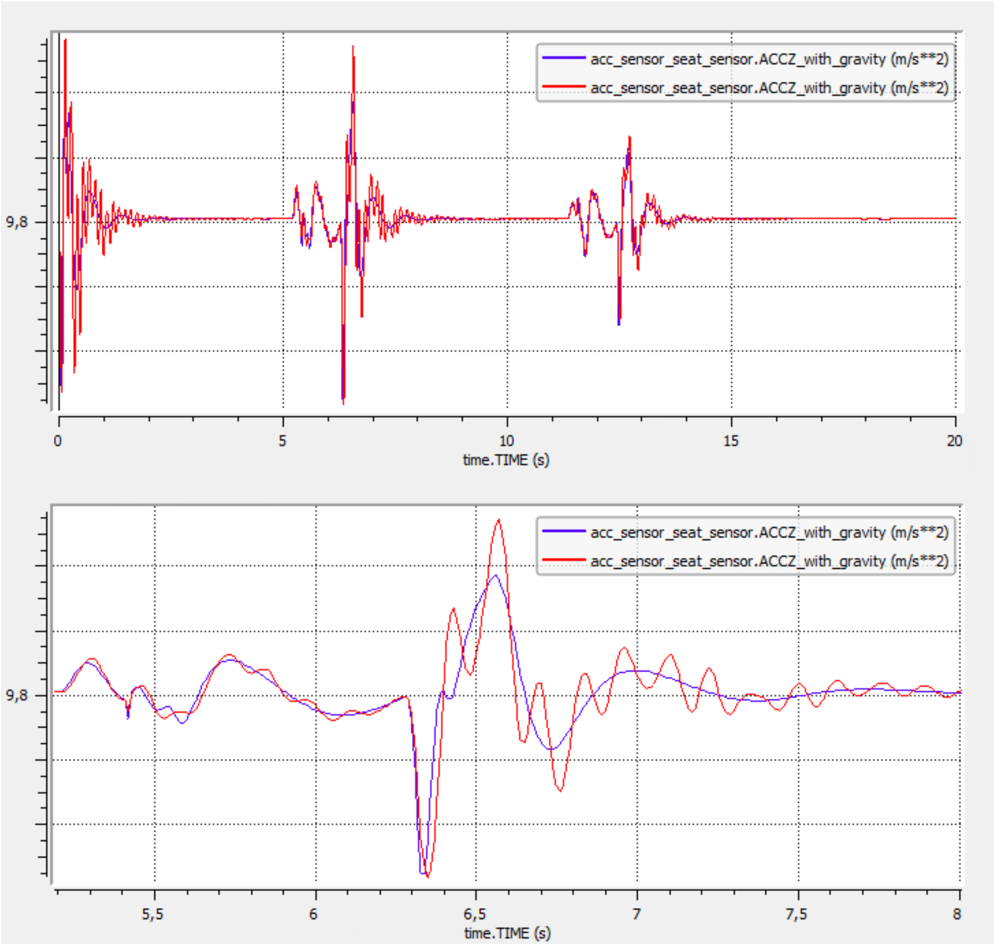

Figure 4.7: *Vertical acceleration perceived at vehicle seat*

In a gear change manoeuvre, the engine torque holes translate in almost impulsive loads; from the obtained results it would seem that a rigid link between the powertrain and the chassis could be beneficial and preferable for this type of study case.

The blue curve, corresponding to the rigid powertrain post-processing, shows lower peaks and also a smoother behaviour for what concerns accelerations measured at the vehicle seat and floor.

The obtained analysis could however be misleading because the explained behaviour could be caused by the way in which the rigid powertrain is defined. With the kine-

matic joint assumption, the bond between engine and chassis is perfectly rigid, and the vibrations of the engine are fixed to zero; it is like having a single body, with the powertrain as part of the chassis, meaning that the vibrations of the engine are damped by the inertia of the whole system, that is unrealistic.
When we detach the powertrain from the sprung mass, as reported in the red curve of the results, it will vibrate, according only to its own inertia, and transmit its accelerations to the rest of the chassis. These vibrations, in this case, are concentrated in the engine centre of mass, and not at the sprung mass one, creating an inertial force and influencing the whole dynamics of the system.
Once measured, as can be seen in Figure 4.10, the relative displacements of the engine with respect to the chassis are verified to be null in the case of a rigid joint, while in the subsystem with bushings they depend on the vehicle and engine dynamics.

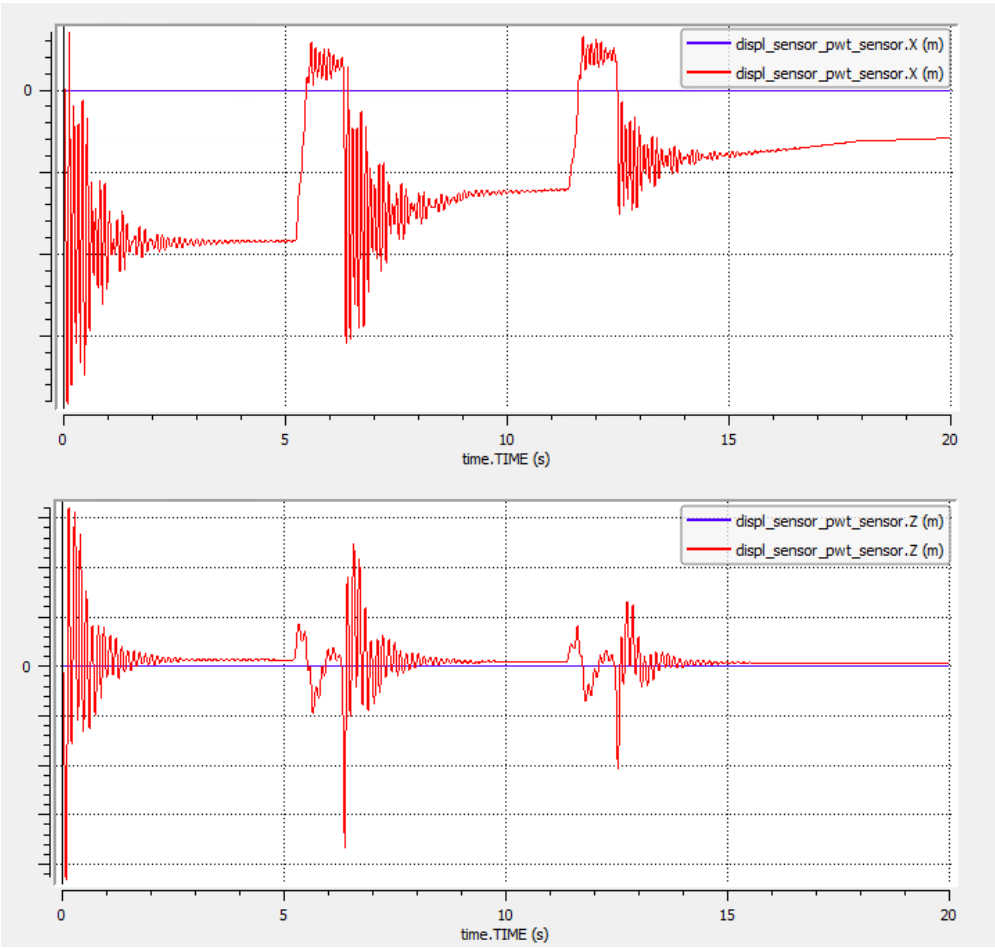

Figure 4.8: *Powertrain displacements in comparison*

This could cause the performed comparison to be inconsistent and obtained results to be not reliable. In order to assess the true effects of engine bushings in the gear change manoeuvre, a detailed analysis of the mounts stiffness and damping property regulation must be made, where in both powertrains the kinematic mount assumption is released.

4.3.3 Bushings regulation analysis

In the performed simulations, bushings displacements recorded are small, even simulating high-load working conditions, so we may think of mounting rubber-metal pads, whose typical characteristic values are in the order of those initially inserted: therefore, they will represent our nominal reference configuration from which start the evaluation.

To assess the suspensions features regulation effects we can work in two directions, acting on their translational damping value, or increasing the elastic stiffness curves slopes. The two effects are separately evaluated.

Firstly, we progressively increase the stiffness of the bushings, operating on their elastic force curve in all three directions.

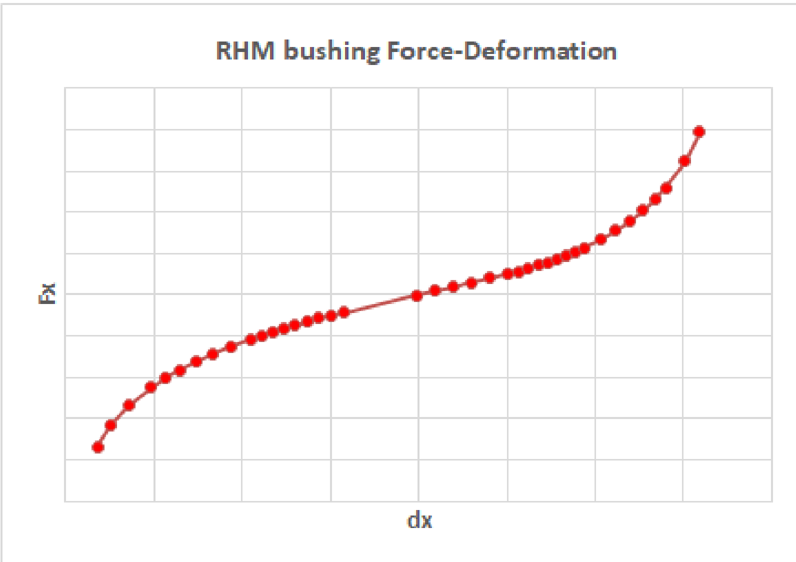

Figure 4.9: *Nominal bushing force-displacement curve*

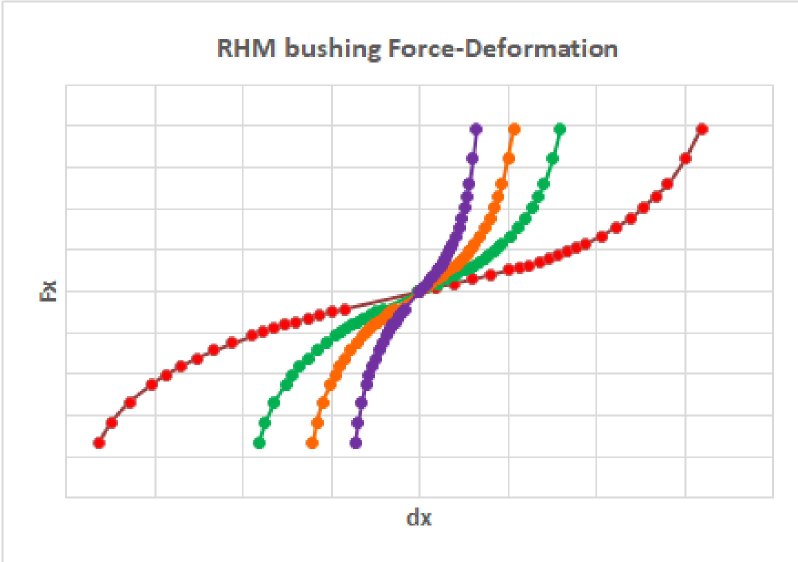

Figure 4.10: *Bushing stiffness progressive increase*

Again we can verify the dynamics of the vehicle and of the powertrain evaluating the sensors' data in an acceleration with gear changes. In particular, to the red curve corresponds the nominal values of the engine suspensions stiffness, to the green curve a doubled stiffness, and to the orange and purple curve a stiffness respectively three and five times higher.

Moving from the nominal values of the bushings stiffness to a progressively more rigid condition, we have that the powertrain displacements are highly affected.

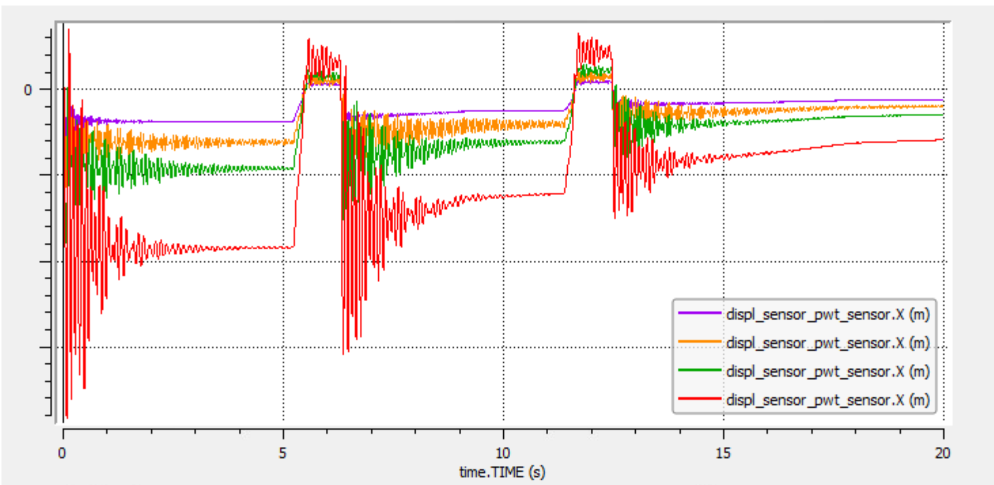

Figure 4.11: *Engine mounts progressive stiffness increase effect on the powertrain longitudinal relative displacement*

First, it can be stated that greater suspension stiffness causes the engine to experience lower displacements due to the longitudinal acceleration of the vehicle; the engine is progressively moving to the rigid mount configuration as the link provided is stiffened.

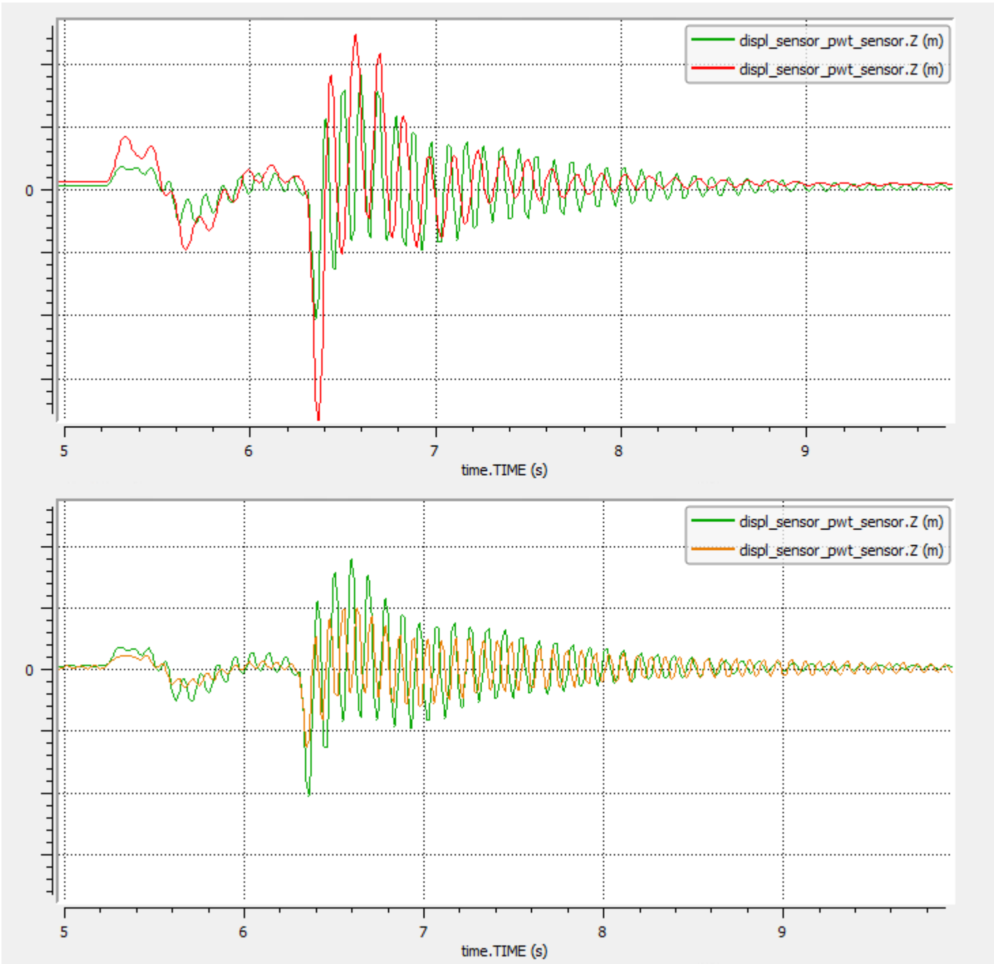

Figure 4.12: *Powertrain vertical relative displacements during the gear change with different engine mounts stiffness*

As can be seen in Figure 4.14, the stiffness increase also has an effect on the vibrations suffered by the powertrain in the gear change manoeuvre. The higher is the stiffness and lower values of relative engine-chassis displacements will verify. It is also true, that the modifications result in increased vibrations frequency and longer time needed for the oscillations extinction.

Eventually, this will end up affecting passenger perception, and even though the powertrain dynamics are moving in the direction of its perfectly rigid configuration, the measured results will take a different turn with respect to the comparison previously made. Both at the vehicle seat and at the floor, the values of the initial acceleration peaks are similar, with a slight increase when stiffening the connection, but in particular, the stiffer the suspension, the lower the progressive absorption of the magnitude of the oscillations will be, resulting in a longer perception time. Also, the perceived vibrations at the case will be characterized by a higher vibrations frequency.

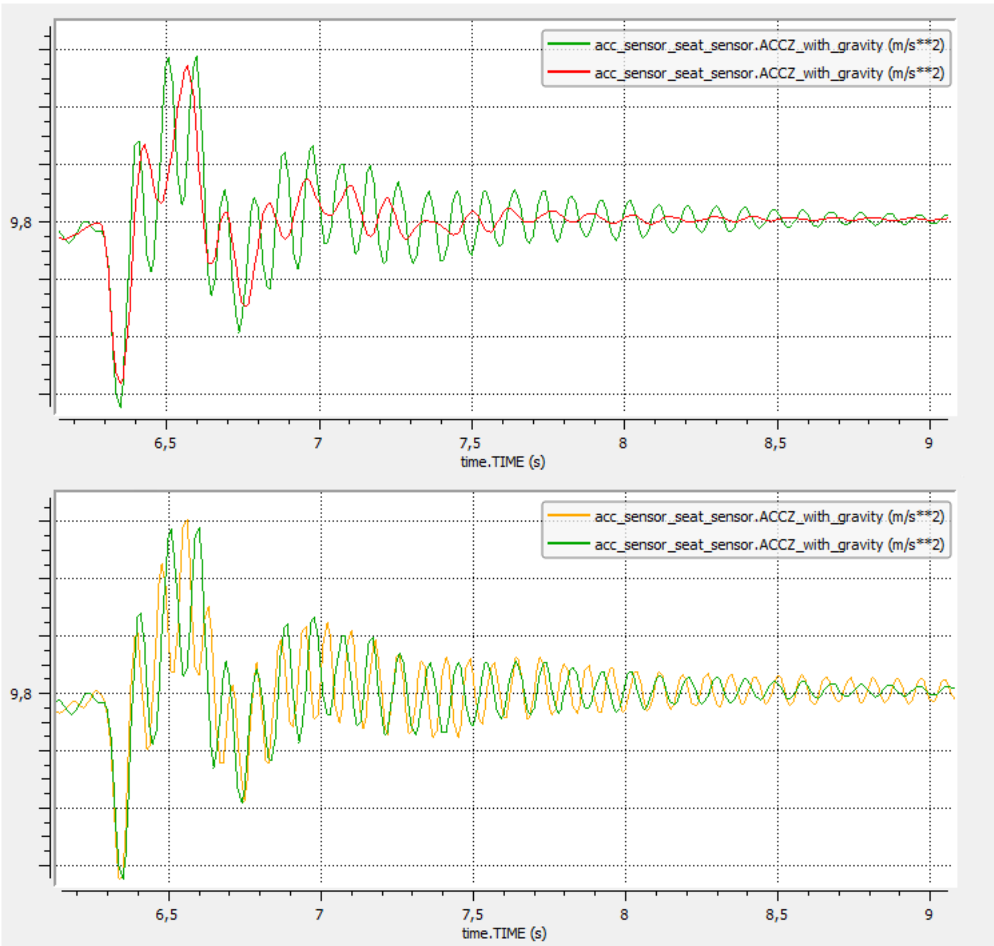

Figure 4.13: *Passenger vertical acceleration perception at seat in the different bushing configurations*

Now an additional analysis can be made, keeping fixed the initial nominal values of the suspension stiffness curves, and progressively increasing the translational damping, again in all three directions.
In this case, by increasing the damping we are not moving towards a rigid powertrain configuration; it is expected a better absorption of the vibrations, but without acting on their relative nominal value, and coherently this is what is obtained in the results.

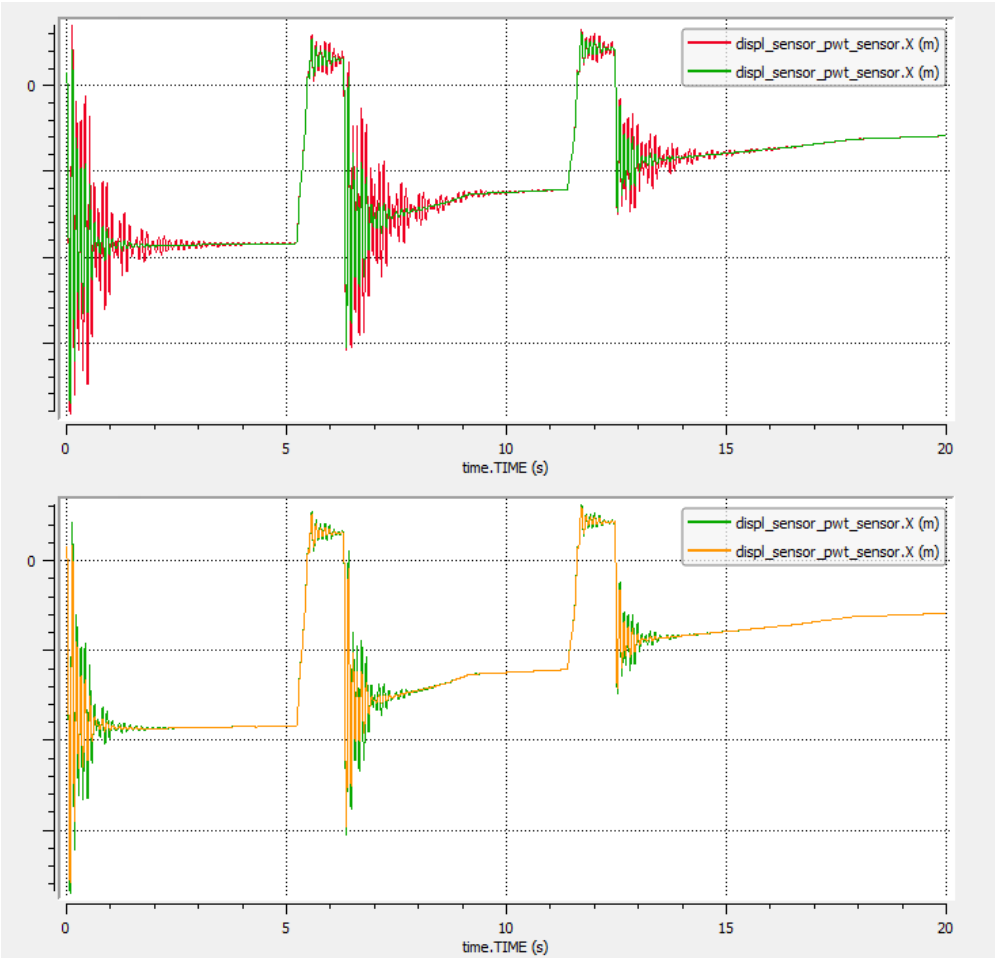

Figure 4.14: *Engine mounts progressive damping constant increase effect on the powertrain longitudinal relative displacement*

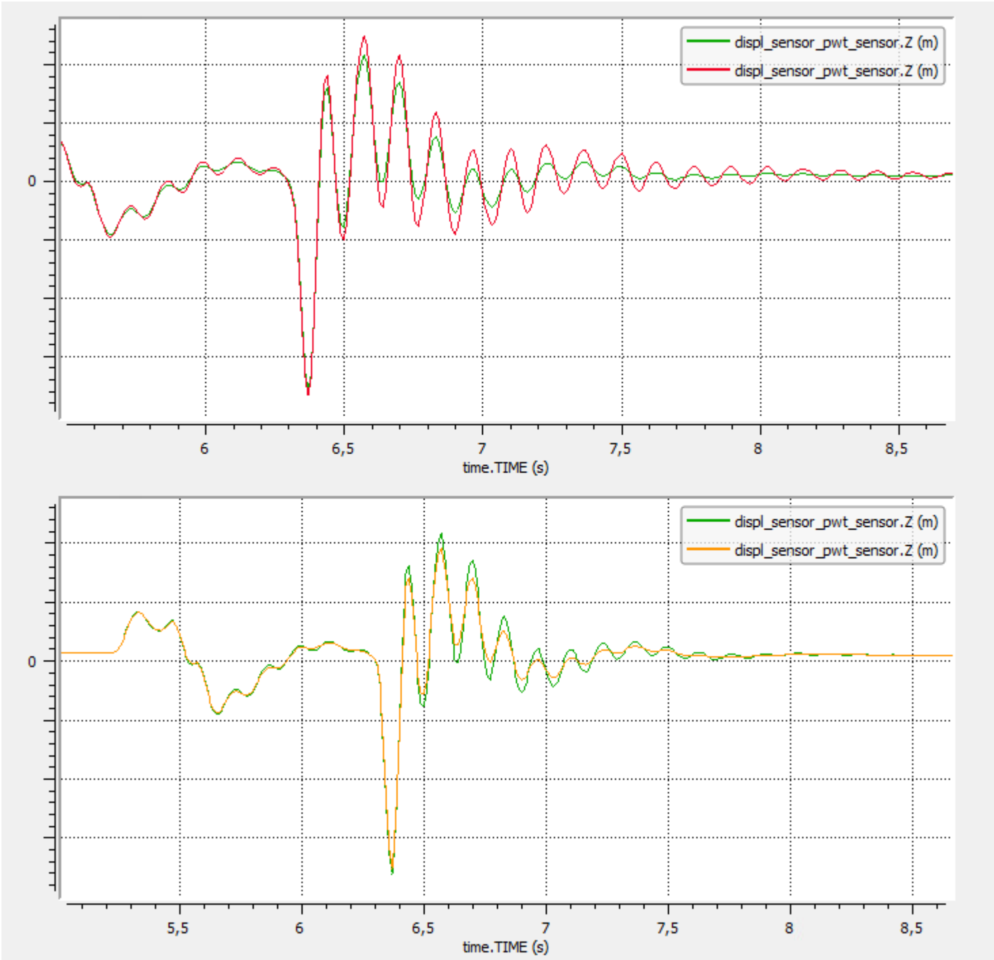

Figure 4.15: *Powertrain vertical relative displacements during the gear change with different engine mounts damping constants*

Both for the powertrain longitudinal relative displacement due to the vehicle acceleration, both for the displacements due to the vibrations in the gear change, the effect of the damping value increase is the same; the vibration frequency is not influenced by the damping capability of the suspension, that instead affects and increases the oscillations absorption.

The same effects are maintained this time when measuring the passengers' perception of the accelerations in the gear shift manoeuvre at chassis floor and at the seat.

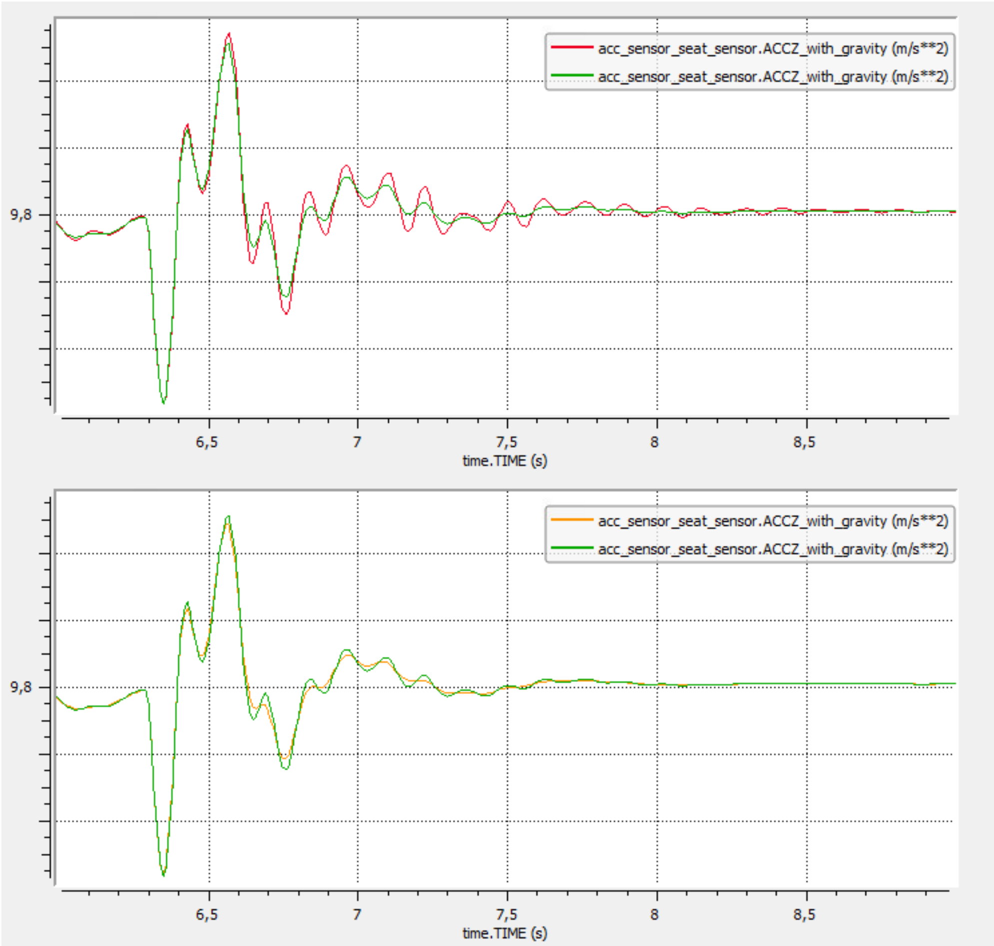

Figure 4.16: *Passenger vertical acceleration perception at seat in the new different bushing configurations*

The described effects can be compared with the one illustrated in Figures 4.13, 4.14 and 4.15.

It is important to state that the performed engine mounts analysis is not absolute, it is relative to the situation hereby assessed. In particular, in VI-CarRealTime, in the computation of the inertia forces given by the torque delivered by the engine, the forces transmitted to the chassis given by the various second order moments, like cylinders motion and firing, are not considered. The only inertia force taken into account is the one given by the engine produced torque, and being the torque output the same, regardless of the mounted bushing, the inertia is also equal in the different cases. Finally, the stress force due to torque output is still constant in the different bushings configurations, but not the one due to the motor displacement in the instantaneous torque hole verifying at gear change, which increases if diminishing the stiffness of the bushing. This increased displacement is what stresses the most the case, and suspensions reaction evolution in the different configurations is coherent with what expected for the related load condition.

In a real-life situation, what happens is that to the nominal engine output, torque irregularities are added, due to its internal components' configuration and dynamics, that are quite relevant for this kind of evaluation. Normally, a less stiff engine suspension is preferred in order to filter these vibrations and for them not to reach completely the passengers. With a stiff mount, the damping would be compromised and comfort negatively affected.

The torque irregularities dynamics can be simulated in Simulink by adding a sinusoidal torque to the engine nominal output, and the consequent effects of suspensions on the vehicle dynamics and comfort can be later assessed in the co-simulation model.

Chapter 5

Co-simulation model

Having the two separated models, the goal now is to create a co-simulation model linking the vehicle model created on VI-CarRealTime with the driveline one present in Simulink. Since it is already possible to easily simulate all the vehicle driving modes in it, MATLAB/Simulink will provide the co-simulation environment and will serve as the master of the co-simulation, determining and controlling the two simulations and integrating the software together.

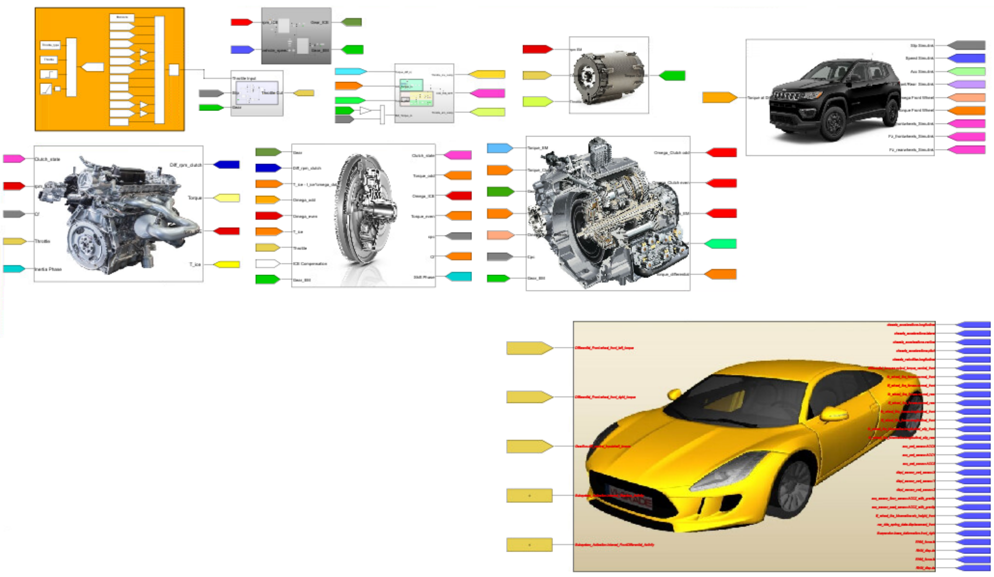

Figure 5.1: *Co-simulation model*

5.1 Co-simulation model setting

In order to link the two models, having decided to use Simulink for the conjoined simulation, we need to integrate the VI model into Simulink. A pre-created block is inserted with the goal of providing to Simulink a link to the VI environment.

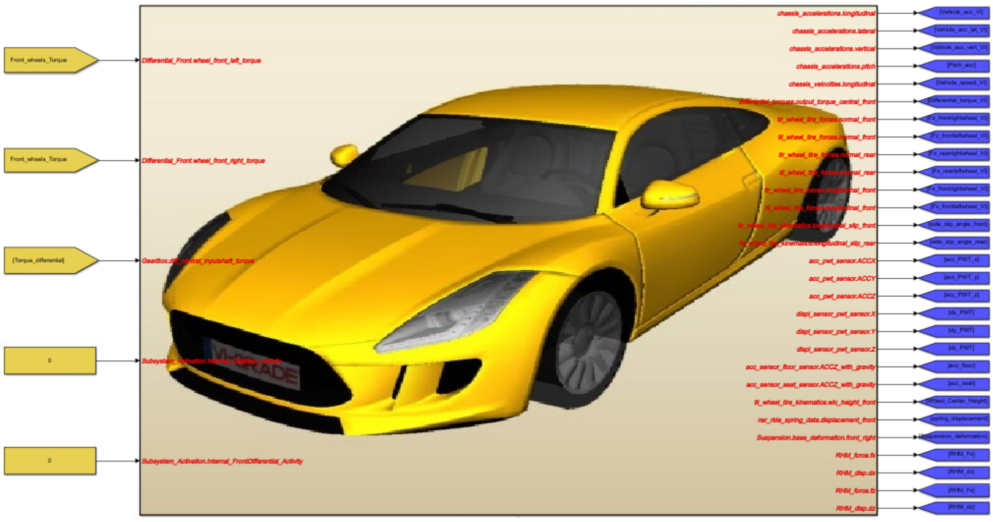

Figure 5.2: *VI-CarRealTime vehicle model on Simulink*

The block providing the two software's connection is present in the VI examples library, and what needs to be done is setting the input parameters according to how we want the link between the two models to be provided, since different possibilities are present.

The linking point that we want to set is the differential input, so it should be found the right combination of input values in order that, once the model is set, the differential torque computed in output by the vehicle model is the same as the one provided in input by the Simulink driveline. It would be preferable to have the lower number of inputs as possible, in order not to provide too many constraints between the two models.

The simulation manager inside this block will supply to the Simulink environment a simulation path in VI-CarRealTime, featuring the vehicle model we want to co-simulate. The input signals needed, and the output values that we want to evaluate are set here.

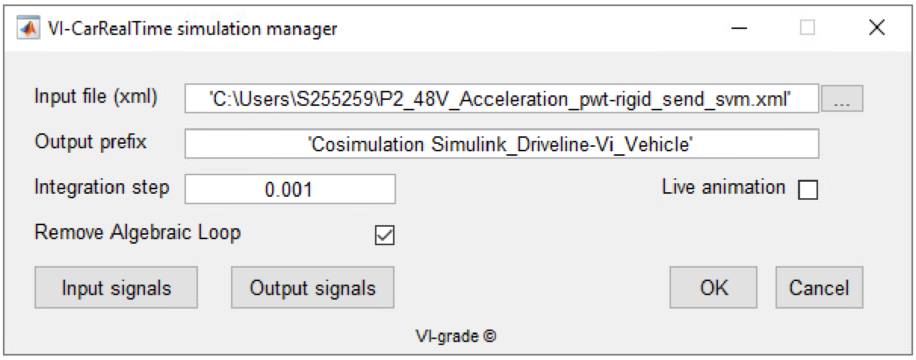

Figure 5.3: *VI simulation manager*

After some analysis, it is found that, in order for the model to behave as desired, the essential inputs to provide from the driveline model to the vehicle model are the torque at the differential input signal, and the torque at the two driving wheels. Also the information about the differential and the gearbox activation is needed.

To verify the correct functioning, the possible manoeuvres are simulated in order to check that in all conditions, the torque at the differential measured by the VI vehicle model is following the constrained value. Some examples are here reported.

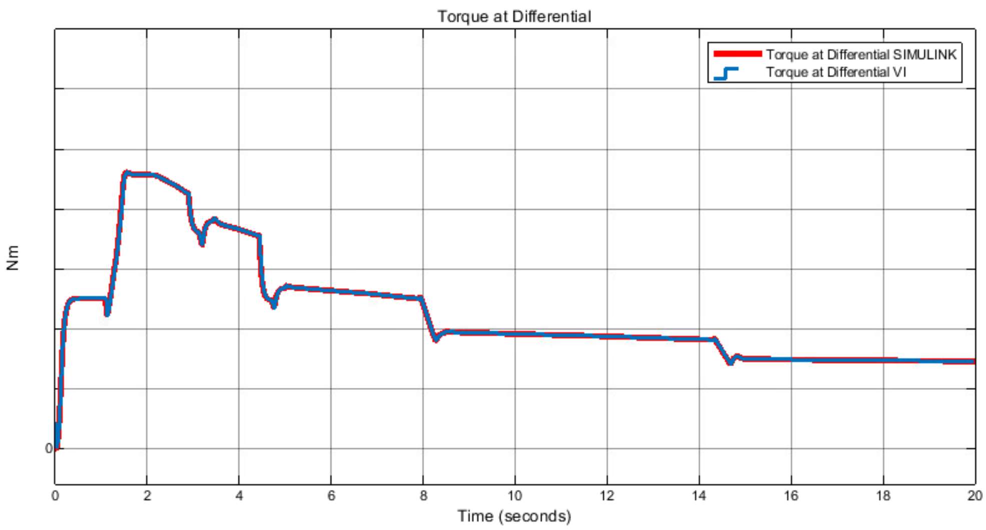

Figure 5.4: *Torque at differential of the two vehicle models in a pure thermal drive manoeuvre*

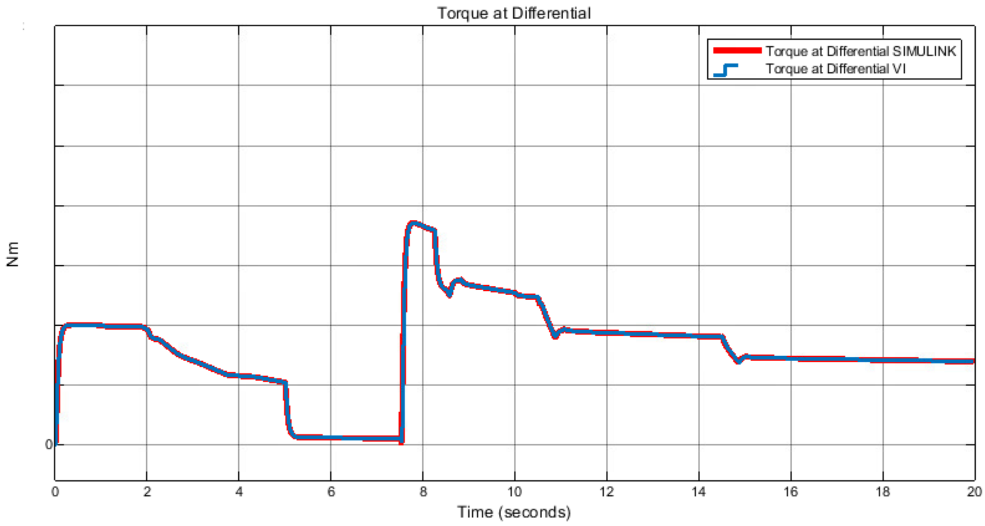

Figure 5.5: *Torque at differential of the two vehicle models in an engine clutch start manoeuvre*

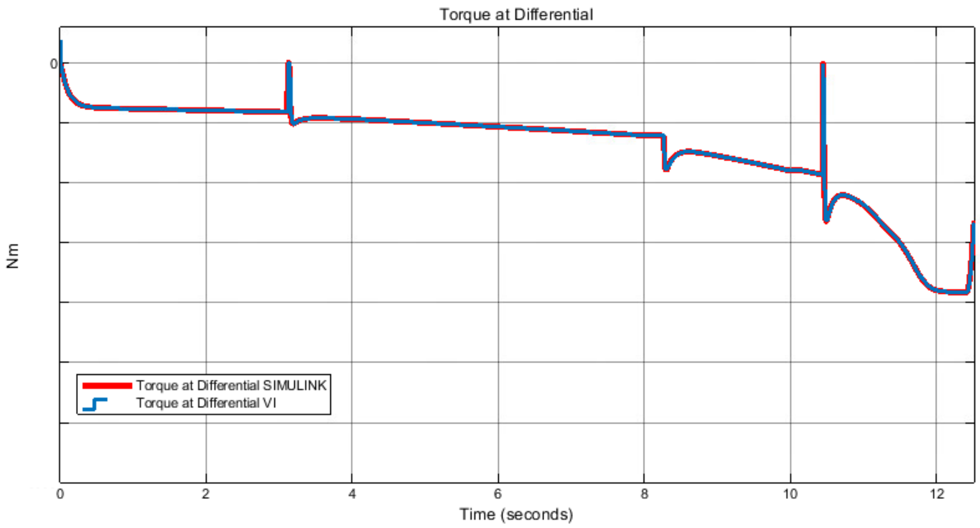

Figure 5.6: *Torque at differential of the two vehicle models in a regenerative braking manoeuvre*

Whichever is the manoeuvre selected, and whichever is the throttle path imposed, the VI model is always able to successfully receive exactly the right torque at the differential that the Simulink environment provides as input.

5.2 Vehicle models comparison

Now that the vehicle model is implemented in the co-simulation model, and verified that the two vehicle models are receiving the same inputs, let us analyse the main features about the vehicle longitudinal dynamics, in order to assess the correct functioning and to compare the results of the new complete model with the simple vehicle one that was present before. In order for the co-simulation to work properly, in the VI-CarRealTime simulation provided to the Simulink environment as link to its vehicle model, it is only needed to set the boundary conditions of the MATLAB/Simulink simulation: in particular, the desired time of simulation and the initial vehicle speed must correspond.
Let us start the analysis with a WOT manoeuvre of pure thermal drive.

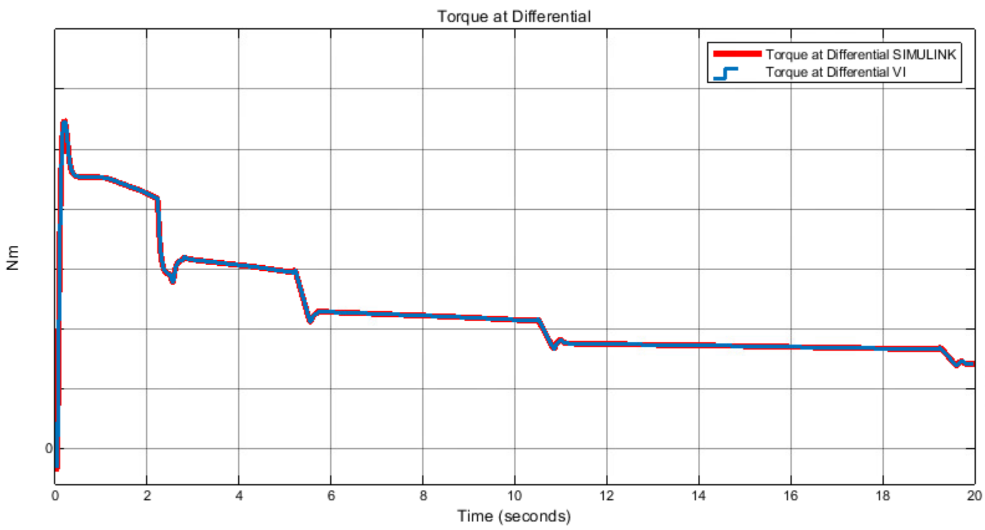

Figure 5.7: *Torque at the differential in a WOT pure thermal drive manoeuvre*

Figure 5.7 shows the torque signal created, and it has already been verified that it arrives correctly in input to the vehicle model, independently on how it was created; now we want to check how differently the models react to it.
Good results are obtained in terms of vehicle speed and longitudinal acceleration, having the longitudinal forces at the driving wheels comparable values.

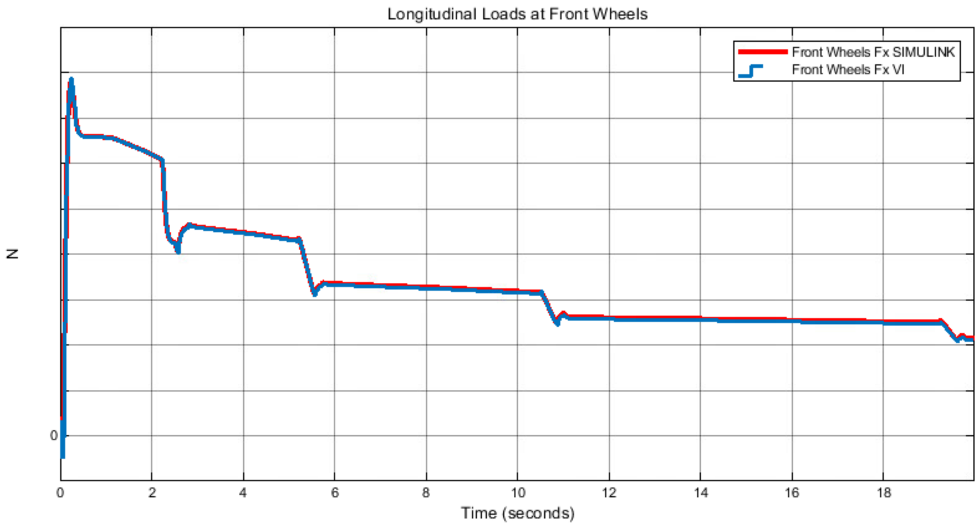

Figure 5.8: *Longitudinal forces at the front wheels of the two vehicle models*

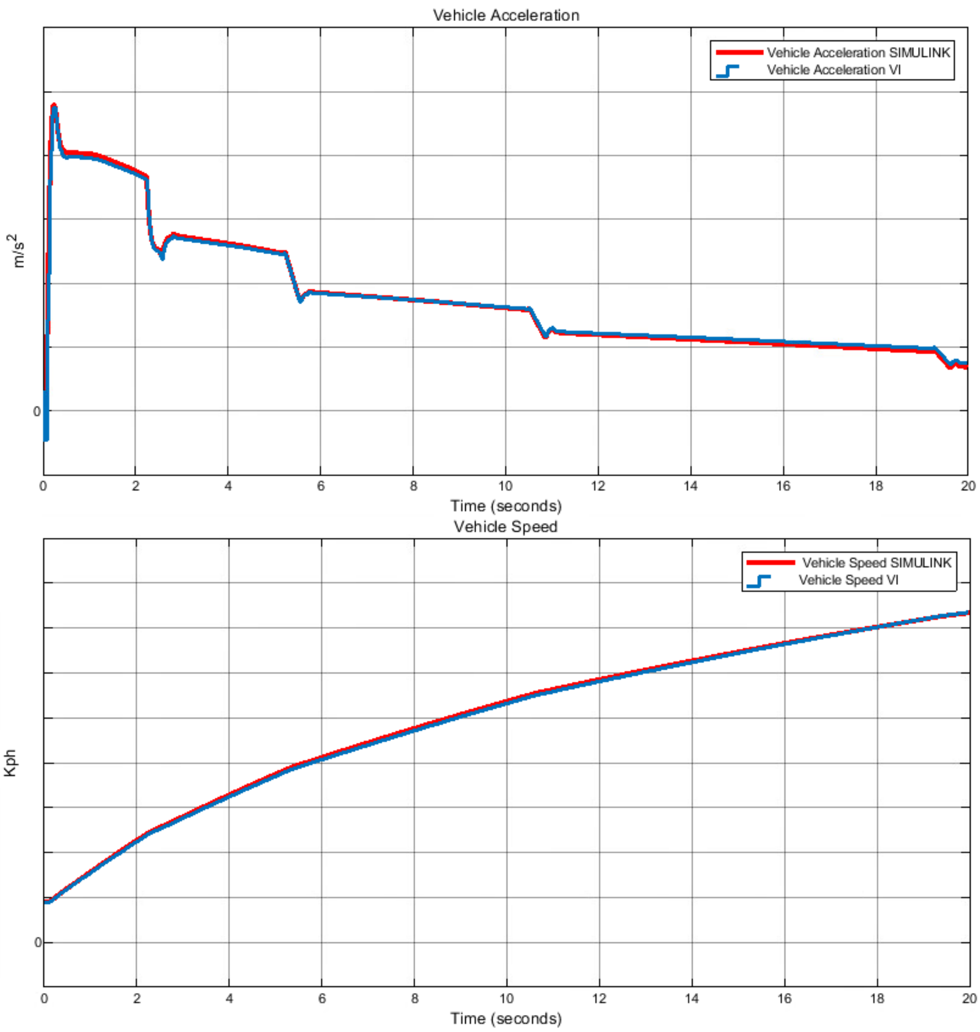

Figure 5.9: *Longitudinal acceleration and speed of the two vehicle models*

The main difference found between the two vehicle models outputs lies in the normal loads' values computed at the wheels, both in terms of single axles and of total loads at the four wheels.

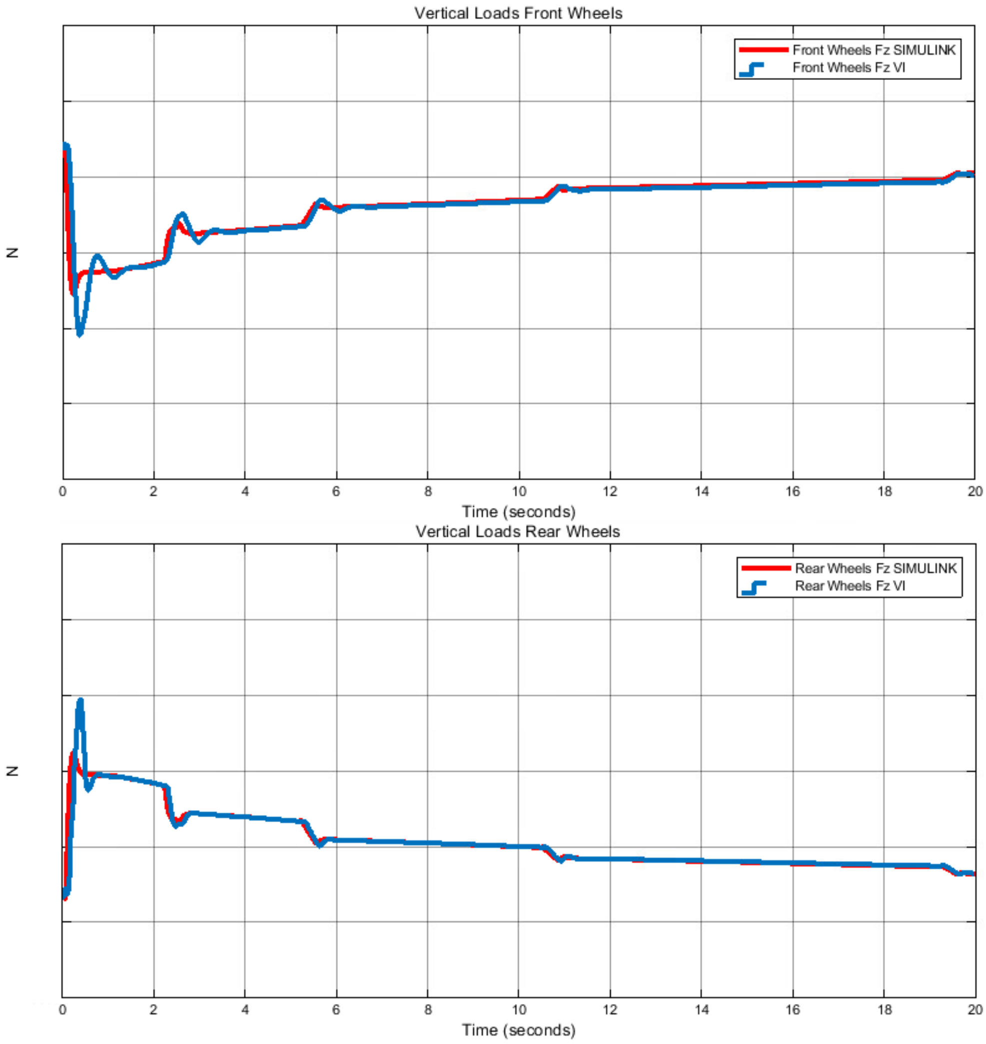

Figure 5.10: *Normal forces at the two axles of the two vehicle models*

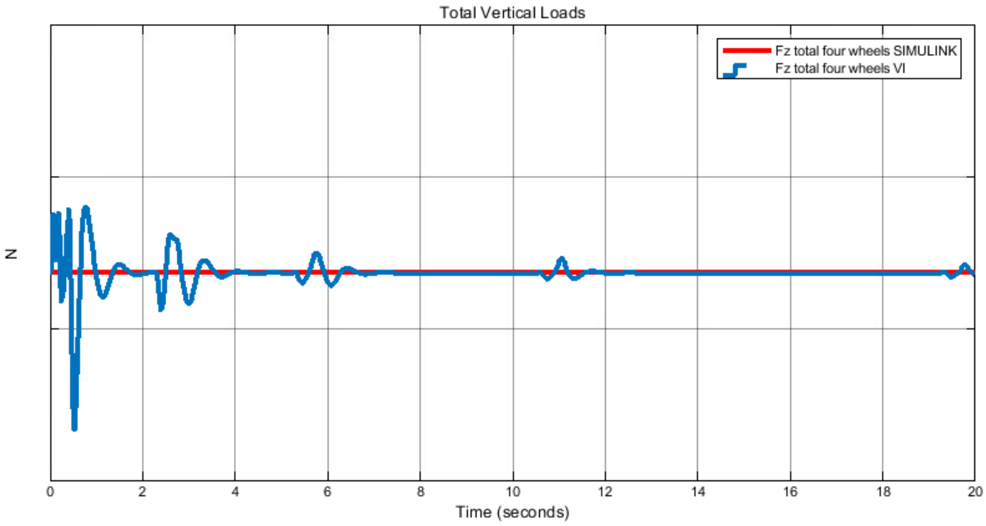

Figure 5.11: *Normal forces at the four wheels of the two vehicle models*

After some verifications, it was found that the inconsistency was due to the fact that high torque ramps cause the VI vehicle model to experience some vibrations. These vibrations are imposing the vehicle to register some unexpected accelerations out of the impressed one, principally a vertical acceleration and a pitch movement.

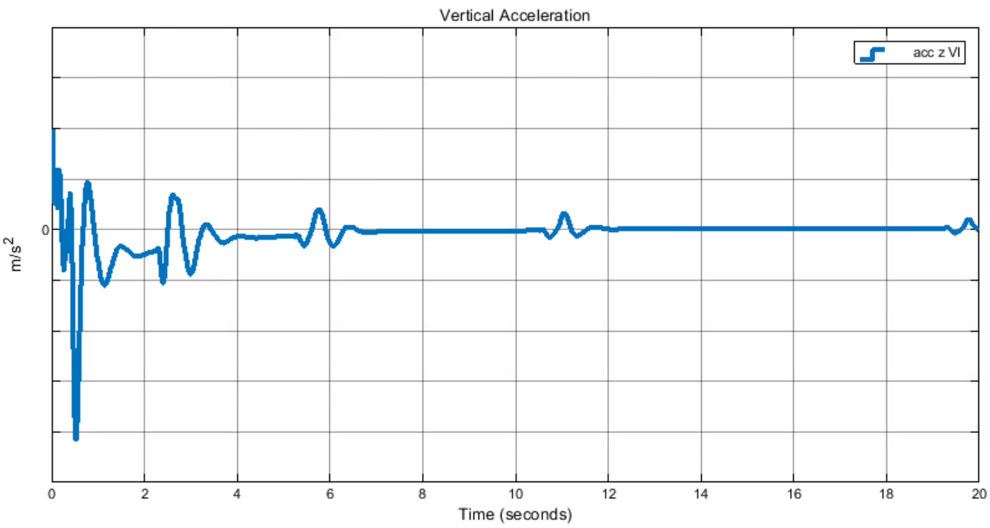

Figure 5.12: *Vertical acceleration of the VI vehicle model*

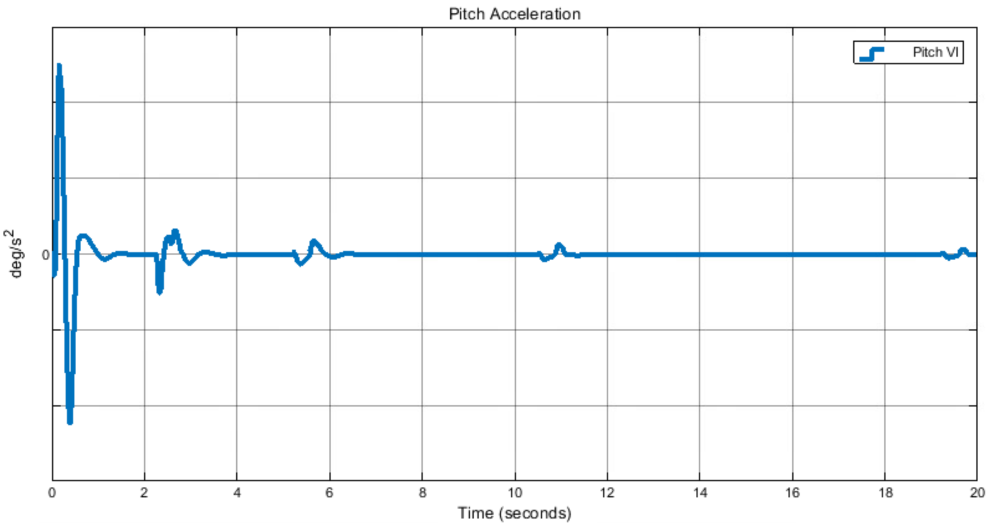

Figure 5.13: *Pitch acceleration of the VI vehicle model*

The pitch acceleration oscillation is causing the vehicle to measure an additional load transfer, out of the one due to the longitudinal acceleration. Moreover, with the impressed vertical acceleration, the total load at the wheel will be influenced; in the Simulink model the total normal load is constant and given only by the vehicle weight contribution, while in the VI results this load will change coherently with the vertical acceleration measured. In correspondence of a negative peak of vertical acceleration is registered a lower total load at the wheels, as a positive value of pitch will cause a load transfer to the front wheels, and vice versa. When the non-impressed accelerations value is null, the loads at the wheels of the two vehicle models coincide.

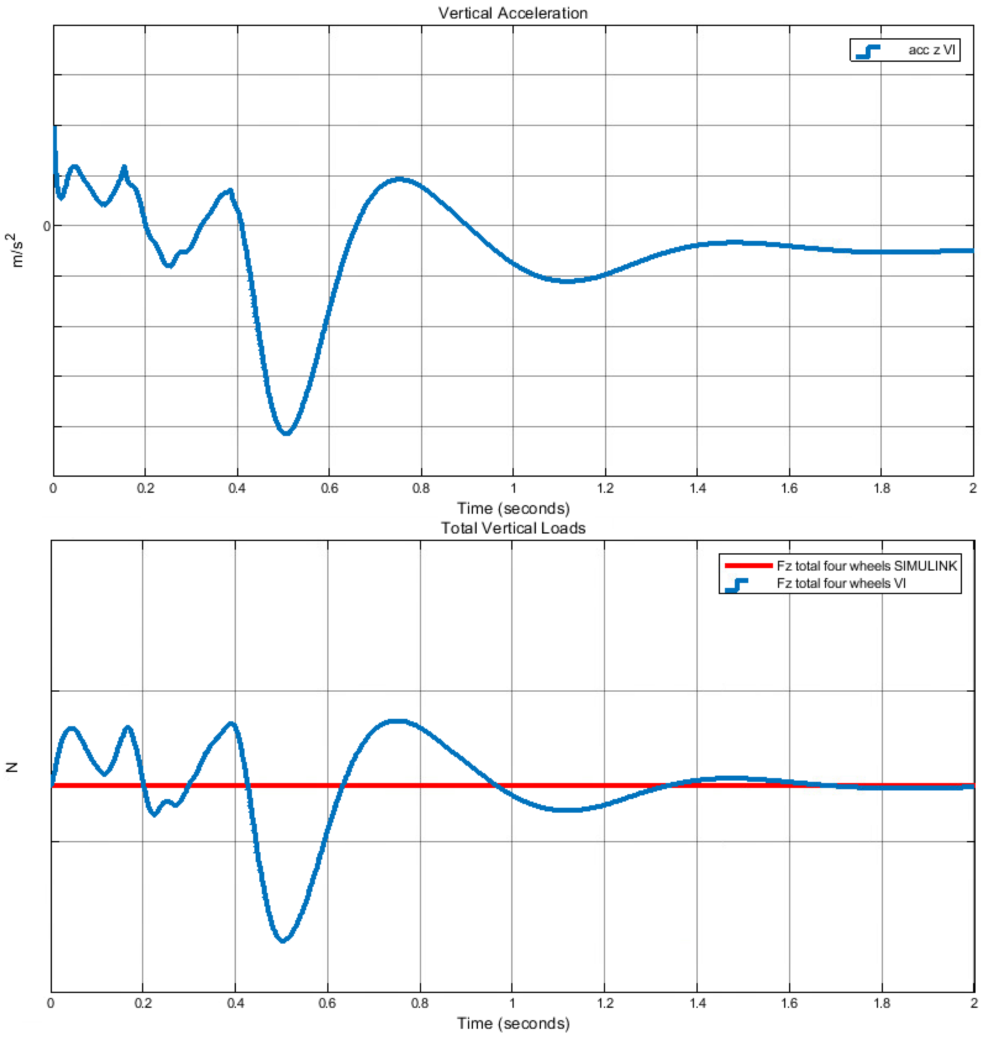

Figure 5.14: *Correspondence of the total normal load change with the vertical acceleration trend*

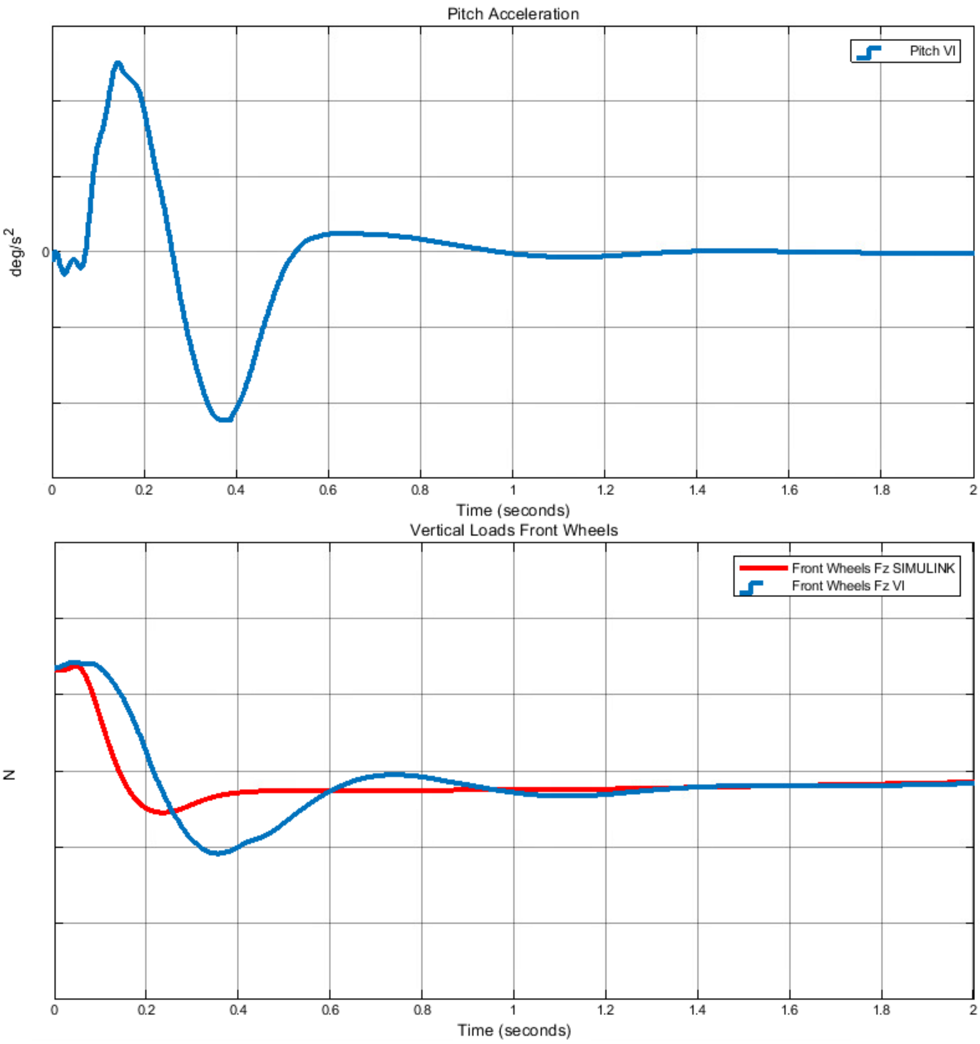

Figure 5.15: *Correspondence of the load transfer with the pitch acceleration trend*

As can be appreciated in the detailed Figures 5.14 and 5.15, the effect is particularly relevant at the start of the manoeuvre: this is because the first peak of torque is the one of greater magnitude, when the simulation environment is impressing a throttle almost instantly rising from zero to maximum. Another contribution was found to be caused by the fact that the VI-CarRealTime model needs about 2 seconds in order to set and stabilize, seconds in which it presents its own irregularities whichever is the manoeuvre impressed. The effects are still visible later in the manoeuvre, in the torque transients present at the gear changes, but with lower impact.
Some improvements are verified to be registered if impressing the same final throttle value, but starting after some seconds and with a more gradual ramp path.

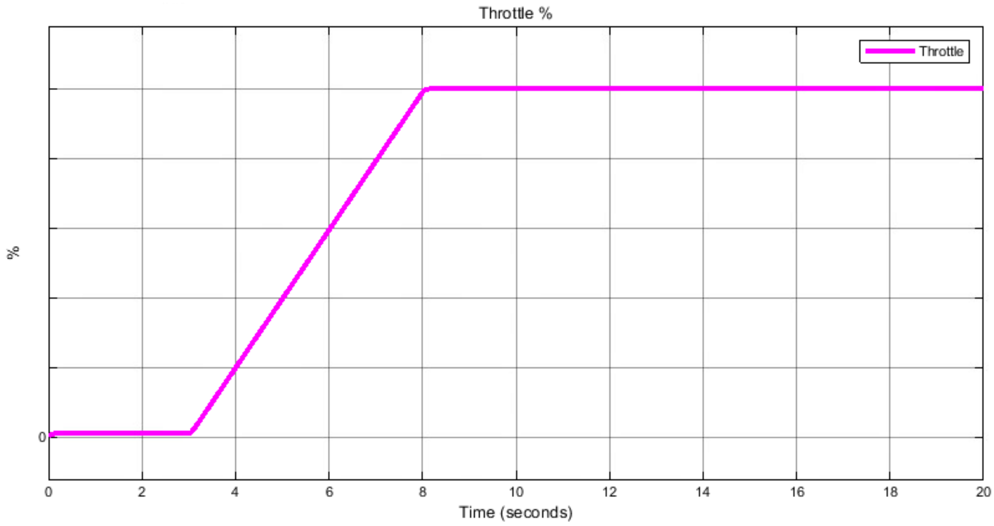

Figure 5.16: *New throttle increase*

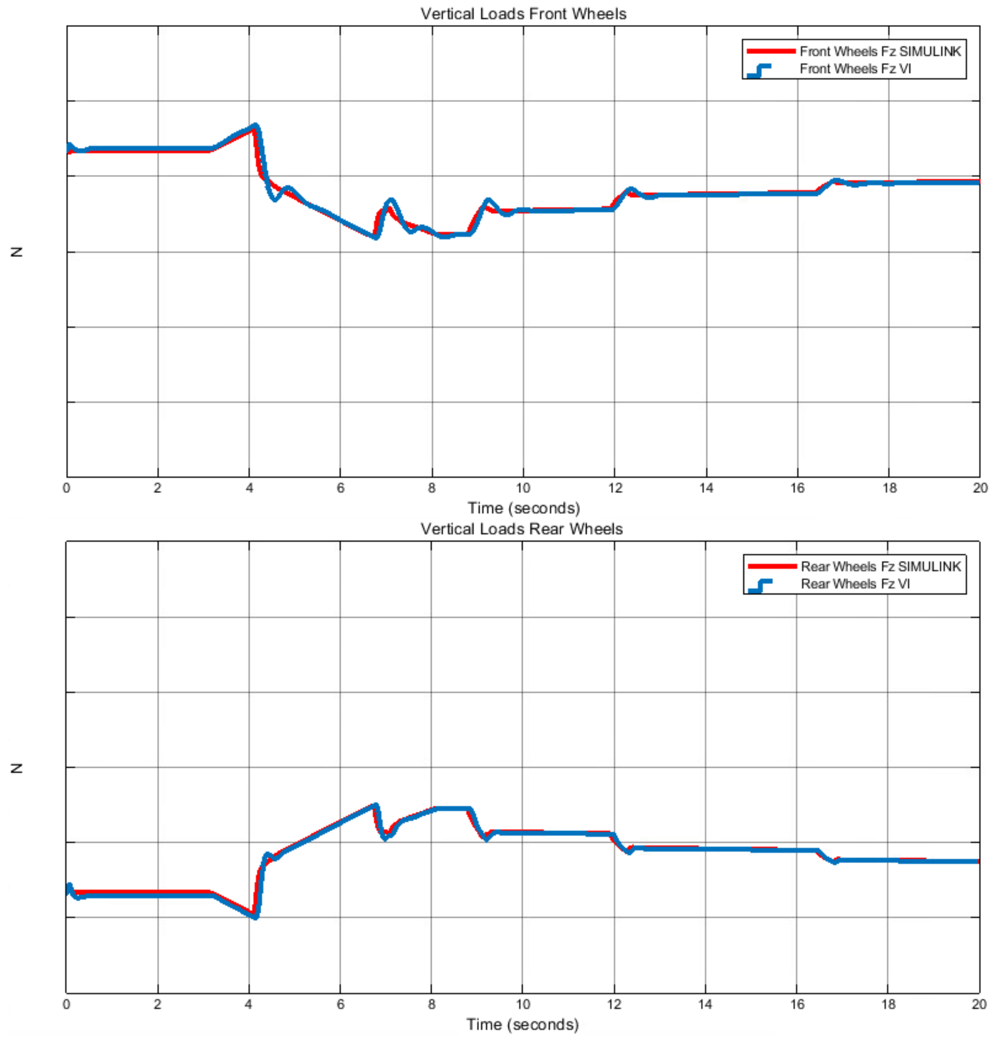

Figure 5.17: *Normal loads at the two axles with the new throttle path*

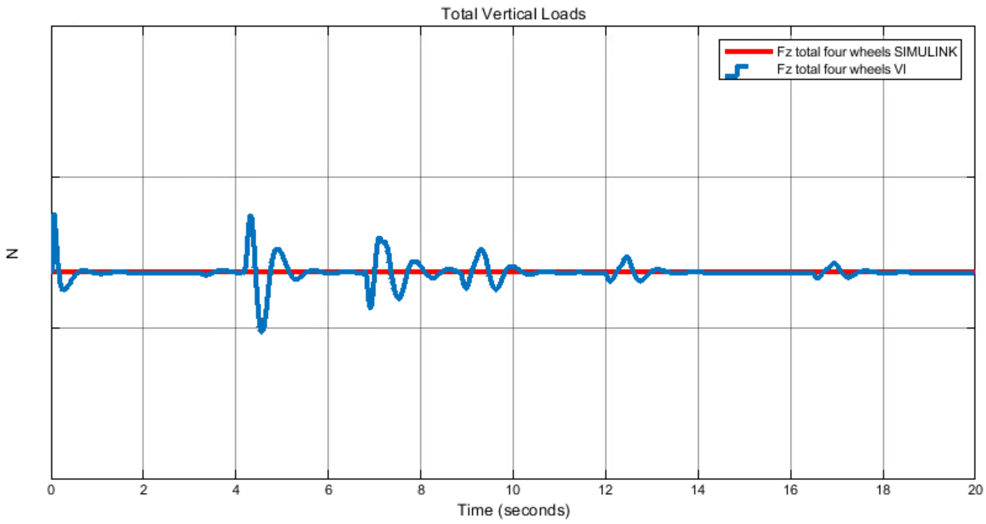

Figure 5.18: *Total vertical load at the four wheels with the new throttle path*

The two vehicles model are now showing satisfyingly similar results. The remaining vibrations are mostly due to the gear change manoeuvre, while the throttle increase effect is lowered. Isolated first seconds' oscillations of the VI model are now evident, and from now on they can be excluded from analysis.
In a simulation with lower torque transients, like could be a pure electrical drive, we can appreciate the consistency of our results.

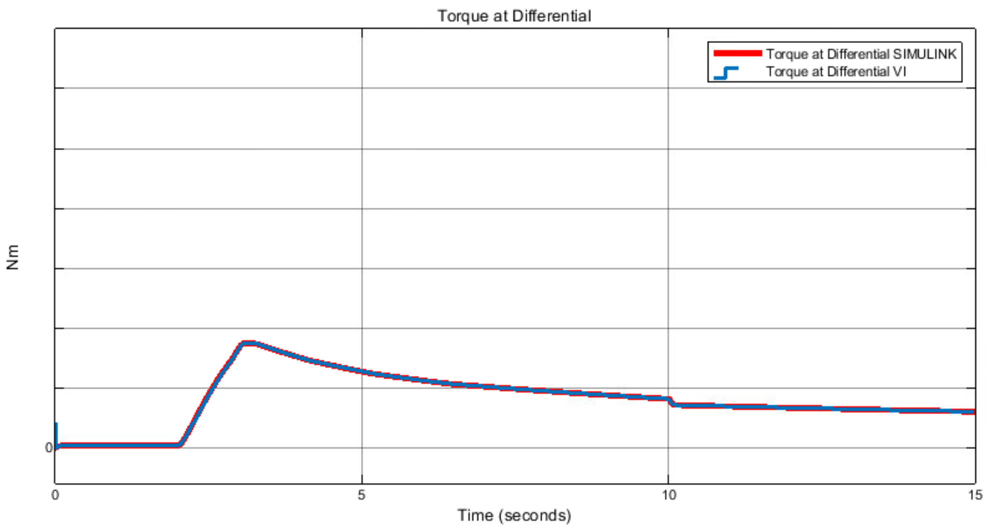

Figure 5.19: *Torque at the differential in a pure electric drive manoeuvre*

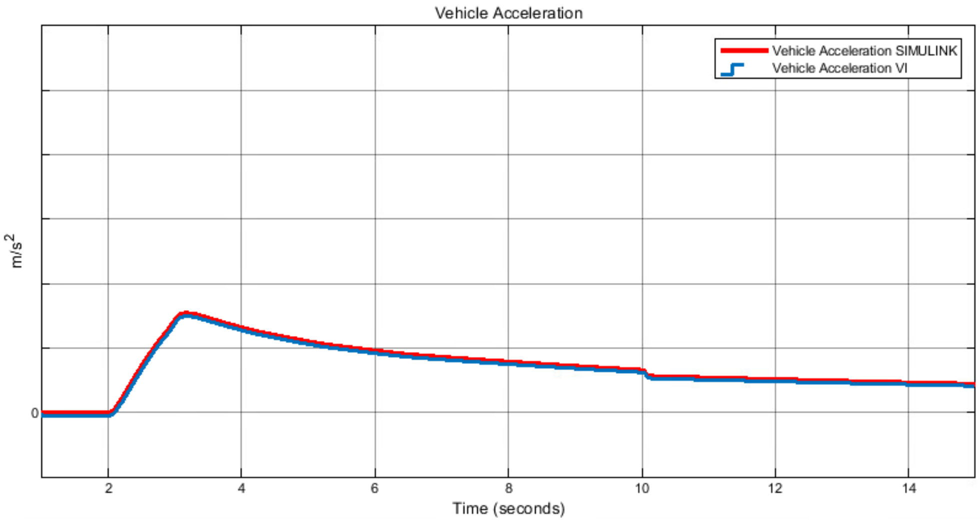

Figure 5.20: *Longitudinal acceleration of the vehicle models in a pure electric drive manoeuvre*

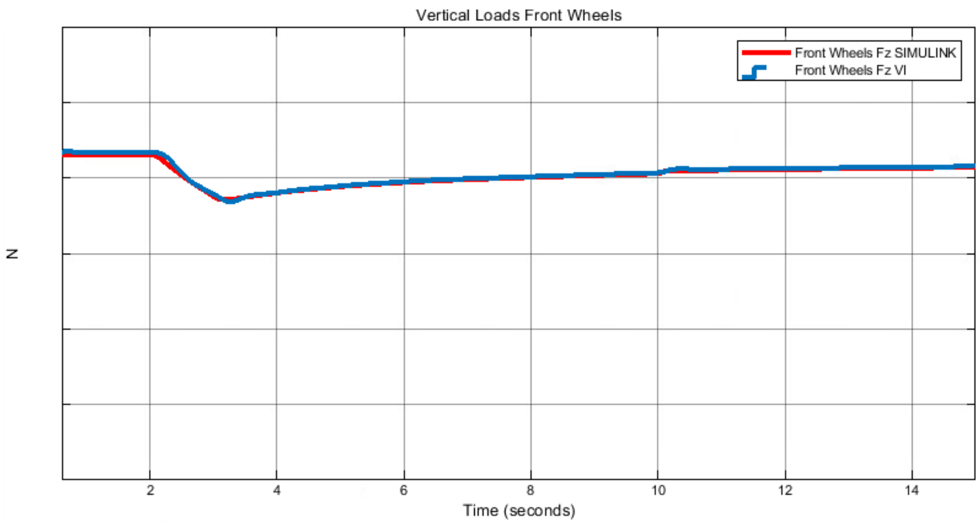

Figure 5.21: *Vehicle models normal loads at the front axle in a pure electric drive manoeuvre*

Even when simulating mixed power sources manoeuvres, the results are satisfactory and give a faithful representation of the correct operation of the vehicle, remaining in the order of what was obtained with the Simulink simple vehicle model.

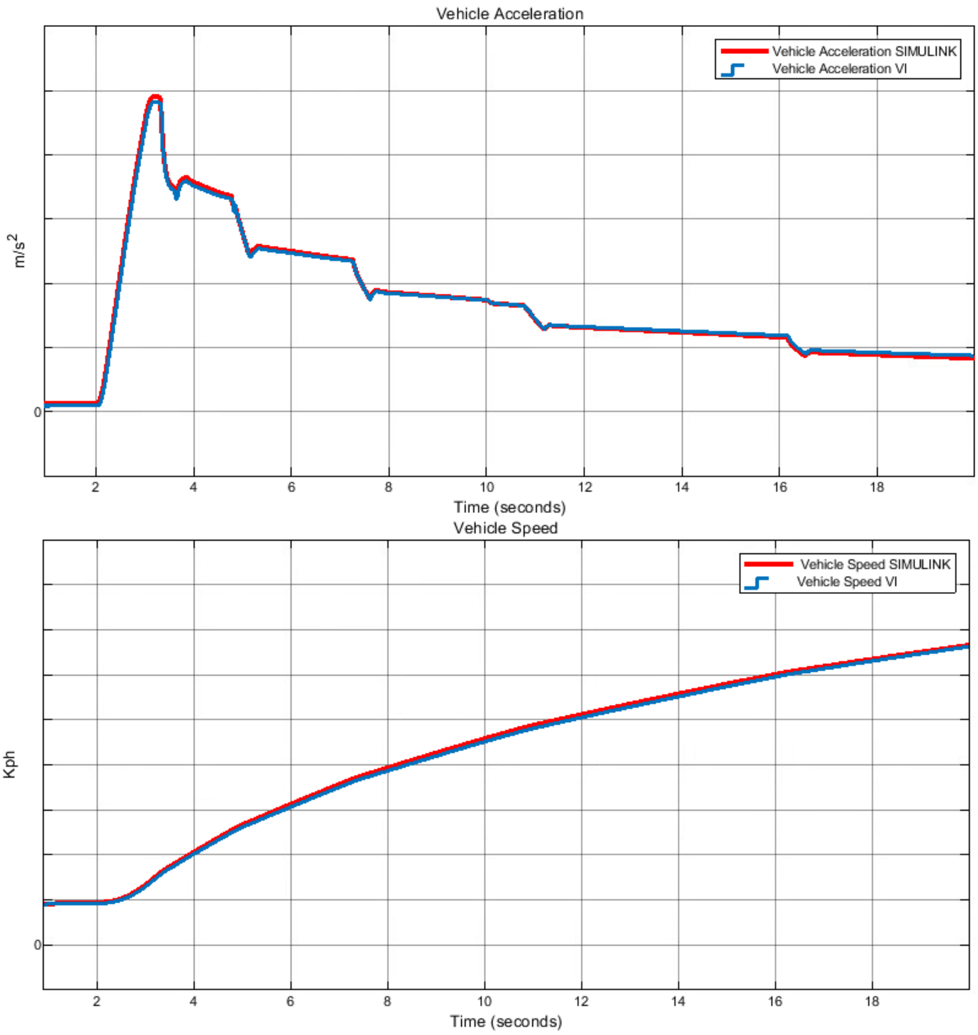

Figure 5.22: *Vehicle models longitudinal acceleration and speed in an overboost manoeuvre*

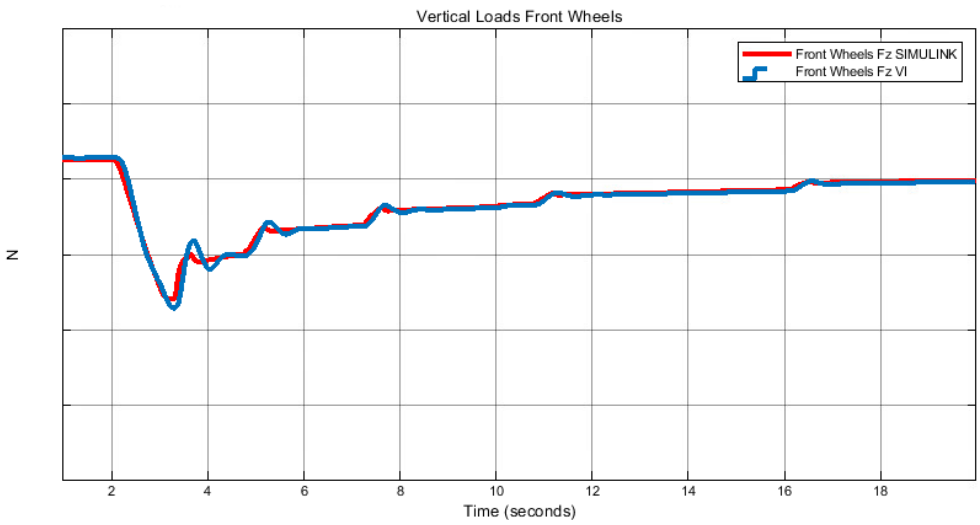

Figure 5.23: *Vehicle models normal loads at the front axle in an overboost manoeuvre*

Each manoeuvre type gives quality results, since in the co-simulation the vehicle model is not interested in how the torque is produced, with which source of power, or with which gear engaged, it only receives the torque trend during the simulation. In general, the VI vehicle model presents a slightly higher resistance to motion at low speeds, that results in lower longitudinal forces at the wheels, a fact that can result more evident in the braking manoeuvre. Differences are anyway accepted, since the behaviour of the vehicle model is still compatible with the performed manoeuvre.

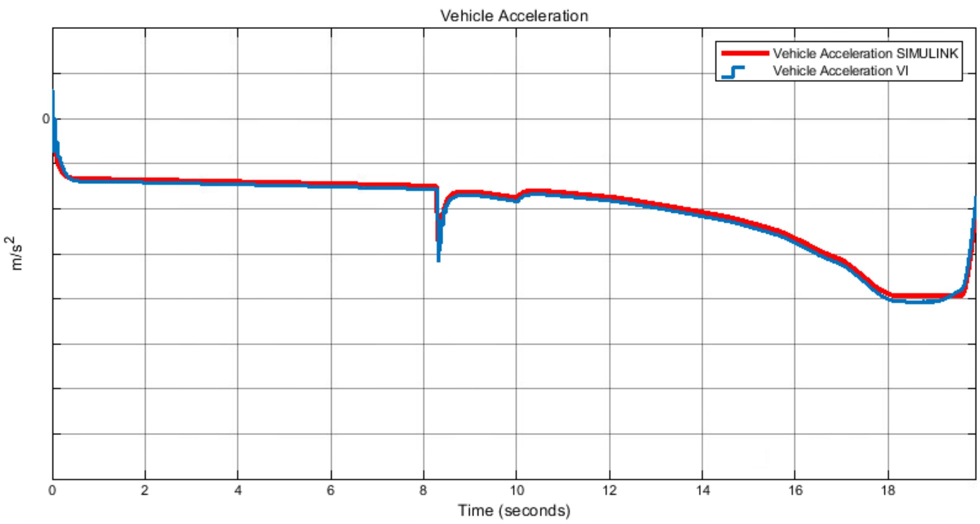

Figure 5.24: *Deceleration of the two vehicle models in a regenerative braking manoeuvre*

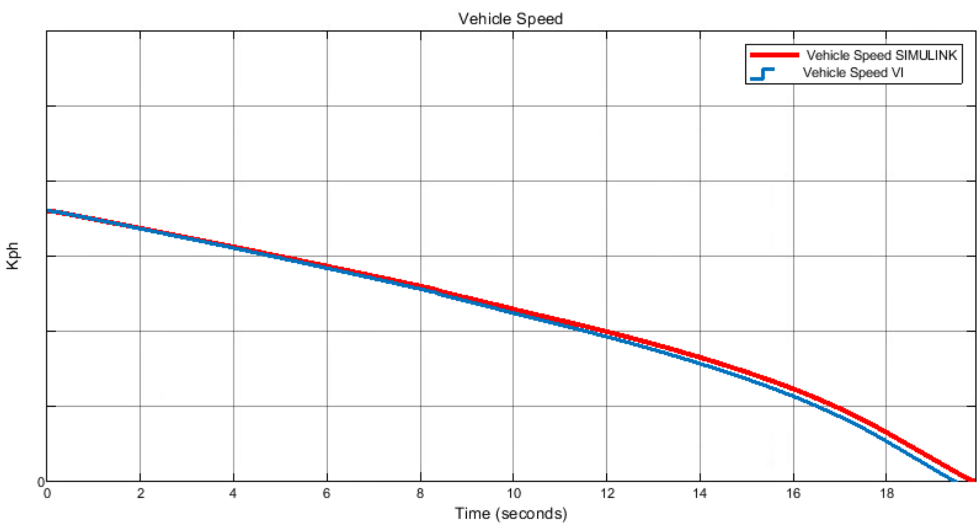

Figure 5.25: *Speed of the two vehicle models in a braking manoeuvre*

5.3 Co-simulation model possibilities

The correct synchronization and the correct functioning of the two co-simulated models is verified; now let us evaluate the benefits and the possibilities of the complete model created.
With the new complete vehicle model insertion, a much more extended pool of output data can be obtained and studied, like the suspensions working conditions, engine mounts forces and displacements, the information perceived by the mounted sensors. Moreover, characteristics about the vehicle are easily modifiable in the dedicated tool and effects of the changes can be assessed, without having to modify the complete model or create new dedicated complex blocks.

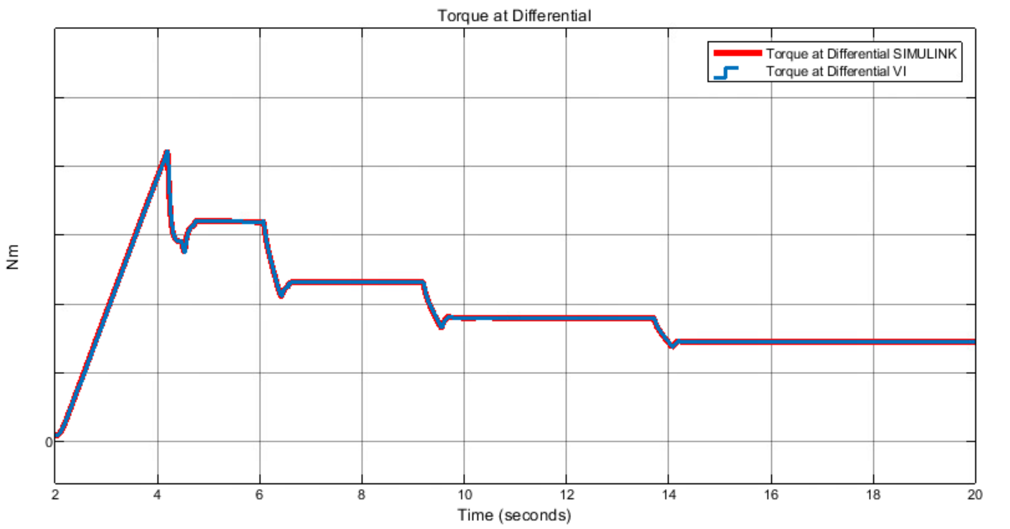

Figure 5.26: *Torque at the differential trend in the performed simulation*

Given the torque in input at the differential showed in Figure 5.26, proper of a pure thermal drive manoeuvre, some of the associated results that can be obtained with the co-simulation model can be observed in the figures below, demonstrating the wide range of study possibilities offered by the co-simulation.

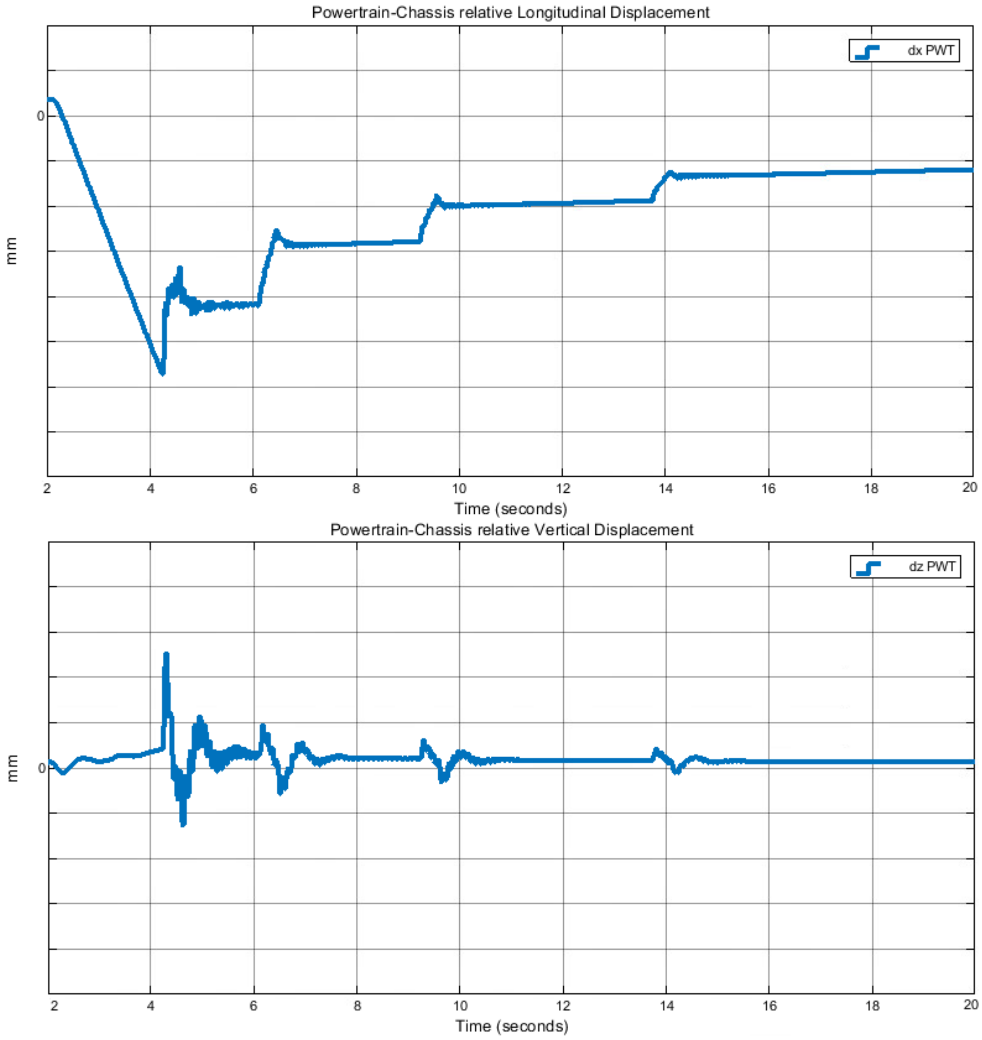

Figure 5.27: *Powertrain-chassis vertical and longitudinal relative displacements*

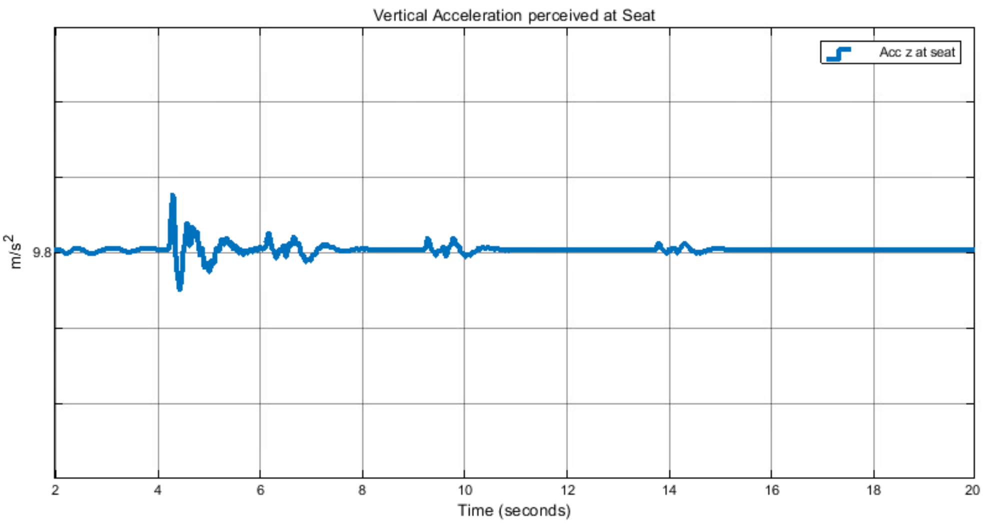

Figure 5.28: *Vertical acceleration perceived at passenger seat*

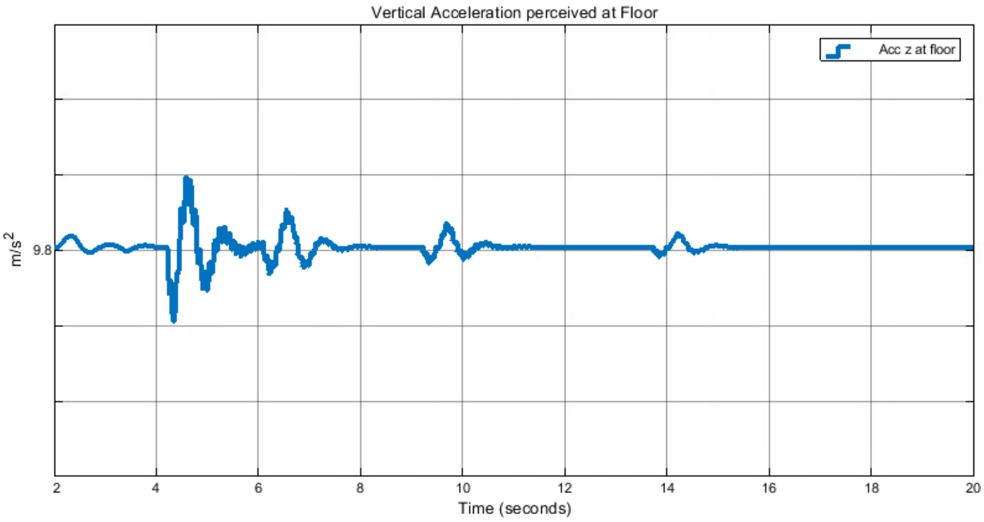

Figure 5.29: *Vertical acceleration perceived at vehicle floor*

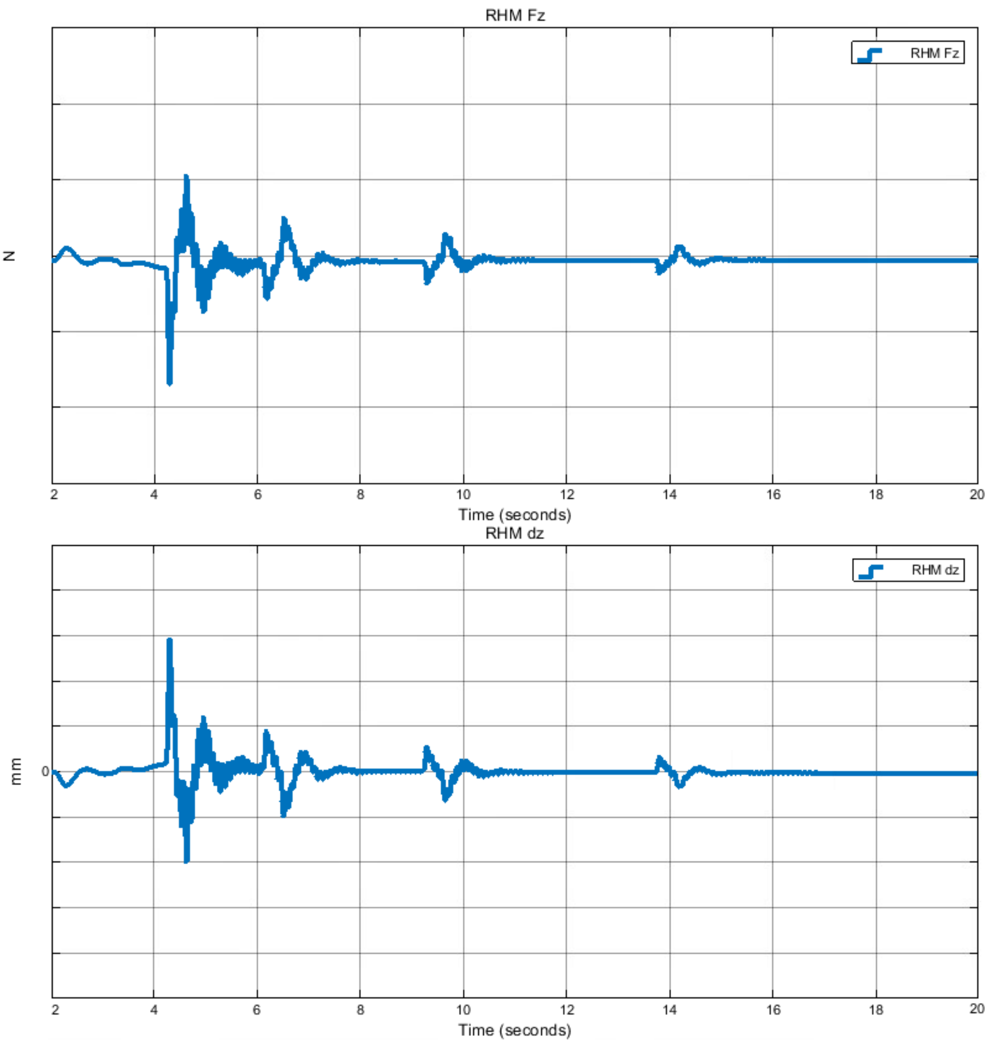

Figure 5.30: *Engine mount working condition in vertical direction*

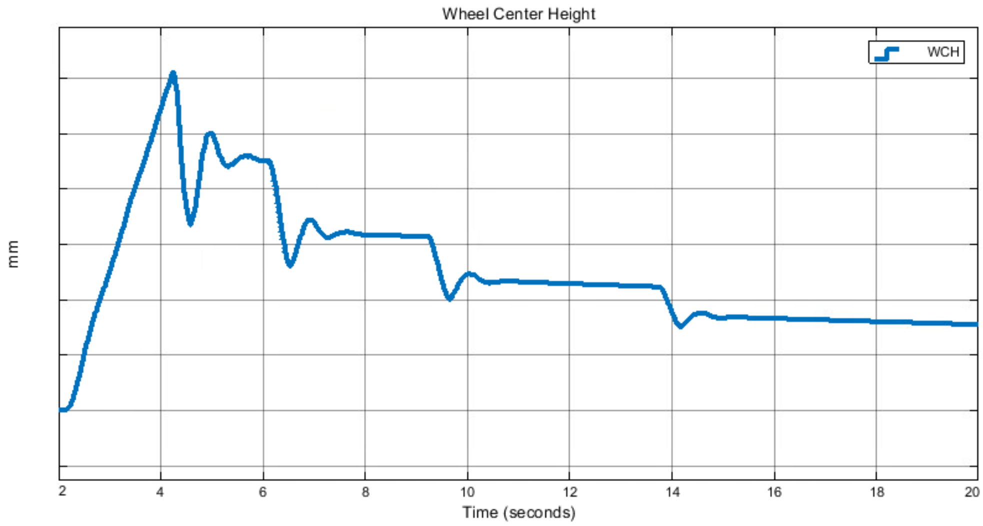

Figure 5.31: *Front wheel center height*

5.3.1 Powertrain suspensions regulation co-simulated analysis

As previously introduced, a more detailed evaluation of the impact of engine mounts on vehicle dynamics and comfort can be carried out using the co-simulation model. In order to have a complete understanding of their usefulness, the engine torque irregularities should be comprehended in the analysis in order to assess the effective capabilities of the powertrain suspensions. For simulating the torque ripple and have a first qualitative analysis to highlight the impact of the bushings in filtering a torque irregularity generated by the engine, a sinusoidal signal is inserted into the ICE block and added to the nominal torque output of the lock-up table T_{ICE_m}.

$$T_{ICE} = T_{ICE_m} + T_{irr} \tag{5.1}$$

$$T_{irr} = A\, sin\,(2\pi\ f\ t) \tag{5.2}$$

The amplitude of the oscillations varies with the engine speed and nominal torque, but in our survey is set to be equal to $\frac{T_{ICE_{nom}}}{2}$, while the frequency can be obtained as:

$$f = \frac{n_{ICE}}{60}\,\frac{i}{m} \tag{5.3}$$

Where n_{ICE} is the engine angular speed in rpm, i is the number of cylinders of the engine, and m is a constant given by the number of strokes of the engine divided by two.

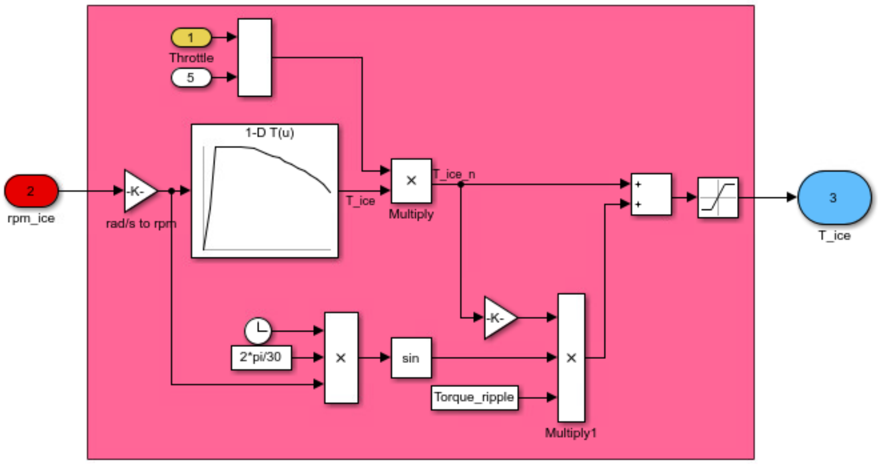

Figure 5.32: *Torque irregularities consideration in the engine output*

In this way the torque irregularities contribution due to the firing order of the cylinders is considered. In the co-simulation, the new torque at the differential dynamics is passed to the VI vehicle model, which verifies and returns the powertrain suspensions effect with a more irregular and representative path of the engine torque.
We can evaluate the more convenient bushings configuration by repeating the same simulation on the different powertrain subsystems analysed in section 4.3.3, where we progressively modify the suspensions stiffness curve in the three dimensions. In this analysis, an high-speed scenario with no gear change is simulated, in order to isolate engine irregularities effects and show the related driver perception.

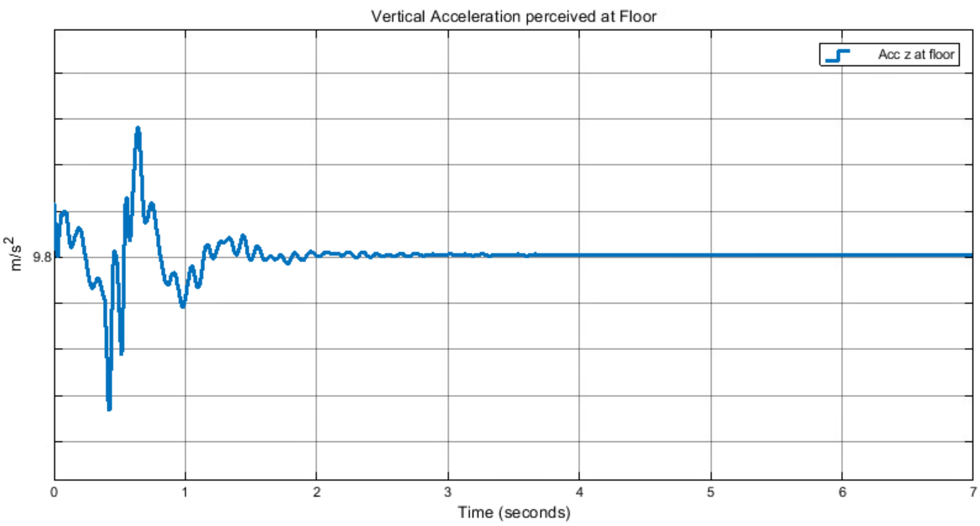

Figure 5.33: *Vertical acceleration perceived at chassis floor with the nominal bushings configuration*

Progressively increasing the stiffness of all the suspensions mounted on the power-train, it can be immediately observed how the vibrations perceived are increasing, in terms of both amplitude and frequency, consequently jeopardizing passengers comfort.

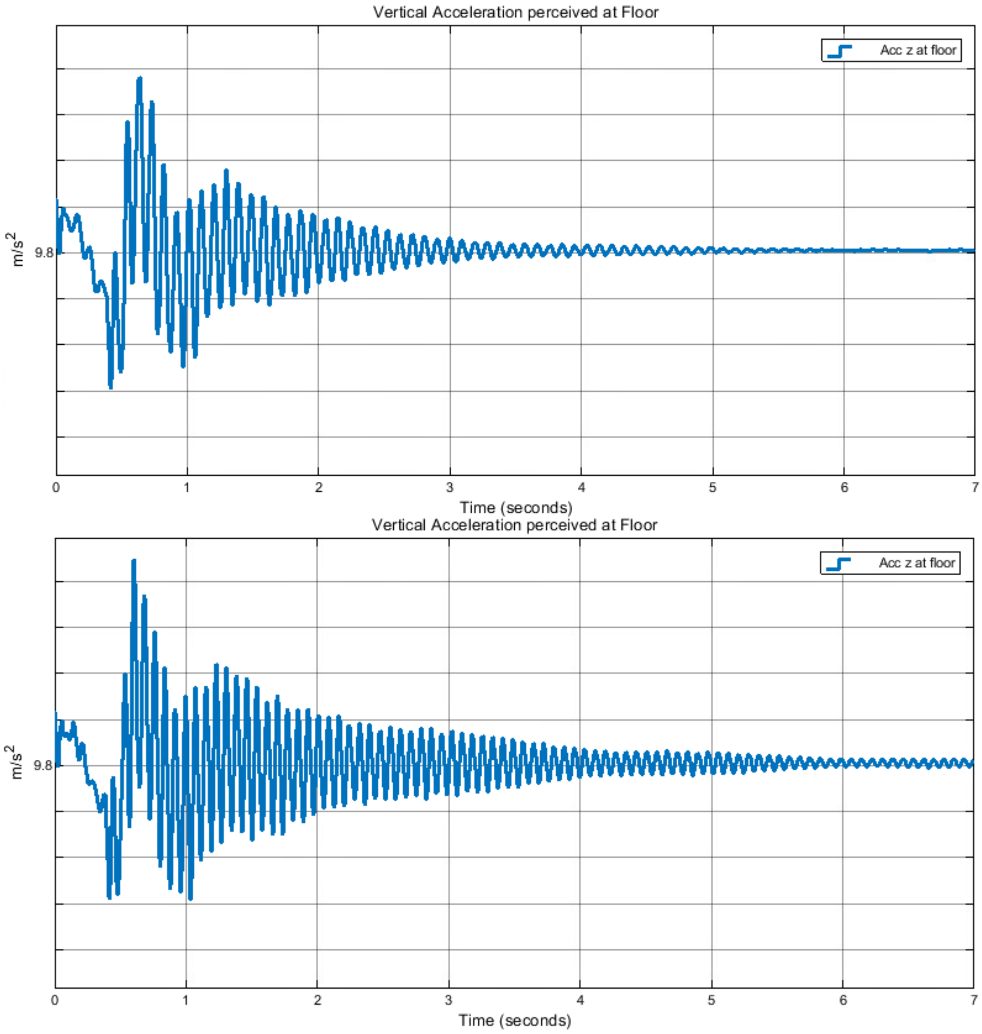

Figure 5.34: *Evolution of the vertical acceleration perceived at chassis floor with the progressive increase of the stiffness from nominal up to tripled value*

As expected, as the link between the powertrain and the chassis is stiffened, the filtering capability of the suspension regarding the engine torque irregularity is proportionally compromised, and higher discomfort will be perceived by the passengers. For this reason is generally preferred a more loose connection, hence installing less stiff engine suspensions. Results are confirmed with the analysis of the frequency response of the oscillations: by plotting their spectrum it can be observed how the peak is progressively moving to higher frequencies and at higher magnitude levels.

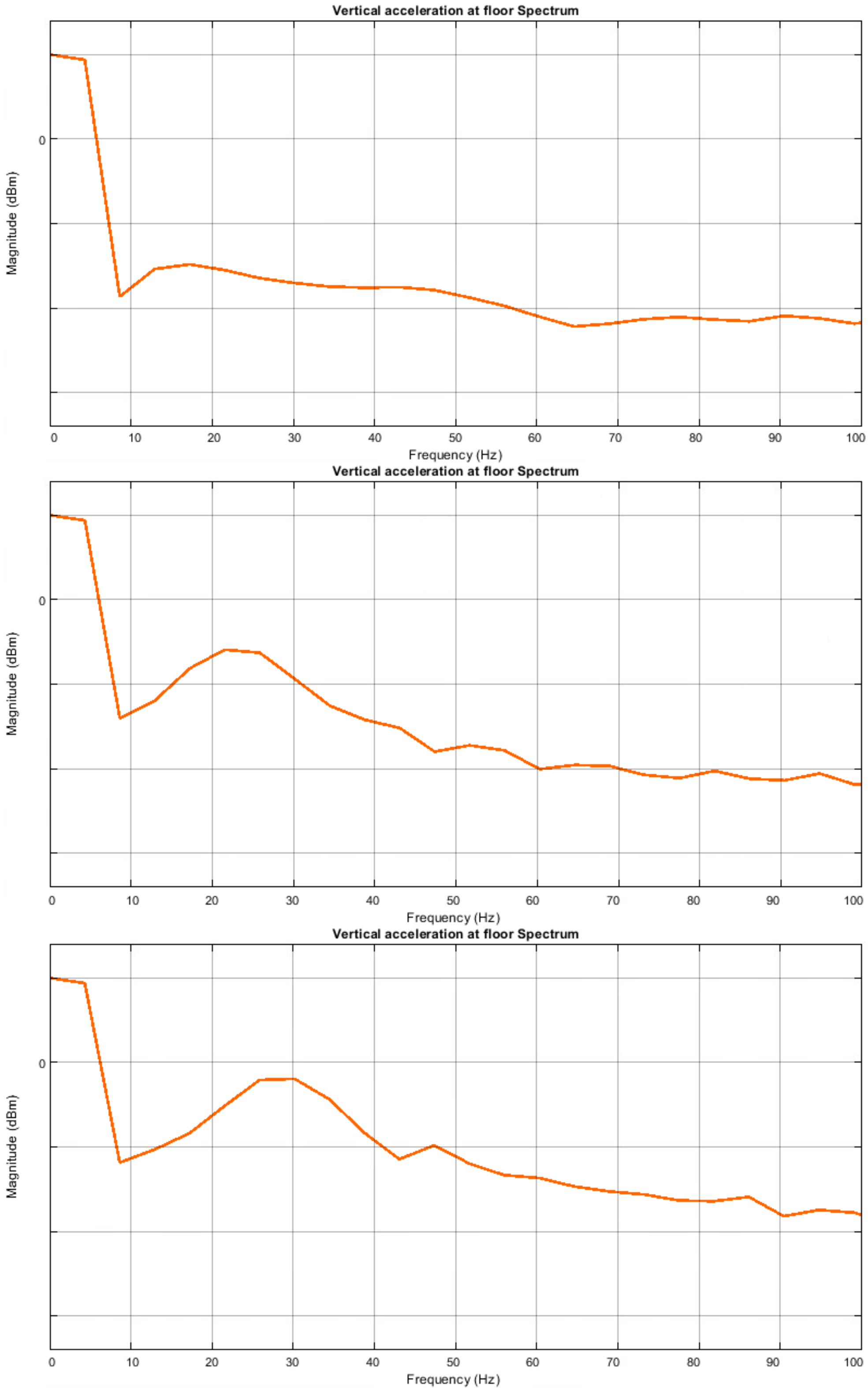

Figure 5.35: *Evolution of the vertical acceleration at chassis floor spectrum with the progressive increase of the stiffness from nominal up to tripled value*

Same results can be obtained assessing the driver feeling at vehicle seat.

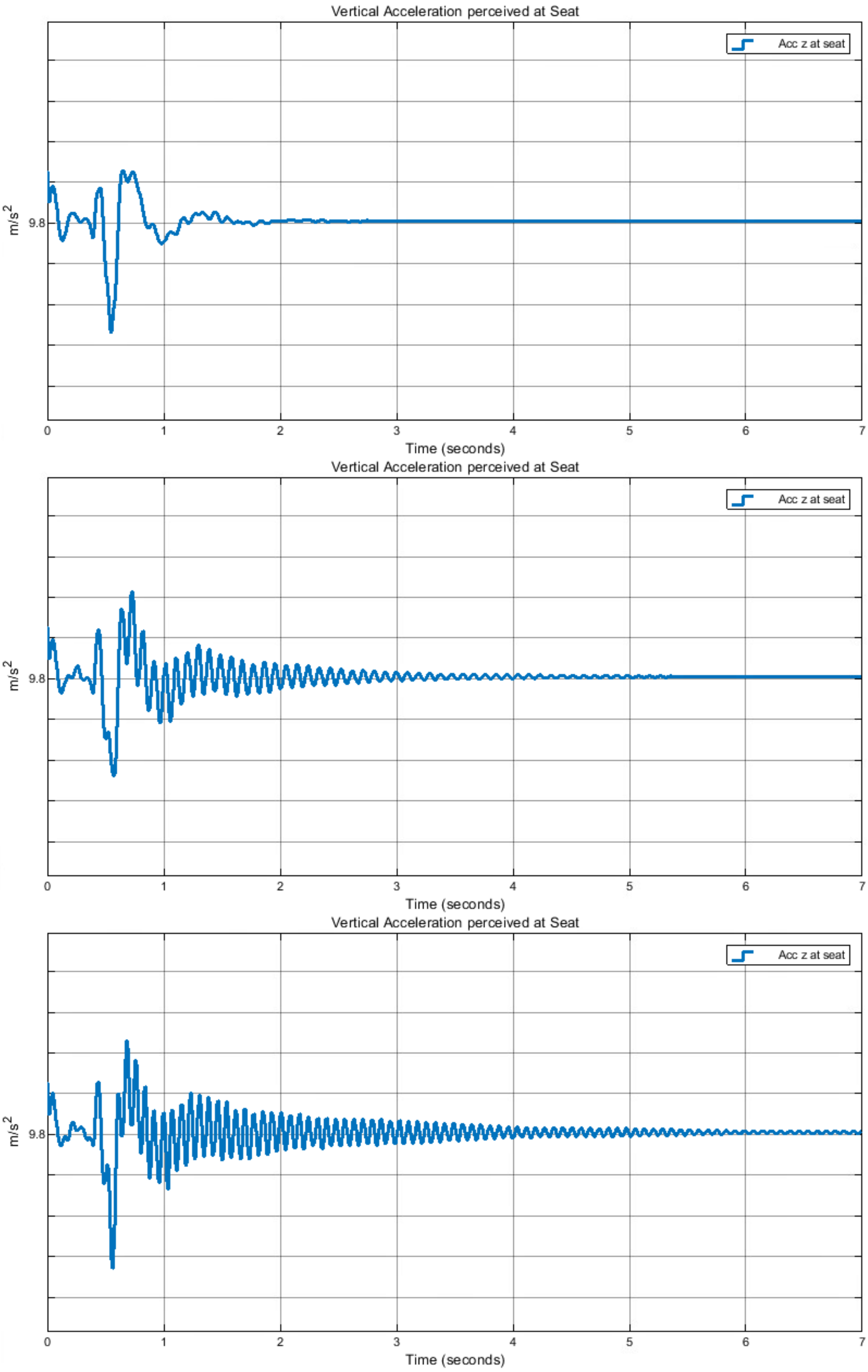

Figure 5.36: *Evolution of the vertical acceleration perceived at driver seat with the progressive increase of the stiffness from nominal up to tripled value*

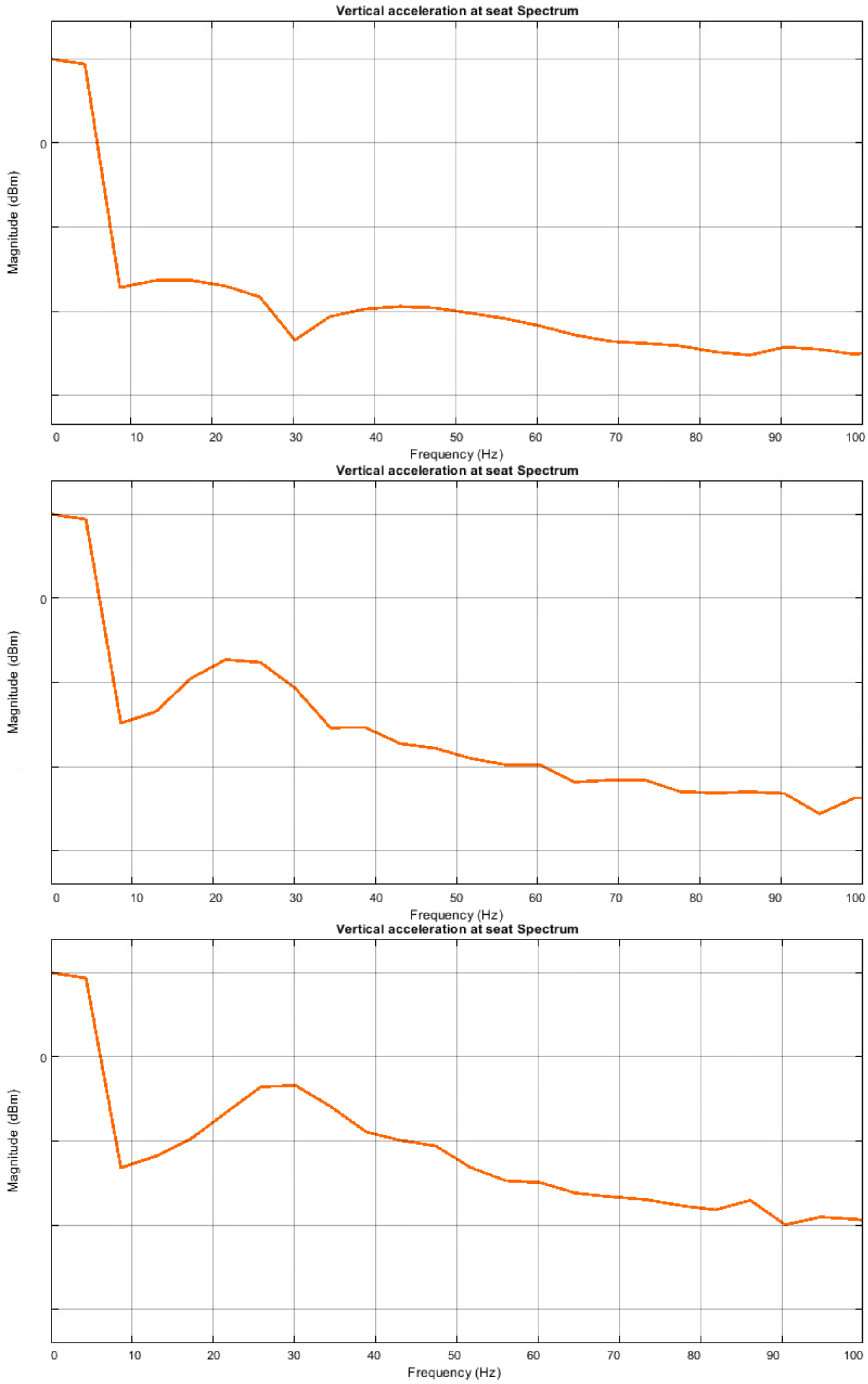

Figure 5.37: *Evolution of the vertical acceleration at driver seat spectrum with the progressive increase of the stiffness from nominal up to tripled value*

Also in longitudinal direction, the vibrations perceived by the driver follows the same pejorative results trend as the powertrain suspensions stiffness is increased.

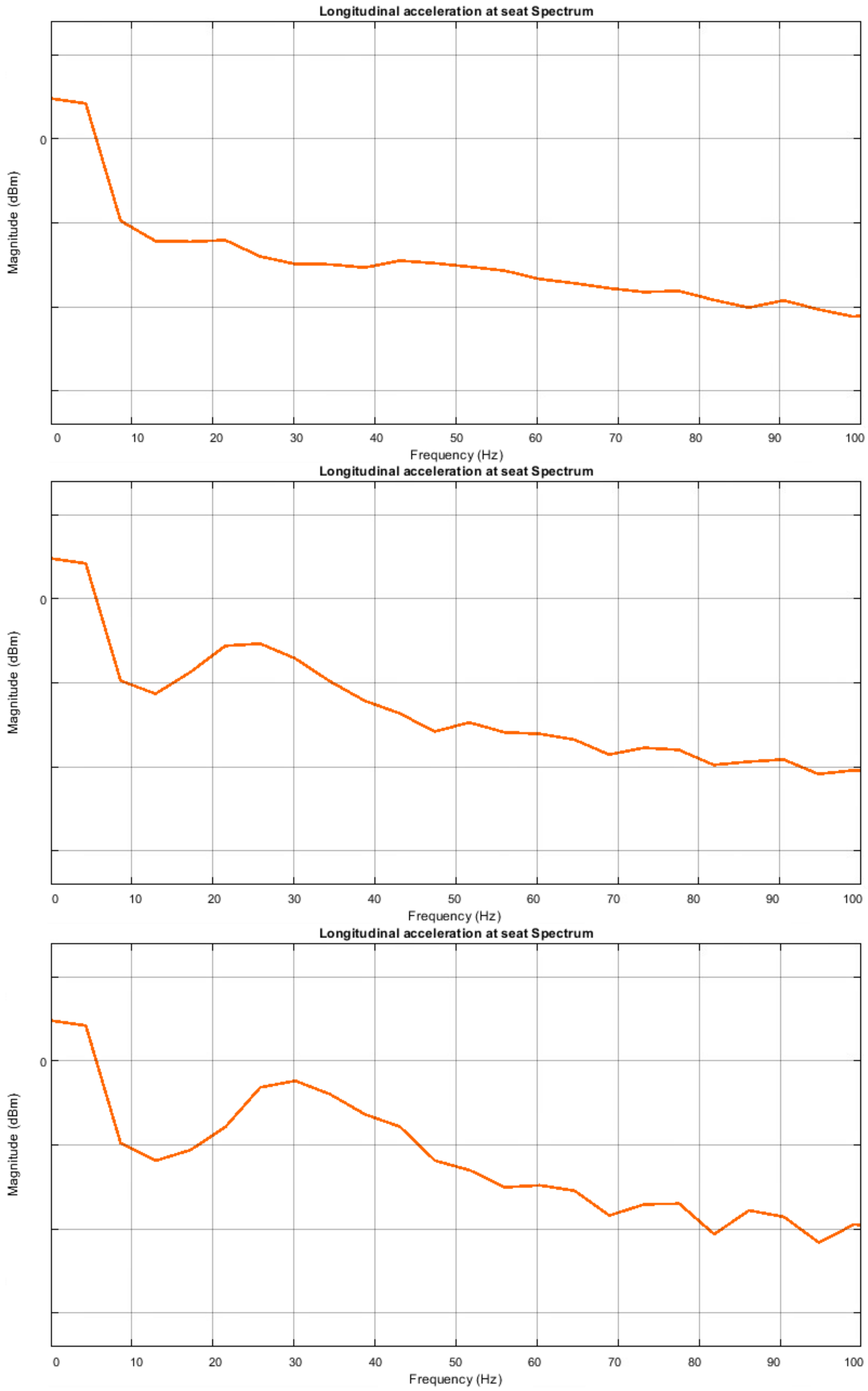

Figure 5.38: *Evolution of the longitudinal acceleration at driver seat spectrum with the progressive increase of the stiffness from nominal up to tripled value*

As obtained in section 4.3.3, acting on the translational damping capability will reduce the magnitude of the vibrations perceived, in the range of the resonance frequency. However, a too high damping value can have detrimental effects on the filtering capability of the suspension when exciting the high frequencies.

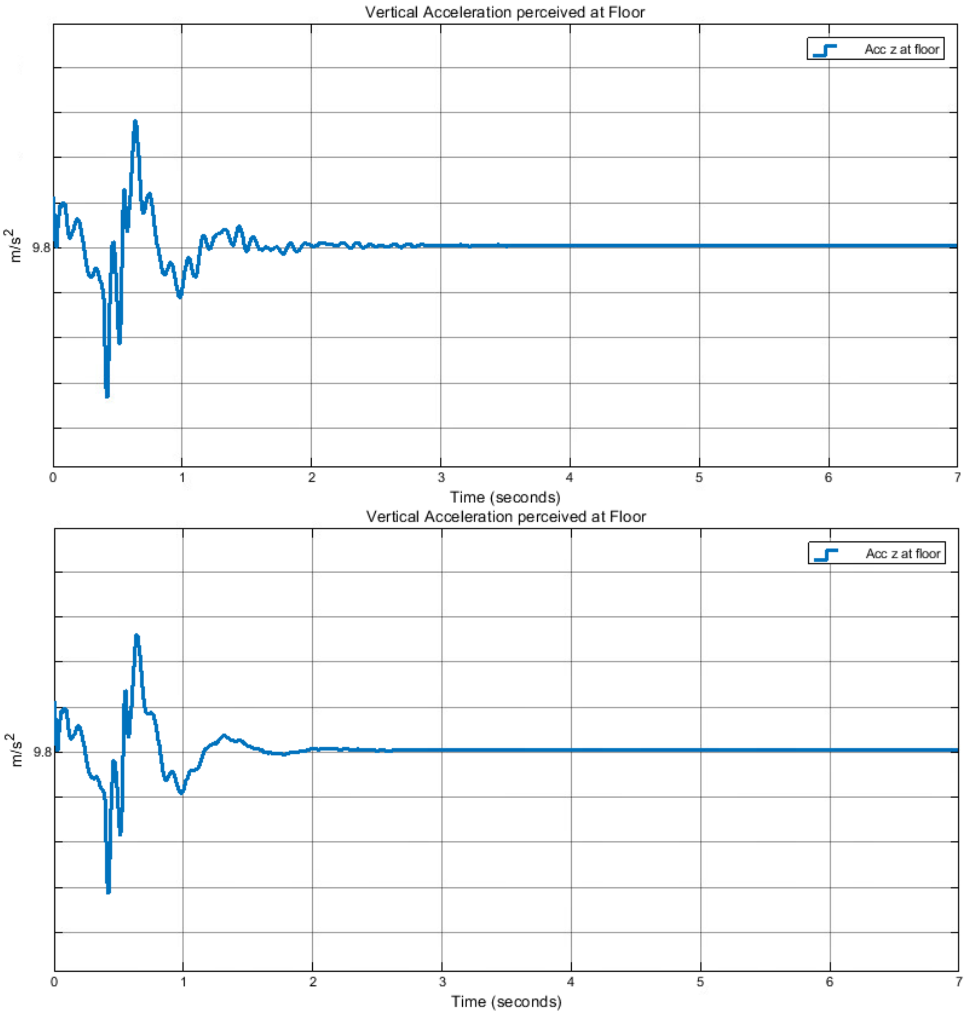

Figure 5.39: *Evolution of the vertical acceleration at chassis floor with the increase of the translational damping constant from nominal to tripled value*

For the reasons just highlighted, it now appears clear the advantages of mounting powertrain suspensions with respect to a rigid link; in order to optimize the passenger comfort, it would be preferable to use low stiffness bushings with the adapt damping properties.

It is evident that the stiffness cannot be reduced indefinitely, since the powertrain vibrations will proportionally increase their magnitude, risking to cause the suspension to reach the end of its stroke, area in which its rigidity greatly increases, thus compromising its filtering capability.

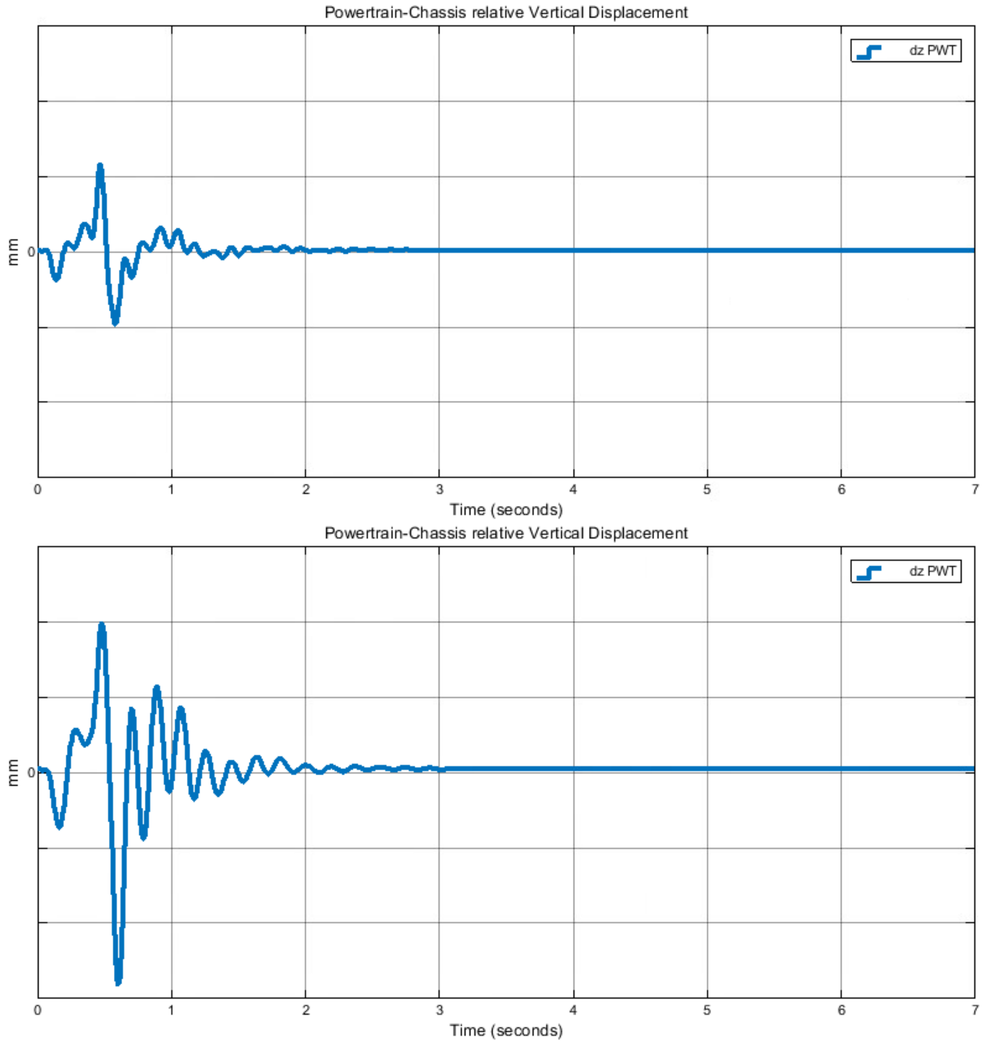

Figure 5.40: *Powertrain-chassis relative vertical displacement evolution modifying bushings stiffness from nominal value to halved*

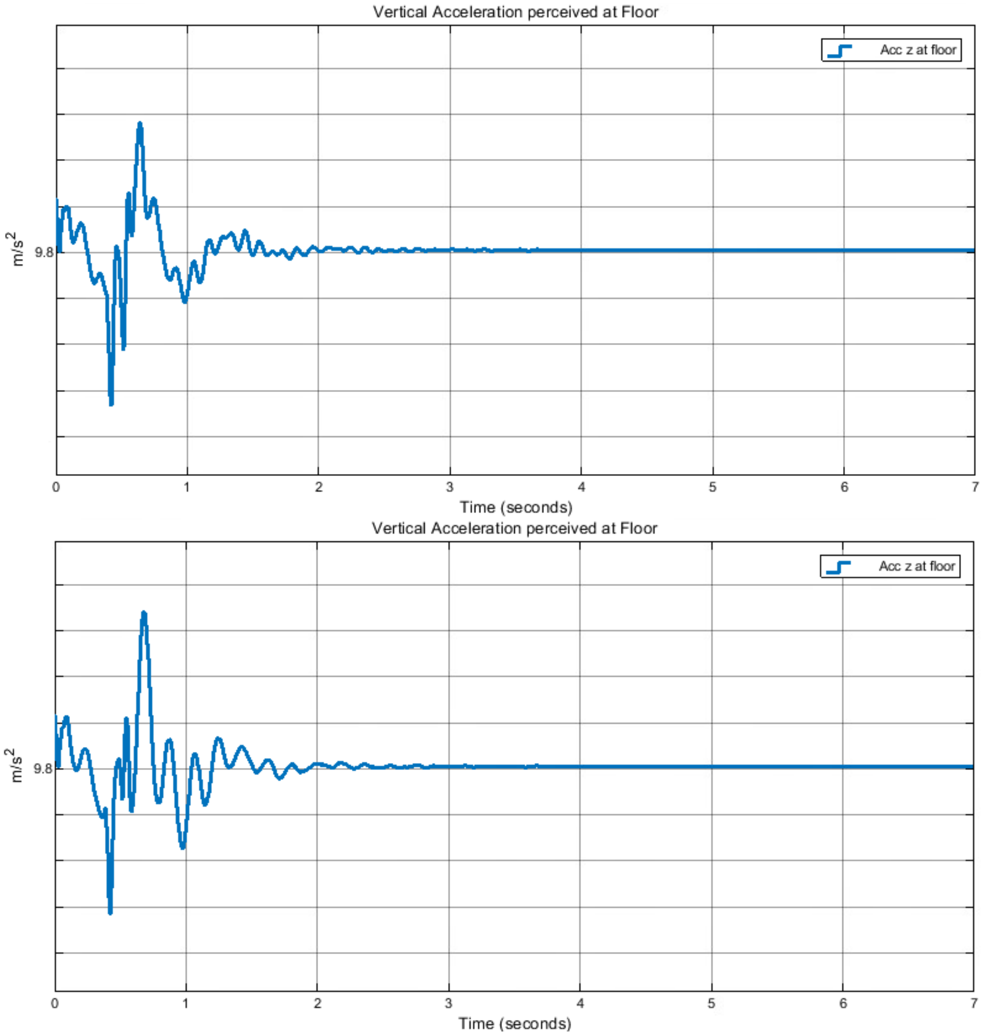

Figure 5.41: *Vertical acceleration perceived at chassis floor with nominal and with halved bushings stiffness values configurations*

Conclusions

The aim of this project was to investigate the possibilities and advantages in co-simulating a functional driveline model with the associated vehicle model, developed in two different dedicated environments. The work carried out allowed the realization of a complete conjoined model in which most of the features regarding vehicle dynamics can be effectively captured and studied.
The initial part focused on extending the previously created and already functional driveline model, and having to work on a pre-structured logic was the first difficulty encountered during the development, as it was necessary to modify part of the model without affecting the general and ultimate functioning. Finally, the correctness of the initial results has been maintained and the expansion has added new flexibility to the model and enhanced its representation of the real vehicle, in particular conferring:

- **The possibility to change gear during regenerative braking**: being able to downshift during braking permits to always use the most suitable gear ratio, resulting in a more efficient braking, as confirmed by the simulations performed.

- **The possibility of using the odd-numbered side of the transmission also for the electric motor**: new intermediate transmission ratios can be useful for the torque supplied, both in terms of maximum performance and when performing the compensation manoeuvres. By redirecting the torque flow through the clutches some losses are introduced, that are taken into account in the evaluation, but that in general seem not to affect the dynamics and the electric motor torque contribution, except if present in the first phases of the manoeuvre.

The general logic of simplicity of the model has been maintained, keeping also the annexed limits. Some improvements can still be made on the driveline modelling:

in particular, further considerations should be made in the transition of the electric motor power to the odd side of the transmission, including its torque in the dynamic equation of the clutches, an impact that, not to over-distort the initial model, has been bypassed. Another refinement would be necessary in the gear change phase, which is very simplified, being that the gear selection is immediate and without any attached losses. Therefore, the analysis derived results quite approximate, in particular the evaluation carried out on regenerative braking with gear change.

It followed the creation of the VI-CarRealTime vehicle model, that was facilitated by the dedicated environment. The greatest difficulty encountered here was in the engine bushings implementation, mainly for the initially unfamiliar software calculation logic and its approximations, which required additional verifications.

Finally, the model was incorporated on Simulink and the initial purpose was finalized, with the co-simulation model that proved to be successfully functioning, for all the simulated manoeuvres. The joined model establishes the torque dynamics and evaluate the qualitative response of the vehicle. The VI model is at a more refined level of detail, and suffers more from excessive and unrealistic power transitions which can be created in the Simulink environment, justifying unexpected vibrations of the VI model and slight discrepancies between the two vehicle models.

Final results were confirmed by the correlation with the previous simple vehicle model, and additional data and studies are now available for the design. An evaluation of the engine suspensions effectiveness was developed, demonstrating their usefulness for ride comfort, and evaluating the impact on it as their properties vary.

Future developments following this project could be the creation of a complete Multi-Body vehicle model in Adams Car. The new MB Adams model would be subsequently co-simulated with the Simulink driveline to obtain even more reliable and representative results. The co-simulation could potentially be avoided, representing the accurate driveline with all the components directly in Adams, but the simplicity of the model must be maintained in order to have reasonable simulating times, therefore the Simulink driveline could represent a better trade-off from that point of view. Subsequently, a numerical-experimental correlation with real data would be necessary for the validation of the various models and related results.

Bibliography and Sitography

[1] Pietro Scandale and Massimo Violante. "Model Based Design of Automotive Embedded System." In: (2019). URL: http://webthesis.biblio.polito.it/id/eprint/12441.

[2] Mathworks Documentation. *Model-Based Design with Simulink*. URL: https://it.mathworks.com/help/simulink/gs/model-based-design.html.

[3] Yaryna Myrka. *Why Model-Based Design Makes Traditional Automotive Software Development Obsolete*. URL: https://medium.com/the-research-nest/why-model-based-design-makes-traditional-automotive-software-development-obsolete-b3abb2cbe794.

[4] Anu Maria. "Introduction to modelling and simulation." In: (1997). URL: https://doi.org/10.1145/268437.268440.

[5] Anylogic. *Why use simulation modeling?* URL: https://www.anylogic.com/use-of-simulation/.

[6] Claudio Gomes et al. *Co-simulation: State of the art: Technical Report*. ArXiv, Feb. 2017.

[7] Open Simulation Platform. *Co-simulation*. URL: https://opensimulationplatform.com/co-simulation/.

[8] Riccardo Benevento, Enrico Galvagno, and Alessandro Vigliani. "Modeling of a P2 hybrid vehicle with dual clutch transmission". In: (2020). URL: https://webthesis.biblio.polito.it/14239/.

[9] VI-Grade. *VI-CarRealTime. One vehicle model from concept to sign-off*. URL: https://www.vi-grade.com/en/products/vi-carrealtime/#av_section_form.